

Early events in cytokine receptor signaling

DISSERTATION

Zur Erlangung des akademischen Grades

Doctor of Philosophy

(Ph.D)

Vorgelegt

der Fakultät Mathematik und Naturwissenschaften

der Technischen Universität Dresden

von

Hetvi Gandhi

Geboren am December 11, 1984 in Surat, India

Gutachter

Prof. Dr. Petra Schwille

Prof. Dr. Gerhard Roedel

Contents

Summary	1
Chapter 1.....	3
Introduction	3
1.1 Signaling from plasma membrane	3
1.2 Receptor endocytosis.....	5
1.3 Signaling and endocytosis	6
1.4 Spatio-temporal regulation of signaling through endosomes	6
1.5 Pathways of receptor endocytosis.....	9
1.6 Endocytosis in cytokine signaling.....	9
Chapter 2.....	13
Materials and methods.....	13
2.1 Materials	13
2.1.1 Constructs	13
2.1.2 Cloning strategy	14
2.1.3 Primer sequence	15
2.1.4 esiRNA sequence.....	15
2.1.5 Antibodies	16
2.1.6 Solutions and media.....	16
2.2 Methods	17
2.2.1 Cell culture and maintenance	17
2.2.2 Cell seeding and transfection.....	17
2.2.3 Cell fixation and immune staining	17
2.2.4 Cell lysis.....	18
2.2.5 Pull down	18
2.2.6 Western blot	18
2.2.7 IL-4 labeling	19
2.2.8 Immunogold labeling and electron microscopy	19
2.2.9 Pulse chase experiment and drug inhibition	20
2.2.10 Loading assay	20
2.2.11 Fluorescence recovery after photobleaching (FRAP).....	22
Chapter 3.....	23
Results part I: Characterization of the endosomes.....	23

3.1 Preface	23
3.2 Endosome formation is ligand independent.....	25
3.3 IL-2R γ positive cortical endosomes are multi-vesicular bodies	27
3.4 Multivesicular bodies are associated with actin meshwork	32
3.5 Multivesicular bodies are positive for Hrs	33
3.6 Endosomes are separate compartments from the plasma membrane.....	34
Chapter 4.....	36
Results II: Quantitative analysis of trafficking of Interleukin receptors	36
4.1 Preface	36
4.2 Signaling components accumulate in the endosome	37
4.3 Dynamics of receptor trafficking in to the endosome	37
4.4 Receptor trafficking is independent of the type of receptor	41
4.5 Receptor trafficking to the endosomes is independent of the presence of IL-4	41
4.6 Signaling and receptor internalization is sensitive to perturbation of Rac1/Pak1 driven endocytosis	42
4.7 Endosomes maintain signaling.....	44
Chapter 5.....	46
Results Part III: Regulation of receptor at the molecular level	46
Preface 5.1	46
5.2 Interaction of GEF with endosomes.....	49
5.3 Domain specific interaction of Vav2	50
5.4 The IL-2R γ cytoplasmic region is important for the endosome formation.....	52
5.5 Interaction of Vav2 with IL-2R γ truncations	54
5.6 Vav2 can modulate signaling	56
5.7 Outlook.....	58
JAK3 mutant fails to form endosome	58
Future directions.....	60
Discussion	61
Abbreviations	69
References	71

Summary

Ligand-activated signal transduction is a process critical to cell survival and function as it serves as a means of communication between the cells and their environment. Endocytosis is generally thought to down-regulate incoming signals by reducing the surface availability of receptors. However, increasing evidence in many systems suggests a notion which is referred to as the 'signalling endosome' hypothesis - that endocytosis can also actively contribute to signalling apart from clearance of activated receptors and thereby attenuation of signalling. The functional aspect of signalling endosomes has been well-characterized in several pathways including RTK and TGF- β signalling. There are, however, various other signalling pathways where the active mechanism of endocytotic regulation is yet to be understood.

In this study, we probe this aspect in the cytokine signalling system, where the receptors are known to internalize but the significance of such internalization and precise mechanism is unclear. My thesis aims to elucidate the function and molecular details of internalization of cytokine receptor using interleukin-4 receptor (IL-4R) signalling as a model. IL-4 and IL-13 ligands can induce assembly of three distinct complexes: IL4 induced IL-4R α – IL-2R γ (type I), IL-4 induced IL-4R α – IL-13R α 1 (type II) or the IL-13 induced IL-13R α 1-IL-4R α (type II). The formation of any of these complexes triggers signalling through the JAK/STAT pathway. However, models of how the oligomerization of the transmembrane receptors and activation takes place are very diverse and lack a clear molecular and biophysical understanding of the underlying receptor dynamics.

Previous results of the lab had shown that the affinities between subunits are low, precluding complex formation at the plasma membrane at physiological concentrations. In addition, IL-4R subunits localize in to endosomal structures adjacent to the plasma membrane. It had already been shown that the shared IL-4R subunit IL-2R γ is internalized by a specific, actin dependent, Rac1/Pak1 regulated endocytosis route in the IL-2 context. We could show that pharmacological suppression of this endocytosis pathway also prevented IL-4 induced JAK/STAT signalling, placing endocytosis upstream of signalling.

Here I show using immuno-EM techniques that these endosomal structures are multivesicular bodies. Importantly, I could show that receptor subunits are highly enriched in the limiting membrane of these endosomes relative to the adjacent plasma membrane. Using quantitative loading assays I could furthermore demonstrate that this enrichment is achieved by constitutive internalization of receptors from the cell surface into cortical endosomes. The trafficking kinetics of the receptor subunits is independent of ligand occupancy. Pharmacological inhibition shows that receptors and ligand traffic via the previously identified Rac1/Pak1 pathway. Finally, Vav2 was identified as a candidate Guanine Exchange Factor (GEF) that may regulate Rac1 activity and thereby control the actin polymerization cascade driving IL-4R endocytosis. Immunoprecipitations showed that Vav2 interacts both with the cytoplasmic tail region of the receptors and the receptor associated

kinase JAK3. Vav2 may thus couple the receptor/JAK complexes to the Rac1/Pak1 mediated endocytosis route.

Taken together, our results suggests that stable ‘signalling endosomes’ adjacent to the plasma membrane act as enrichment centres, where ligand and receptor concentrations are locally increased by constitutive trafficking. The confined environment of the endosome then compensates for the weak affinities between the ligand and receptor and facilitates ligand-mediated receptor dimerization. Importantly, overexpression of both type II IL-4R subunits renders signal transduction resistant to endocytosis inhibition, strongly suggesting that the critical factor effecting signalling is sufficient concentration, which the endosomes facilitate achieving. The endosomes are thus dispensable as signalling scaffolds when the receptors are in sufficient concentration, where activated receptors could interact with downstream pathway components.

Endocytosis thus provides a crucial means for the signalling process to overcome the thermodynamic hurdles for receptor oligomerization. In conclusion, our data propose a novel, purely thermodynamic role of endosomes in regulating cytokine receptor signalling not seen in any other signalling pathway.

Chapter 1

Introduction

Cells must sense their environment and respond to stimuli in order to maintain homeostasis and to coordinate cellular events depending on their context. All cells have a plasma membrane as the first barrier to the extracellular milieu. Among the many mechanisms to sense the external signals, the most diverse are the ligand-based signal process. In this chemical-based signaling, a secreted compound - typically a small protein or peptide - binds to its specific trans-membrane receptor on the extra cellular side, thereby activating it. Therefore, the receptors at the plasma membrane are usually the first sensors of signals. However, “sensing” is a broad term and further in this thesis, a distinction between binding of receptors and subsequent activation will be made. When discussing the mechanistic basis of signal transduction, it is important that the subtle difference between binding and activation is kept in mind.

1.1 Signaling from plasma membrane

The occupation of receptors by ligand must be transduced across the plasma membrane. This happens mainly through two distinct mechanisms. The first mechanism is through a conformational change upon ligand binding, which affects protein interactions on the intracellular side. G protein coupled receptors (GPCRs) are a prime example of this [1]. The primary architecture of these receptors is seven transmembrane domains linked by extracellular and intracellular loops. Upon binding of a ligand, conformational changes allow

GPCRs to act as a guanine exchange factor (GEF) by bringing together the intracellular loops. This sets off an intracellular signal transduction cascade through the activation of heterotrimeric G-proteins, which often eventually results in transcriptional modulation. The GPCRs have a wide variety of ligands ranging from small molecules to large proteins [2]. Chief examples of GPCR activating molecules are neurotransmitters, pheromones, hormones etc.

The second mechanism involves receptor oligomerization upon binding to ligand. The general model is that the inactive receptor monomers are in equilibrium with the dimeric receptors in a way that the equilibrium greatly favors the monomeric forms. Upon binding of ligands, the equilibrium is shifted to “active” homo dimers or hetero dimers. This dimerization brings together active enzymatic molecules into close proximity, resulting in reactions which give rise to downstream signaling [3]. Using either of these general mechanisms, the signal sensed at the extracellular side is transmitted across the plasma membrane to the cytoplasm. The precise mechanism of how the oligomerization may be facilitated, or the equilibrium shifted upon ligand binding depends on many finer details of the system and may vary substantially. Cytokine receptor signaling [4, 5], which is the receptor system investigated in this thesis, belongs to the second group of receptors which depend on oligomerization to transmit the activation across the plasma membrane. The details of the oligomerization in this system are described later in this thesis.

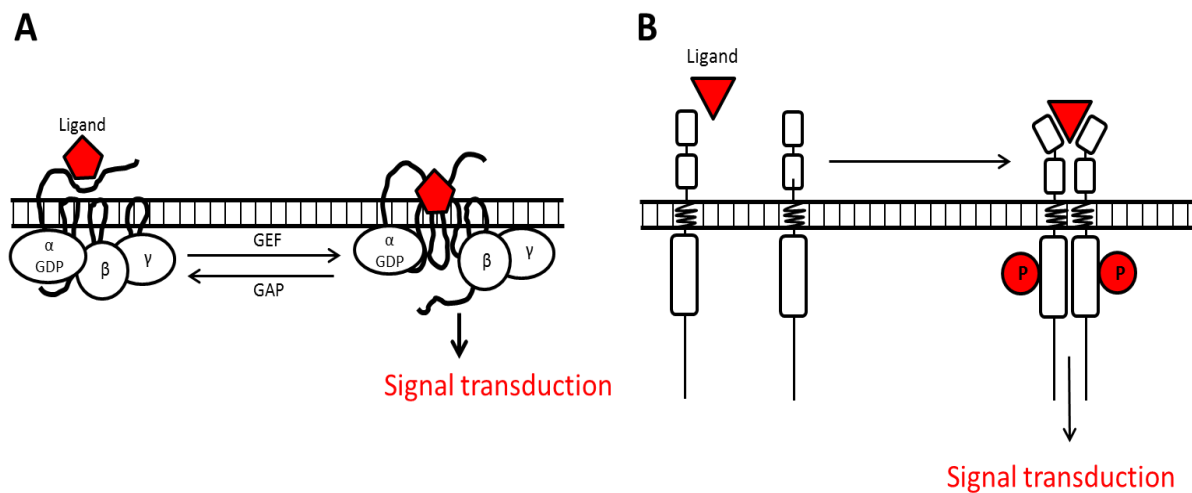


Figure 1.1: Signaling from the plasma membrane. (A) Ligand binding to GPCR triggers conformational changes in the receptor. These changes are translated into dissociation of associated signal transduction molecules (heterotrimeric G proteins) (B) Ligand binding to the receptor chain causes a recruitment of a second receptor. This brings the receptor subunit in close proximity, which allows cross-phosphorylation of tyrosine or serine/threonine residues kinases. This activity can either be provided by the receptor itself or by associated kinases. Phosphorylation typically provides docking sites for downstream signaling molecules.

1.2 Receptor endocytosis

It was also observed that, upon activation, many receptors enter the endosomal trafficking system [6]. The endosomal system is a dynamic system of internalization of membrane compartments, which undergo membrane remodeling and extensive directed transport. The typical cascade of events that follow any endocytosis is trafficking and fusion of the endocytic carriers to early endosomes and their subsequent maturation into recycling endosomes, late endosomes, and lysosomes, as represented in Figure 1.2. These compartments are distinct in their lipid and protein composition. This facilitates recruitment of specific proteins to them. All these intracellular compartments are highly dynamic and exchange cargo and lipids with other membrane compartments. Each endosomal compartment is also characterized by a particular set of associated Rab GTPases which serve to recruit additional molecules that provide its specific, cell biological functions [7].

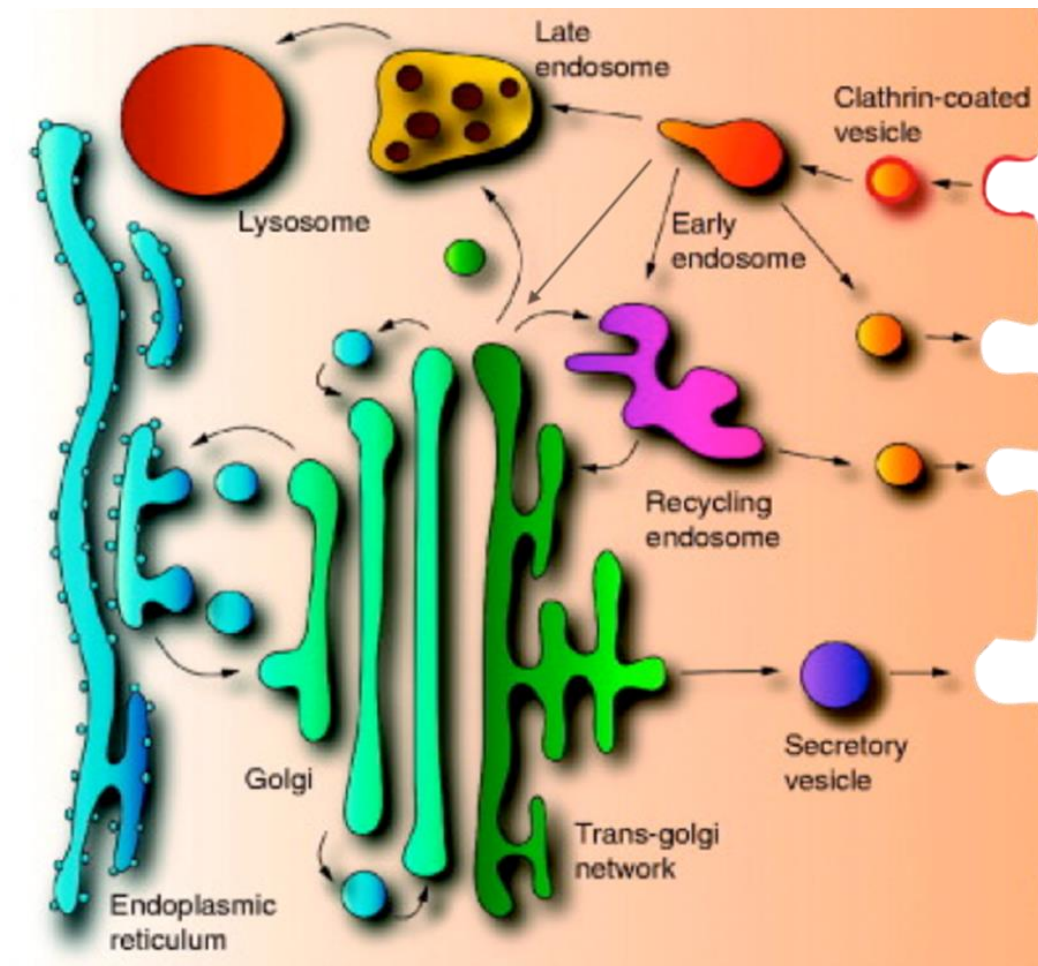


Figure 1.2: Membrane compartments in Trafficking. Cargo is internalized at the plasma membrane by different pathways. Endocytosed cargo proteins are sorted in early endosomes, which may recycle back to the plasma membrane or are targeted to late endosomes and lysosomes. Late endosomes are characterized by the presence of intra-luminal vesicles and are known as multivesicular bodies. Cargo molecules may also undergo retrograde transport from early endosomes to reach the endoplasmic reticulum via the Golgi. Modified from [8]

1.3 Signaling and endocytosis

The process of receptor endocytosis was classically thought to be only meant for clearing the activated receptor population from the plasma membrane to attenuate signaling [9]. Accordingly, receptor endocytosis was generally thought to be triggered by pathway activation. However, this view has been evolving with findings that in many cases, endocytosis of receptors and signaling may be tightly coupled and internalized membrane compartments may be sites of signaling [9, 10]. This is not surprising as the receptors have to be expressed at the plasma membrane to sense extracellular cues, and the signaling molecules must be carried to the intracellular milieu. Therefore, it is foreseeable that the membrane trafficking and signaling components interact strongly to manifest signaling events.

Ligand-induced endocytosis is typical of signaling receptors like receptor tyrosine kinases (RTKs) [11-14]. In the case of RTKs, one of the important roles of endocytosis is to remove activated receptors from the plasma membrane and funnel them towards degradation. This particular pathway leading to degradation achieves a negative-feedback loop resulting in inhibition of signaling and modulates the response of the cell to an external signal. The pathway of endosomal maturation leading to degradation involves the formation of multi vesicular bodies (MVBs) which are characterized by the presence of intra-luminal vesicles. The formation of the MVBs depends on the Endosomal Sorting Complex Required for Transport (ESCRT) machinery [15, 16]. Internalization of vesicles into the MVB lumen cut off any cargo that is associated with the vesicles from the cytoplasm of the cell. However, receptor endocytosis does not necessarily turn off the signaling process initiated by the ligand binding. Internalized receptors rather continue or in many cases begin active signaling after activation from the surface of the endosomes. This link between endocytosis and signaling has been established to be biologically significant for at least some pathways. Internalized receptors in the endosomes can give rise to spatial and temporal differentiation of signaling as has been exemplified by some specific receptor systems like Nerve Growth Factors (NGF) [17], Epidermal growth factor (EGF) [18] and transforming growth factor-beta (TGF β) [19].

1.4 Spatio-temporal regulation of signaling through endosomes

An extreme case of role of endocytosis in spatial regulation is demonstrated by studies on NGF [20]. Growth factors released from tissues, which bind to the NGF receptor TrkA, a member of the RTK family, must carry out signaling events sustainable across the long distance from the axon of a neuron to the cell soma. This is facilitated by the internalization of activated TrkA receptors into ‘signaling endosomes’, which are actively transported from the axon to the soma through the retrograde pathway [21]. This results in the signaling components being present at an effective proximity to carry out robust and sustained signaling, even if the receptors sensed the ligands at an otherwise ineffective distance.

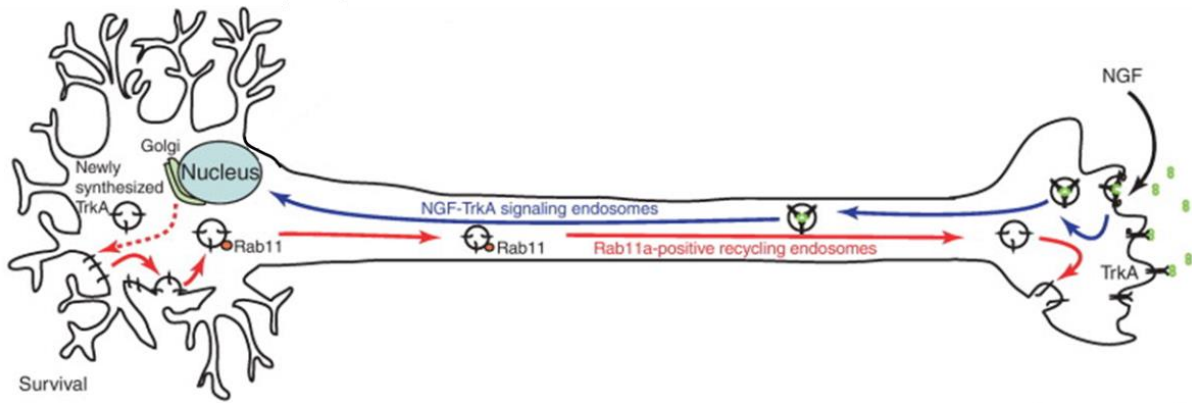


Figure 1.3: Spatial regulation in signaling through endosomes. NGF binds to its receptor TrkA at the axonal growth cones, far away from the cell soma. Diffusion kinetics will be too slow to allow signaling molecules to reach the cell soma resulting in a response. The activated receptors are instead internalized into endosomes, which are actively transported through the axon back to the cell soma, thus overcoming the long distance resulting in effective signaling. The receptors are also replenished in the axon through active forward transport of Rab11 positive recycling endosomes Modified from [22]

Temporal regulation by endosomes is chiefly achieved by tuning of the kinetics of the events leading to internalization and further recruitment of downstream proteins. Different members of the GPCR family differ in their kinetics of internalization upon activation by agonists. In general, activation results in phosphorylation of GPCRs and binding to β -arrestins, resulting in clathrin dependent receptor internalization. β -arrestins provide a scaffolding function for intracellular assembly of further downstream signaling complexes, which includes the Mitogen-activated protein kinases (MAPK) and c-Jun N-terminal kinase 3 (JNK3) pathways. Dissociation of β -arrestins results in recycling via Rab4 and Rab11 dependent mechanisms or degradation in lysosomes. The kinetics of different GPCRs is controlled by the affinity of β -arrestins for different GPCRs and this leads to differential lifetimes of the receptors in the endosomes. This results in different degrees of signaling by different GPCRs from endosomes [23-25].

EGFR signaling provides an example of how subcellular spatial sorting through endocytosis leads to coordinate temporal regulation of the signaling output [26]. EGF receptors signal through phosphatidylinositide 3-kinases (PI3K) from the plasma membrane and via the MAPK pathway from early and late endosomes. Receptors are activated upon ligand binding at the plasma membrane. Activated receptors at the plasma membrane signal through PI3K pathway, but this signal is abrogated following receptor internalization [27, 28]. Instead, binding of the scaffold protein MP1-p14 to the receptor, which only happens at the endosome, and then drives extracellular signal-regulated kinases (ERK) mediated signaling. Thus, activation of the EGFR gives rise to a temporally coordinated sequence of signaling events.

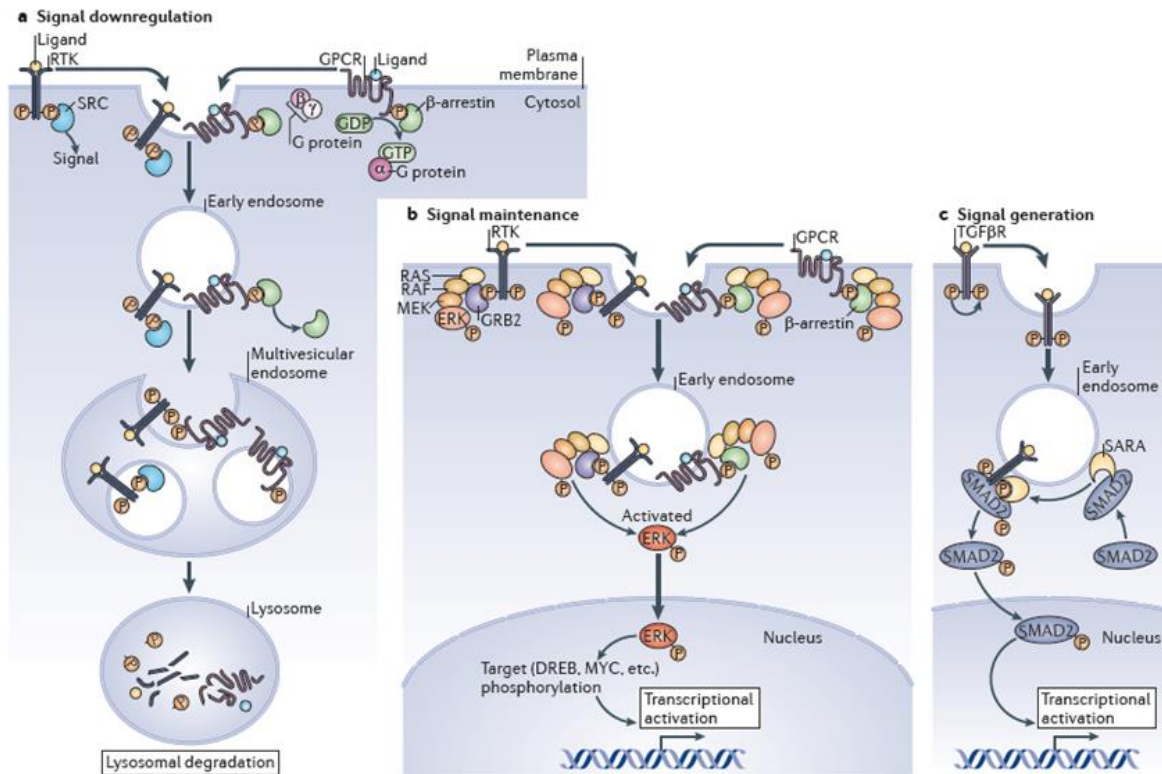


Figure 1.4: Endosomes and signaling. (A) Downregulation of signals through the degradation of receptor complexes. Receptors trafficked to multilamellar endosomes fuse with lysosomes, where receptors are degraded. (B) Receptor Tyrosine kinases (RTKs) and GPCR are an example of downstream signaling being maintained by early endosomes. (C) Downstream signaling of transforming growth factor- β -receptors (TGF β R) is only generated on endosomes. The endosomal protein SMAD anchor for receptor activation (SARA) brings the activated receptor and the SMAD transcription factor into contact which results in downstream signaling. Modified from [29].

While EGFR signaling at least partially occurs from the membrane, in the case of TGF β , the activation by ligands takes place at the plasma membrane, but signaling takes place only after receptor internalization. The activated TGF β receptor localizes into Rab5-positive early endosomes. On these endosomes, SMAD anchor for receptor activation (SARA) is also recruited. Coordination of SARA and TGF β is necessary to phosphorylate SMAD2 and achieve propagation of signal [30, 31]. This exemplifies the role of endosomes in proper signaling where the endosome, by virtue of its specific recruitment of different components, bring together a functional unit to result in active signaling, even if the receptor activation took place in the plasma membrane.

Various other studies also highlight the significance of endocytosis in a range of critical processes of biological systems. Examples can be found in establishment of morphogen gradient [32], EGFR, symmetric distribution of signaling components following cell division [33] etc. Therefore, it appears that endocytosis has not only evolved as a mechanism of receptor clearance, but has strongly co-evolved with various signaling mechanisms to fulfill certain functional requirements.

1.5 Pathways of receptor endocytosis

Many of the receptor uptake pathways known so far are ligand-triggered, Clathrin-dependent pathways. Typically, in this pathway, receptor phosphorylation leads to recruitment of ubiquitin ligases [34]. Ubiquitination of receptor triggers recruitment of clathrin adaptors and then endocytosis via Clathrin-coated pits. However, receptors are also internalized by other mechanisms. Many receptors including GPCRs, RTKs, WNT, NOTCH, and TGF β R can take multiple portals of entry into the cell [10]. For example in EGFR and TGF β R signaling, internalization of receptors via Caveolin-mediated pathway leads to their degradation thus, limiting signaling. However, there are several other pathways that are not marked by the presence of coat proteins, for example GPI-AP-enriched early endosomal compartments (GEECs) and Clathrin independent carriers (CLICs) [35]. A second mode of coat independent mechanisms seems to be utilizing the actin cortex and its regulatory proteins. In these pathways, the actin machinery is required for providing structural support for trafficking intermediates as well to generate forces for membrane deformation. Regulation of actin in most of the processes in the cell occurs through a large number of signaling cascades. This involves the members of the Rho family of small GTPases- rhoA, cdc42 and rac1 and their activators (GEFs), as well as their protein kinase effectors [36]. These molecules may directly interact with actin or regulate it through other actin nucleating/branching proteins. In general, they act as coupling factors that converge to regulate the dynamics and organization of the actin cytoskeleton and have been implicated in regulation of endocytosis by coupling cargo proteins to cytoskeletal changes and signaling events.

1.6 Endocytosis in cytokine signaling

Cytokines are ligands belonging to a diverse group of soluble proteins and peptides, which act as signaling molecules with functions in immunomodulation. These immunomodulating agents generally refer to interleukins and interferons. Interleukins are produced by a wide variety of cells. The receptors for these ligands fall under the cytokine receptor family [5]. The principle behind their transmembrane signaling is generally thought to be ligand induced oligomerization.

A unique type of signaling pathway that is clathrin independent has been reported for certain cytokine receptors. Previous studies have established that IL-2R, the first interleukin receptor to be characterized in this respect, internalizes through a clathrin independent mechanism [37-41].

The internalization in this case occurs through a Rac1/Pak1-mediated pathway and is also thought to involve ordered domain forming lipid components (“rafts”) [39]. This pathway is a general actin polymerization regulatory pathway utilized for a broad range of processes. Internalization of cytokine receptor was thought to terminate signaling [42-45]. However, this is contradicted by studies describing positive effects of endocytosis on signaling. For

example, in IL-7R and in *Drosophila* Domeless receptors, endocytosis is implicated in cytokine receptor activation [44, 46]. But the mechanistic link between endocytosis and signaling components is unknown.

Using the IL-4 receptor system, our labs have characterized the oligomerization dynamics of the receptors *in vivo* ([47] and unpublished data). It was observed that the expression of the receptor components resulted in localization of the receptors into endosome like structures, suggesting that they undergo endocytosis, as has been previously reported for IL-2R and IL-7R systems. Furthermore, measurements of the dissociation constants using fluorescence correlation spectroscopy revealed that the lateral affinities between subunits were very low, such that receptor complexes would not be detectable without overexpression to higher concentrations. Therefore, the receptor complex formation resulting in active signaling may be thermodynamically unfavorable due to insufficient concentrations of the receptors at physiological conditions.

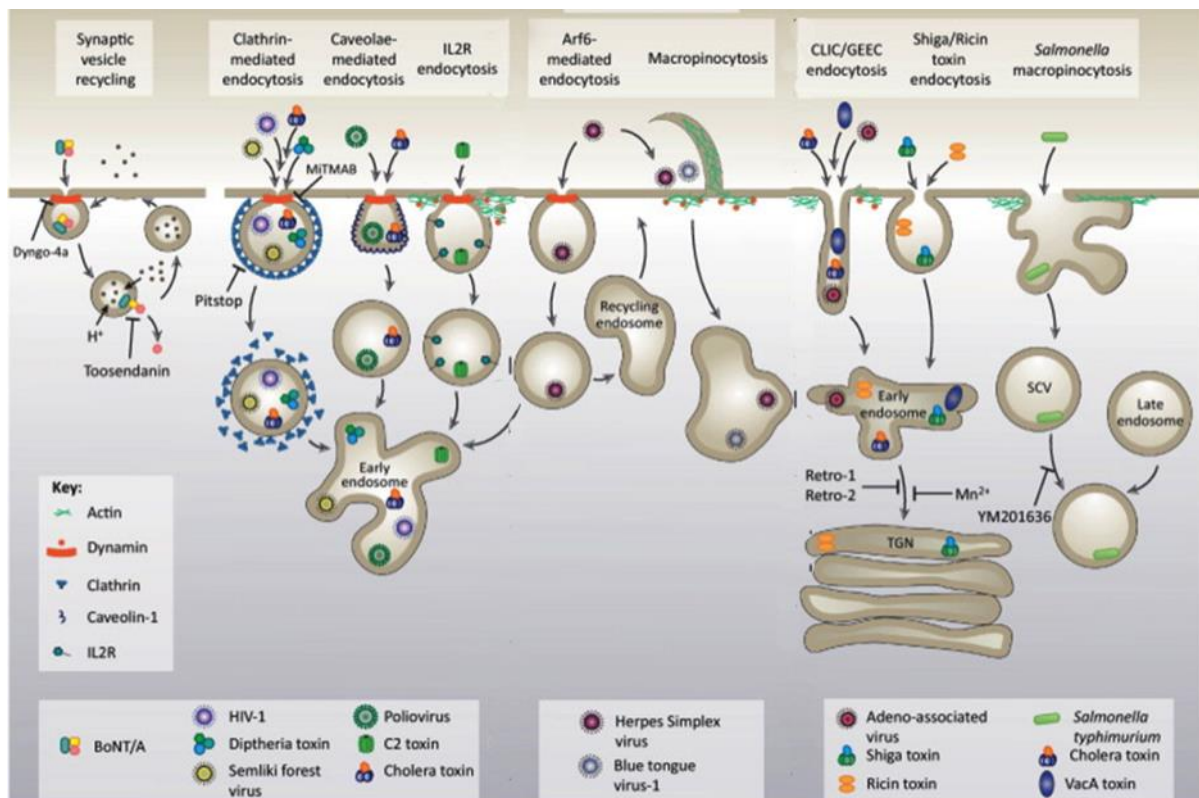


Figure 1.5: Major endocytic pathways with focus on clathrin-independent pathways and their cargoes. Apart from the canonical clathrin mediated pathway many pathways are dependent on actin machinery. These pathways are characterized by specific cargo proteins that use them for their internalization. For e.g. RTKs are known to be internalized by clathrin mediated endocytosis, whereas cholera toxin is a marker for CLIC/GEEK pathway. IL-2R is known to be internalized by a clathrin independent, actin mediated pathway. Figure modified from [48].

The Rac1/Pak pathway has been implicated in endocytosis of IL-2R [41]. Therefore, our working hypothesis was that IL-4R was also internalized via Rac1/Pak mediated pathway. Previous work in the lab had also shown that signaling by IL-4R was dependent on Rac1/Pak pathway activating actin polymerization machinery, suggesting a positive role of internalization of receptors into endosomes in active signaling, given that inhibition of Rac1/Pak also blocks endocytosis.

The three major facts observed in the lab – consistent observation of receptor components in endosomes, low affinity of the receptors, and requirement of internalization for active signaling suggests that endosomes play a very significant role in signaling.

Therefore, the work in this thesis is aimed at understanding the role of endosomes in IL-4 receptor signaling mainly at two complementary levels: ultrastructural and molecular characterization of the signalling endosomes and the dynamics of receptor trafficking. Based on the previous observations, we hypothesized IL-4R systems use endosomes to fulfill a function relating low affinity of the receptors and formation of active complexes. Since both endosome formation and signaling are highly dynamic processes, I seek to employ a range of static and dynamic analyses to elucidate their interplay. Further, I aim to confirm the role of Rac1/Pak-mediated actin regulation in the endocytic pathway used by IL-4R. This pathway is known to be involved in lamellipodia and filopodia formation as well and it is not yet clear how general actin polymerization machinery could be coupled to the internalization of a specific receptor system. I address this question by using a candidate-based approach to find the specific molecular link between actin modulation and IL-4R internalization. Thus, the aims of this study can be summarized as follows:

- **Aim1: What is the molecular nature of the compartments containing cytokine receptors? How are they organized at the morphological and ultra-structural level?**
- **Aim2: What are the dynamics of receptor trafficking between the plasma membrane and the internalized compartments? Are they dependent on ligand activation or are internalized constitutively? What functionality do they serve?**
- **Aim3: What molecules regulate the process of receptor internalization at the plasma membrane? What links the receptors to the actin polymerization machinery?**

To achieve these aims I used a variety of cell biological, biophysical, biochemical, and imaging approaches.

In **Chapter 3**, I will describe the cytokine system and characterization of the endosomes at molecular and ultrastructural level using immunocytochemistry and electron microscopy.

Chapter 4 focuses on a biophysical analysis of interleukin receptor endocytosis to quantify trafficking kinetics using live cell imaging.

Chapter 5 focuses on the identification of the upstream regulator molecule that links IL-4R subunits to the actin dependent endocytic machinery using biochemistry and a candidate-based approach.

Chapter 2

Materials and methods

2.1 Materials

All chemicals, unless otherwise mentioned, were purchased from Roth or Sigma. All restriction enzymes were purchased from New England Biolabs (NEB) or Fermentas. The manufacturer of other reagents is indicated in the respective section.

2.1.1 Constructs

pJAK3-TagRFP was created from pJAK3-eGFP by removing the eGFP sequence via AgeI/NotI, followed by insertion of TagRFP. pNHIS-IL-2R γ -N2 plasmid was derived from pNHIS-IL-2R γ -eGFP-N2 by NotI/SmaI digest followed by Klenow fill-in and re-ligation. pCMV-STAT6 was generated by replacing the eGFP ORF in pEGFP-N1 with the ORF of human STAT6 excised from the Flexi clone F1KB4980 (Kazusa DNA Res. Inst., Kisarazu, Japan.). pCMV-Vav2 was generated by replacing the ORF in pEGFP-stat6-C1 with the ORF of human Vav2 excised from the Flexi clone F1KB4980 (Kazusa DNA Res. Inst., Kisarazu, Japan.). Truncated mutants of IL-2R γ – Δ 25 to Δ 40 were a kind gift from Dr. Sigrun Hofmann (Department of Pediatrics, University Hospital Carl Gustav Carus).

For all PCR amplification, native Pfu polymerase was used. PCR products were cloned in pJet vector. For digestion all the enzymes were used from New England Biolabs. For ligation, Fast link DNA ligation kit from EPICENTRE Biotechnologies was used. Mutagenesis was

achieved by QuickChange lightning single or multi mutagenesis kits (Agilent Technologies). New clones were evaluated by restriction digestion. Clones were sequenced at MPI-CBG DNA sequencing facility.

2.1.2 Cloning strategy

Plasmid	Template for PCR	Forward primer	Reverse primer	PJet clone	Insert digested with enzymes		Vector digested with	
					Insert	Enzyme	Vector	Enzyme
pCMV Vav2-Nterm-HA	pCMV-Vav2	cmv_fwd	linker rev SpeI	pJet Nterm	pJet Nterm	NotI/SpeI	pCMV-Vav2	NotI/RsrII
							pCMV-Jak3-1xFK	SpeI/RsrII
pCMV-Vav2 ΔSH2SH3-HA	pCMV-Vav2	cmv_fwd	SH3_1 rev SpeI	pJet ΔSH2SH3-HA	pJet ΔSH2SH3	NotI/SpeI	pCMV-Vav2	NotI/RsrII
							pCMV-Jak3-1xFK	SpeI/RsrII
pmRFP-Vav2SH3a-HA	NO PCR	NA	NA	NA	pCMV Vav2-SH3a-HA	NotI+kleno w/SpeI	pmRFP-Vav2SH323-HA	BglII+kleno w/SpeI
pmRFP-Vav2SH3b-HA	NO PCR	NA	NA	NA	NA	NA	pmRFP-Vav2SH323-HA religation	Scal
pmRFP-Vav2SH2-HA	NO PCR	NA	NA	NA	pCMV Vav2-SH2a-HA	NotI+kleno w/SpeI	pmRFP-Vav2SH323-HA	BglII+kleno w/SpeI
pmRFP-HA	NO PCR	NA	NA	NA	NA	NA	pmRFP-Vav2SH323-HA religation	Scal/SpeI+kleno w
pSig-eGFP_IL2Rcg_Δ50-Δ80	pSigEGFP_hIL2Rcg_Flag	IL2Rcg-seqF1	50-80 rev	pJet IL2Rshort	pJet IL2Rshort	BstXI/XhoI	pSigEGFP_hIL2Rcg_Flag	BstXI/XhoI
pC2_IL2R_eGFP_Δ50-Δ80	pSigEGFP_hIL2Rcg_Flag	IL2Rcg-seqF1	50-80 rev	pJet IL2Rshort	pJet IL2Rshort	BamHI/XhoI	pC2-IL2Rg-EGFP	BamHI/BstXI
pcs2+2x mem-cg-cyt-GFP	pNhis_IL2Rcg_EGFP	GFP rev BglII	cg cyt fwd BspEI	pJetcg-cyt-GFP	pJetcg-cyt-GFP	BspEI/ BglII	pCS2+mem Cerulean	AgeI/BglII

2.1.3 Primer sequence

50_rev	TGGATCCGCCTCGAGCTCACTGACGAG GC
60_rev	TGGATCCGCCTCGAGCTCCCAAG
70_rev	TGGATCCGCCTCGAGATGCTGGTTGCA
80_rev	TGGATCCGCCTCGAGGGTGTAACATGG
FW2 (Y172D)	GACGACATCGACGAGGACATC
RW2	GATGTCCTCGTCGATGTCGTC
FW3 (Y142D)	CGATGACGTCGACCGCAGCC
RW3	GGCTGCGGTCGACGTCATCG
FW4 (Y159D)	GGGGAGGACATCGACGACTGC
RW4	GCAGTCGTCGATGTCCTCCCC
IL-2R_seq_F1	TCCCAGAGGTTTCAGTGTTTTGTGT
SH3_1 rev SpeI	ACTAGTAGGGCAGGGCTTCAC
CMV fwd	ATGGGAGTTTGTGTTTGGCAC
GFP rev BglII	AGATCTTTACTTGTACAGCTCGTC
cg cyt fwd BspEI	TTTCCGGATAACCTAGAGGATCTTGTT
Linker rev SpeI	ACTAGTG CAGTTCCTCTTGTC
Vav2-Y174D FW	GACGACATCGACGAGGACATC
Vav2-Y174D RW	GATGTCCTCGTCGATGTCGTC
Vav2-Y142D FW	CGATGACGTCGACCGCAGCC
Vav2-Y142D RW	GGCTGCGGTCGACGTCATCG
Vav2-Y160D FW	GGGGAGGACATCGACGACTGC
Vav2-Y160D RW	GCAGTCGTCGATGTCCTCCCC

2.1.4 esiRNA sequence

Vav2 (EHU058751)	CCCGAGATATGAGGGAGCTTTCGCTGCGGGAGGGTGACGTGGT GAGGATCTACAGCCGCATCGGCGGAGACCAGGGCTGGTGGAAAG GGCGAGACCAACGGACGGATTGGCTGGTTTCCTTCAACGTACG TAGAAGAGGAGGGCATCCAGTGACGGCAGGAACGTGGACAAG ACTCGCAGATTTTCTTGGGAGAGTCACTCCAGCCCTGAAGTCTG TCTCTAGCTCCTCTGTGACTCAGAGGGGAAATACCAACCT
RULC (esiRNA1)	GATAACTGGTCCGCAGTGGTGGGCCAGATGTAAACAAATGAAT GTTCTTGATTCATTTATTAATTATTATGATTCAGAAAAACATGC AGAAAATGCTGTTATTTTTTTACATGGTAACGCGGCCTCTTCTT ATTTATGGCGACATGTTGTGCCACATATTGAGCCAGTAGCGCGG TGTATTATACCAGACCTTATTGGTATGGGCAAATCAGGCAAATC TGGTAATGGTTCTTATAGGTTACTTGATCATTACAAATATCTTA CTGCATGGTTTGAACCTCTTAATTTACCAAAGAAGATCATTTTT GTCGGCCATGATTGGGGTGCTTGTGTTGGCATTTCATTATAGCTA TGAGCATCAAGATAAGATCAAAGCAATAGTTCACGCTGAAAGT GTAGTAGATGTGATTGAATCATGGGATGAATGG

2.1.5 Antibodies

Antibody	Experiment	Dilution	Species	Primary/Secondary	Company
Anti- eGFP	WB	1:4000	Rabbit	Primary	Clonetech 632460
Anti- HA	WB	1:2000	Mouse	Primary	Cell signaling 2367S
Anti- GAPDH	WB	1:4000	Mouse	Primary	Abcam Ab8245
Anti- Stat6	WB	1:2000	Rabbit	Primary	Santacruz Sc-136019
Anti-pStat6	WB	1:4000	Mouse	Primary	Santacruz Sc-11762
Anti-VAV2	WB	1:2000	Rabbit	Primary	Abcam Ab52640
Anti- pVAV2	WB/ICC	1:1000/1:400	Rabbit	Primary	Santacruz Sc-16409
Anti-Rabbit	WB	1:4000	Donkey	Secondary	GE Healthcare NA9340
Anti-Mouse	WB	1:4000	Goat	Secondary	Sigma A8924
Anti-Vav3	WB	1:2000	Rabbit	Primary	ab52938
Anti-EEA1	ICC	1:400	Mouse	Primary	BD bioscience BD610456
Anti-HGS	ICC	1:400	Rabbit	Primary	Gene tex GTX101718
Anti-mouse	ICC	1:1000	Goat	Secondary	Invitrogen
Anti-Mouse	ICC	1:1000	Goat	Secondary	Invitrogen

WB: Western Blot, ICC: Immunocytochemistry

2.1.6 Solutions and media:

Solution and media	Composition
PEM	80mM PIPES, 5mM EGTA, 1mM MgCl ₂ , pH 7.4
Semi dry buffer	200ml MeOH, 0.37g SDS, 5.81g TRIS, 2.39g Glycin, add H ₂ O up to 1 liter
PBS	1.7mM KH ₂ PO ₄ , 5.2mM Na ₂ HPO ₄ , 150mM NaCl
PBST	PBS, 0.05% Tween
5% milk	5% (w/v) powdered, non-fat, dry milk in PBST
Air buffer	150mM NaCl, 20mM HEPES pH 7.4, 15mM Glucose, 46mM Trehalose, 5.4mM KCl, 0.85mM MgSO ₄ , 1.7mM CaCl ₂ , 0.15mg/ml bovine serum albumin

10X SDS buffer	10g SDS (0.1% w/v) , 30g TRIS (25mM) , 144g Glycin (192mM) for 1 L H ₂ O
25% PFA	25 % (w/v) Paraformaldehyde solution in PEM
PEMT	PEM + 0.2% Tween
Blocking buffer	PEM + 0.2% tween + 0.5% BSA

2.2 Methods

2.2.1 Cell culture and maintenance

HEK293 cells were kept as adherent culture in DMEM medium (Invitrogen/Gibco) supplemented with 10% FCS (Fetal calf serum). They were cultured with 5% CO₂ at 37°C. Cells were passaged by trypsination. Cells were washed 1X with PBS and incubated for 2 min at 37°C with trypsin. Trypsin was inactivated by the growth medium and removed by centrifugation. Cells were resuspended in DMEM medium and seeded in 3X10⁴ /ml in 25cm flask. Cells were passaged every third day.

2.2.2 Cell seeding and transfection

Transfection was done with a traditional protocol. Cells were seeded 24 hours before transfection so that they are 40% confluent on the next day. Cells were transfected with Turbofect (Life Technologies) using a DNA:Turbofect ratio of 100ng:0.3µl. For imaging purposes, 24 hours post transfection cells were washed twice with air buffer or media without phenol red to avoid the auto-fluorescence from Phenol red.

For esiRNA transfection, cells were seeded before 24hr so that cells are 20% confluent on next day. Next day cells are transfected with esiRNA:lipoRNAiMAX (Life Technologies) ratio of 100ng:0.2µl. After 48 hours, cells are transfected again with esiRNA and DNA mix together. Cells were lysed 24 hours later and analyzed by western blot.

For immunostaining, FRAP and imaging experiments, 8-well Lab-tek chambers (Nunc) were used. For pull down assays, 6-well plates were used. For esiRNA experiments, 12-well plates were used.

2.2.3 Cell fixation and immunostaining

24 hour post transfection cells were washed twice with PEM and fixed with 4% PFA/PEM for 10 min, followed by 4% PFA/PEMT for 10min. Cells were washed 3X10min with PEMT. Cells were incubated with NH₄Cl for 15 min and washed 2X10min with PEMT. Blocking was done for 30min at room temperature in blocking buffer. Cells were incubated with

primary antibody diluted in blocking buffer at 4°C overnight. Next day, cells were washed 3X20min PEMT. Secondary antibody staining was done for 1 hr at room temperature followed by subsequent washing step with PEMT for 3X10min and PEM for 1X10min. Cells were imaged directly in PEM or embedded in Mowiol overnight and imaged next day.

2.2.4 Cell lysis

After 24 hours post transfection, cells were washed with PBS and lysed by Lysis buffer. Phosphatase inhibitors cocktail² and cocktail³ (Sigma-Aldrich) and protease inhibitor (Roche, Complete EDTA free) were added to the lysis buffer. Cells were kept on ice with mixing in between for 30min followed by 10min centrifugation at 10,000g 4°C to sediment the cell debris. Supernatant was taken in to a fresh tube and either processed for pull down assay or analyzed by western blot.

2.2.5 Pull down

μ MACS epitope tag protein isolation kit was used according to manufacturer's instruction. After cell lysis 50 μ l anti-eGFP/HA tag micro beads were added to the cell lysate supernatant and incubated for 30min on ice with shaking in between. Cell lysate was applied to pre-equilibrated μ columns placed in a strong magnetic field. Column was rinsed with wash buffers and samples were eluted with 50 μ l elution buffer. Samples were analyzed by western blot.

2.2.6 Western blot

For the separation of proteins 10% or 12% or "anyKd" SDS polyacrylamide *BioRAD* gels were used.

The lysates were boiled with 5x SDS sample buffer for 10 minutes at 95°C before they were loaded on the SDS-PAGE gel. The gels were run in 1x SDS running buffer with 120 V and 300 mA for 20 min to stack the band. Subsequently, the voltage was increased to 160 V. The Precision Plus ProteinTM standard was purchased from BIO-RAD.

For the immune-detection of the separated proteins, the proteins were transferred by western blotting using the *Biometra Semi dry blotter*. The cellulose blotting paper (VWR) and nitrocellulose membrane (Protran, 0.45 μ m pore size) was first soaked in blotting/transfer buffer for several minutes. These components were stacked air bubble free on the blotting cassette in the following order: lower side of the cassette (anode), cellulose paper, nitrocellulose membrane, gel, cellulose paper, upper side of the cassette (cathode). Proteins transferred for 1.5hrs at constant 45mA and maximum Volt. After blotting, the membrane

was blocked with 5% milk for 1 hour at room temperature. Then, the membrane was incubated with the primary antibody in 5% milk in 50 ml falcon tube for 1hr at room temperature or overnight at 4°C. The membrane was washed 4X5min with PBST before incubation with the secondary HRP-coupled antibodies in 5% milk for 1hr at room temperature. Again, the membrane was washed 4x10 min with PBST followed by 2X10min PBS to remove tween. The bioluminescence was detected with the LAS-3000 luminescent image analyzer (Fujifilm) using the ECL™ Western Blotting Analysis System (GE Healthcare). All washing and incubation steps were performed on a tumbler.

2.2.7 IL-4 labeling

For biotinylation- EZ-Link Sulfo-NHS-Biotinylation Kit (Thermo scientific, # 21425) was used. 20nM of IL-4 was suspended in 500µl of BIC buffer. As per instructions, Biotin was dissolved in DMSO. Biotin-DMSO was added to the IL-4 having final concentration of 400nM. IL-4-Biotin solution was incubated overnight at 4°C. Next day, buffer exchange was carried out to replace BIC with PBS using Nap5 column (GE Healthcare). Fractions were aliquoted in Eppendorf tubes containing 1% BSA. Fractions were analyzed by silver staining.

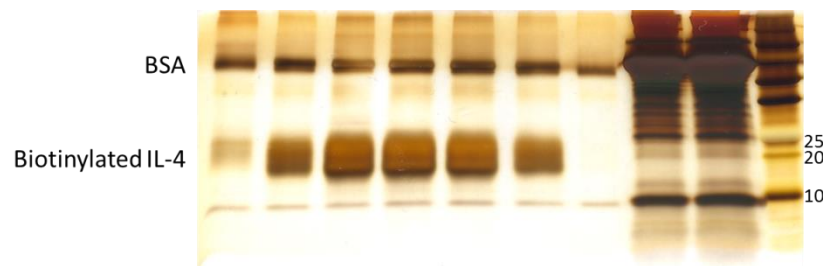


Figure 2.1: Silver stained polyacrylamide gel of Biotinylated IL-4. Analysis of purified fractions after biotinylation. BSA was also added to the sample to prevent adsorption to eppendorf surfaces.

2.2.8 Immunogold labeling and electron microscopy

Cells expressing JAK3-GFP were fixed with 4% paraformaldehyde (PFA) in 0.1 M phosphate buffer (PB, pH 7.4) and processed for Tokuyasu cryo-sectioning as described [49, 50]. Briefly, the cells were washed several times in PB, infiltrated stepwise into 10% gelatin and cooled down on ice. Small blocks (0.5 x 0.5 mm) were cut on ice, incubated in 2.3 M sucrose/water for 24hrs at 4°C, mounted on Pins (Leica # 16701950) and plunge frozen in liquid nitrogen. 70 nm sections were cut on a Leica UC6+FC6 cryo-ultramicrotome and picked up in methyl cellulose/sucrose (1 part 2% methyl cellulose (MC), Sigma M-6385, 25 centipoises + 1 part 2.3M sucrose). For immunogold labelling, the grids were placed upside down on drops of PBS in a 37°C incubator for 20 min, washed with 0.1% glycine/PBS

(5x1min), blocked with 1% BSA/PBS (2x5min) and incubated with primary antibodies for 1hr (anti-GFP: TP 401, Torrey Pines, 1:100). After washes in PBS (4x2min), the sections were incubated with Protein A conjugated to 10 nm gold for 1hr, washed in PBS (3x5sec, 4x2min) and postfixed in 1% glutaraldehyde (5min). Sections were washed with distilled water (10x1min), stained with neutral uranyl oxalate (2% uranyl acetate (UA) in 0.15M oxalic acid, pH7.0) for 5min, washed shortly in water and incubated in MC containing 0.4% UA for 5 min. Finally, grids are looped out; the MC/UA film is reduced to an even thin film and air dried. Alternatively, the primary anti-GFP is detected with secondary antibodies coupled to ultrasmall gold (Aurion, ~ 1nm) followed by silver enhancement using the R-Gent SE/Kit (Aurion) before contrasting and embedding of the sections in MC/UA. Labelled sections are analysed on a Philips Morgagni 268 (FEI) at 80 kV and images were taken with the MegaView III digital camera (Olympus).

2.2.9 Pulse chase experiment and drug inhibition

A similar protocol was used for all pulse chase experiments, unless otherwise specified. 24hr post transfection, cells were kept on ice for 20min to cool down. The cells were then incubated with either 20ng/ml ligand IL-4 or 150nm A647 dye for another 20 min. Cells were washed 2 times with media to remove unbound ligand or dye and transferred onto a pre-warmed metal block inside a 37°C incubator to initiate endocytosis. For inhibitor treatment, cells were incubated with inhibitors 50µM EHT-1864 and/or 10µM IPA3 for 10min before shifting them on ice, followed by same procedure as mentioned above in the presence of drug. Cells were either lysed after different time points and analyzed by western blot or fixed and imaged.

For STAT6 kinetics assay, cells were transfected with 300ng pCMV-STAT6. For IL-4 ligand tracking experiment, cells were co-transfected with JAK3-eGFP (100ng), IL-2R γ (100ng) and IL-4R α (100ng).

2.2.10 Loading Assay

Cells were seeded sub-confluency in an 8-well chambered Lab-tek slide (Nunc) and co-transfected with a DNA master mix. For IL-2R γ kinetics, I transfected pNhis-IL-2R γ -N2 (80ng), pJAK3-eGFP (50ng) and pIL-4R α -N1 (40ng). For IL-4R α kinetics, cells were transfected with pIL-2R γ -N1, pJAK3-eGFP and pNhis-IL-4R α -N1 at equivalent concentrations in the absence or presence of 20ng/ml IL-4 (Life Technologies). The specificity of trisNTA-A647 binding was checked using receptors in which neither receptor subunit carried the His-tag.

24 hours post-transfection, cells were washed twice with air buffer and kept at 4°C for 20min. After 20min, cells were incubated with 150nM trisNTA-A647 in air buffer for 20min on ice

to facilitate binding of dye to the His-tagged receptors. Cells were washed twice to remove unbound dye and transferred onto a pre-warmed metal block inside a 37°C incubator to initiate endocytosis. After different time points, cells were fixed with 4% PFA/PEM. For the drug inhibitor treatment, the whole procedure was done in the presence of 50 μ M EHT-1864 with pre-incubation at 37°C for 10 min.

Confocal imaging was performed on a LSM780 (Carl Zeiss, Jena, Germany) using avalanche photo diode detectors (APD). 16-bit images were recorded with a 40x, NA 1.2 water immersion objective, using a 75 μ m pinhole at a pixel dwell time of 50 μ s. eGFP emission was collected between 505-610nm, for A647 we used a 655nm long pass filter. Laser powers for both channels were adjusted such that the emission intensity did not exceed 1MHz. Each cell was imaged in three different planes (top, middle, and bottom) separated by 1.5 μ m. For image analysis, we manually selected the endosomes in the eGFP channel. A MATLAB script then identified the maximum intensity and extracted the total counts of a centred 3x3 pixel bin (Matlab 2010a, MathWorks, Natick, MA, USA). Endosomes showing intensities exceeding the linear range were excluded. Average values for each individual cell (ca. 100 endosomes) were then calculated for statistical analysis. Fitting of the loading and activity curves was performed using hyperbolic and logistic response functions as implemented in Origin 9.0 (OriginLab, Northampton, MA, USA).

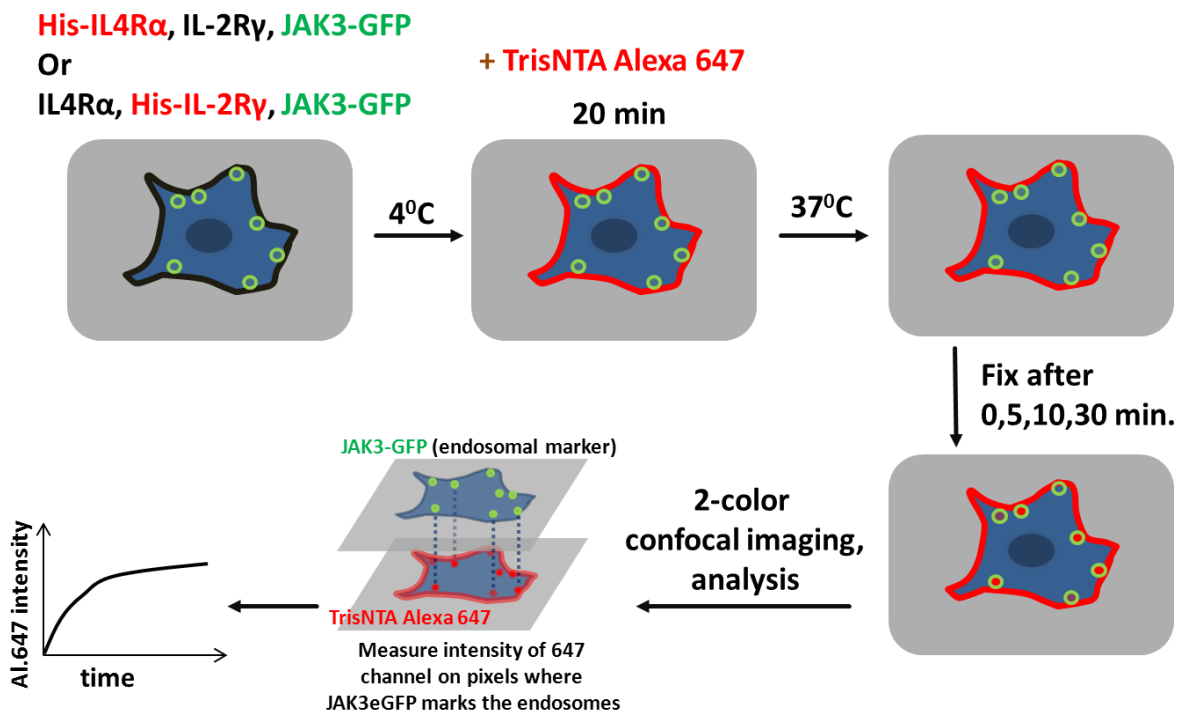


Fig 2.2: Schematic of loading assay. Cytokine positive endosomes are marked by Jak3-GFP. Using the his-tag binding TrisNTAAlexa647 to label the his-tag containing IL-4R α or IL-2R γ , the trafficking kinetics of the receptors can be assayed using colocalization analysis.

2.2.11 Fluorescence recovery after photobleaching (FRAP)

FRAP experiments were performed on the LSM780 with a 40x, NA 1.2 objective using a multi-channel GaAsP detector to collect eGFP emission between 490 and 560nm. HEK293T cells were seeded sub-confluently in an 8-well chambered Lab-tek slides (Nunc) and co-transfected with pJAK3-eGFP and pIL-2R γ -N1. Region of interest (ROI) (2.5 x 2.5 μm^2) were selected on the membrane plane, containing either plasma membrane or both plasma membrane and a cortical endosome. JAK3-eGFP was bleached to about 20% using the combined excitation of the 405 and 488nm laser lines. 50 frames over a period of 5min were recorded.

The raw FRAP curves were normalized using the following equation:

$$C(t) = \frac{A_o}{A(t)} \times B(t) \quad (\text{Equation 1})$$

Where A_o is a prebleach intensity of the an area distant from the bleach area, $A(t)$, the intensity with time during the experiment and $B(t)$ the intensity with time at the area of bleaching. Then the normalized curve is given by:

$$N(t) = \frac{C(t) - C_1}{B_o - C_1} \quad (\text{Equation 2})$$

Where B_o is intensity at the area of bleaching before the bleaching, and C_1 the first point after bleaching from equation 1. Curves are fitted with using following equation adapted from [51]: $y=A (1-e^{-Bx})$.

Chapter 3

Results part I: Characterization of the endosomes

3.1 Preface

In order to understand the role of endocytosis in cytokine receptor signaling we are studying this pathway in human embryonic kidney (HEK293T) cells, using the IL-4R receptor as a model [52, 53]. The IL-4R shares the IL-2R γ chain with several other, related receptors, including the IL-2R and IL-7R receptor complexes, and this recruited subunits is hence also referred to as the common gamma chain [4, 54].

The IL-4R can form three types of active receptor complexes, which can be induced either by IL-4 or IL-13. A type 1 receptor complex is formed when IL-4 binds to IL-4R α and recruits the secondary receptor subunit IL-2R γ . Type 2 receptor complexes comprise of IL-4R α and IL-13R α 1, which can be assembled following binding of either IL-4 or IL-13.

Although cytokine receptors can signal via many different pathways like insulin receptor substrate (IRS) or PI3K (Phosphatidylinositol 3-kinase), their main signaling output occurs via the JAK/STAT pathway. Signaling is generally thought to be initiated when ligand induces receptor dimerization on the plasma membrane where the ligand binding chain recruits the second receptor/co-receptor, which may be shared by several different receptor complexes [53, 55] (Figure 3.2). This brings associated JAKs into close proximity, which facilitates their cross-phosphorylation. This results in further phosphorylation of tyrosine residues on the receptor tail that provides docking sites for STAT family transcription factors. STATs are then phosphorylated on conserved tyrosine residues that facilitate their

dimerization. Finally, STAT dimers are translocated to the nucleus where they and bind to DNA motifs in the promoters of STAT-responsive genes.

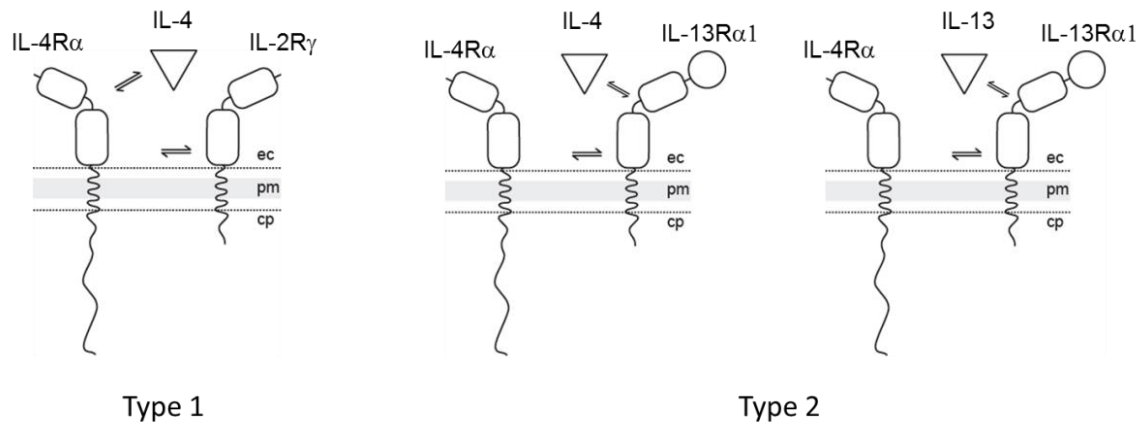


Figure 3.1: Schematic representation of two types of IL-4R complexes. Type 1 receptor complex is formed upon binding of IL-4 to IL-4R α . This is followed by recruitment of co-receptor of IL-2R γ . Type 2 complex can be induced either by ligand IL-4 that binds to IL-4R α and recruits IL-13R α 1 or by ligand IL-13 that binds to IL-13R α 1 and recruits IL-4R α as a co-receptor.

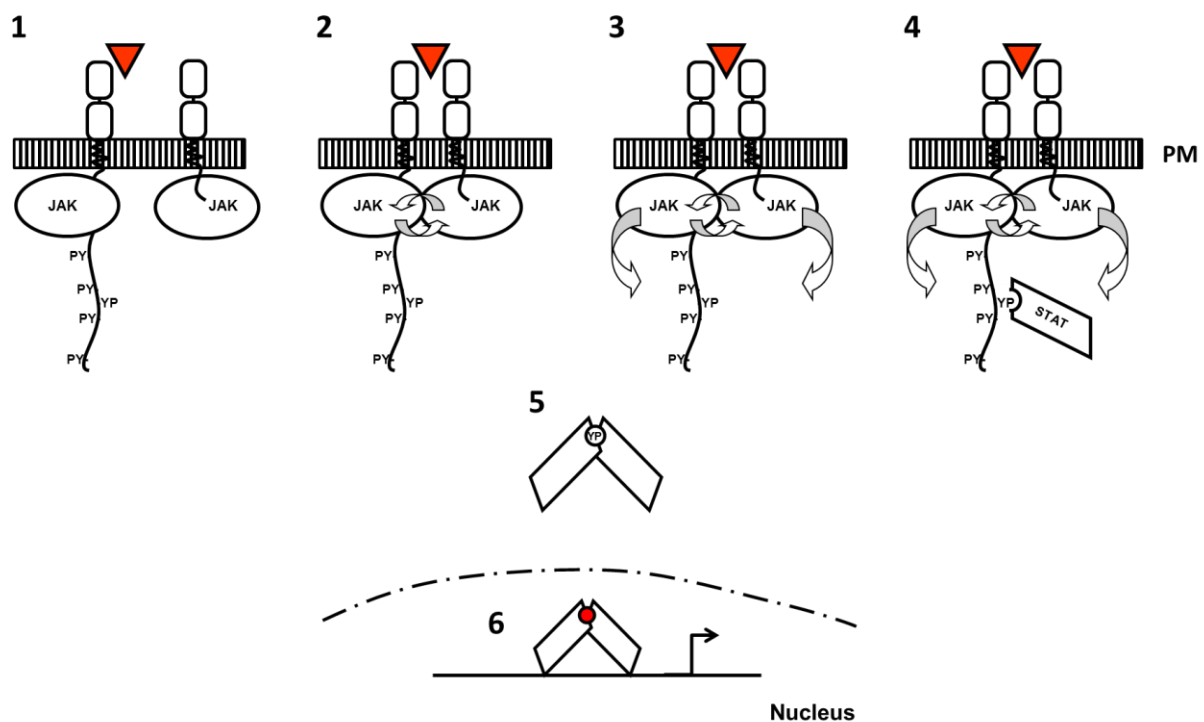


Figure 3.2: JAK/STAT pathway. (1) Each receptor subunit consists of a receptor chain and its associated JAK kinase. (2) Ligand binding to the alpha chain triggers recruitment of a secondary subunit. This brings associated JAK kinases into sufficiently close proximity that facilitates cross-phosphorylation. (3) JAKs furthermore phosphorylate tyrosine residues on the receptor tail. (4) Phosphorylated residues then provide a docking site for STATs. (5, 6) Phosphorylated STATs then forms a dimer and translocate into the nucleus, where they regulate target gene transcription.

All these receptors possess typical structural features of hametopoetin family - 4 conserved cysteine residues, fibronectin type II modules in its distal region from plasma membrane and tryptophan-serine doublet (WSXWS) in its proximal domain. Apart from that, IL-13R α 1 contains an extra IgG-like domain at its N-terminus. These cytokine receptors do not have intrinsic catalytic activity and instead it is provided by their associated JAKs. IL-4R α , IL-2R γ and IL-13R α 1 are associated with JAK1, JAK3 and TYK2 respectively and signal, amongst other pathways, through STAT6 phosphorylation. Importantly, while IL-4R can also activate other STATs such as STAT5, which can also be controlled by other cytokine receptor, Stat6 only responds to the IL-4R. So STAT6 phosphorylation gives specific readout of IL-4R signaling pathway. Upregulation of the IL-4R pathway is related to diseases like allergy and asthma [56], whereas either mutation in IL-2R γ encoding gene or prevention of its association with JAK3 results in X-linked severe combined immunodeficiency (XSCID).

We are studying IL-4R signaling pathway by reconstituting type 1 receptor complex in HEK293T cells. Because of their size and adherent nature, these cells are suitable for different microscopic techniques [47]. HEK293T cells express the endogenous type 2 receptor components IL-13R α 1 and IL-4R α but not the type 1 receptor components IL-2R γ and JAK3. They also do not express signal transducer STAT6 which allow us to study pathway specific effects by transient expression of STAT [53]. By over-expression of the type 1 receptor component, we can re-route the entire pathway via type 1 signaling pathway and can ignore endogenous type 2 background [47]. The cytokine mediated signaling was reconstituted on Jurkat cells lymphocytes also and the results are similar to those in HEK cells (Kristina Kurgonaite, unpublished results).

Initial results in the lab have shown that expression of the type1 signaling components in the HEK293T cells resulted in inhomogeneous distribution of the proteins at the plasma membrane. IL-4R subunits accumulated in speckle-like structures with strong fluorescent signals. These structures were suspected to be endosomes, which was confirmed by the presence of the endosomal marker proteins Rab5 and Rab11. The aim of this chapter is to reconfirm these initial results, and to further investigate and characterize these interleukin-positive endosomal structures in detail.

3.2 Endosome formation is ligand independent

Previous studies in our lab have shown that JAK3 and IL-2R γ expressed in HEK293T cells are mutually required for their plasma membrane localization [53, 57]. If IL-2R γ is expressed alone, it is localized in perinuclear region, while expression of JAK3 on its own resulted in a cytoplasmic distribution. However, co-expression of IL-2R γ recruits JAK3 to the plasma membrane and JAK3 in turn stabilizes IL-2R γ on the surface (Figure 3.3A). Therefore, the co-expression of JAK3 and IL-2R γ is essential for plasma membrane localization of these components. Moreover, we observed that their distribution is not homogenous and they form speckle-like punctate structures - endosomes (close arrows), characterized by bright fluorescent spots along the otherwise homogeneous plasma membrane. Due to the optical

resolution limit of confocal microscopy, it is not clear from fluorescent images whether they are distinct endosomal structures close to the cell surface or protein accumulations within the plasma membrane (Figure 3.3B). Tagging of receptors or kinase with fluorophores does not interfere with endosome formation or protein expression. Surprisingly, these endosomes are formed in the absence of ligand. Since JAK3 is always a component of the speckle-like structures, I used JAK3-eGFP as a positive endosomal marker.

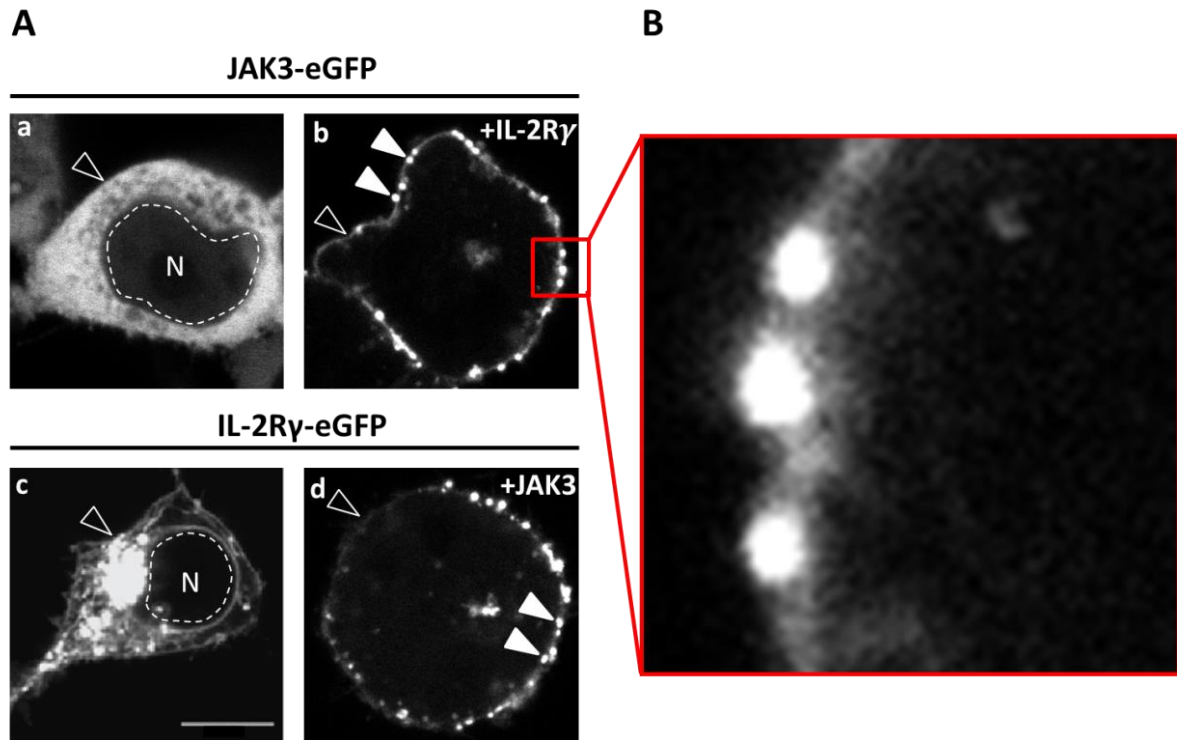


Figure 3.3: Co-expression of JAK3 and IL-2R γ in HEK293T cells. Left panels, (A) JAK3 shows cytoplasmic distribution (a), IL-2R γ is localized in perinuclear region in the absence of JAK3 (c). Open arrow shows no recruitment of IL-2R γ or JAK3 to the surface. (b) and (d) shows co-expression of JAK3 and IL-2R γ makes endosomal structure on the membrane, shown by close arrows. Open arrow shows homogenous distribution in the plasma membrane. (B) Close-up image of the endosomal structure along the plasma membrane.

After confirming that type 1 complex reproducibly localizes to endosomal structures, we checked whether the type 2 receptor subunit -IL-13R α 1 also colocalized within the same JAK3-positive endosome. To directly and simultaneously visualize multiple receptors that are present on the plasma membrane in the absence of ligand, receptors carrying an N-terminal His-tag was used that can be labeled with trisNTA-conjugated fluorescent dyes. The Ni²⁺-trisNTA complex moiety has a low nanomolar affinity towards the hexa-histidine stretch. The N-terminus of the extracellular cytokine-binding domain carrying the hexa-histidine is distant from the IL-4 binding site. Therefore, trisNTA labeling does not interfere with cytokine binding[47]. To stain the surface expressed H6-IL-2R γ , cells were incubated with Tris-NTA-A647 at 4°C (where the membrane dynamics are inhibited) and washed to remove unbound label before endocytosis was started by a shift to 37°C.

Confocal images showed that the type 1 receptor subunit IL-2R γ , and the type 2 receptor subunit IL13R α 1 is accumulated in the same endosomal compartment (Figure 3.4). Taken together, these results show that IL-13R α 1 colocalizes with IL-2R γ and JAK3 within the same endosome population independent of ligand induction.

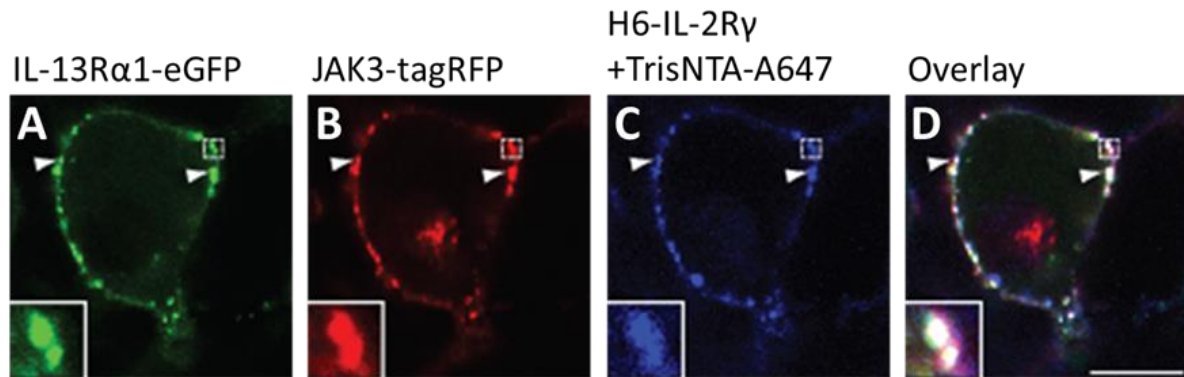


Figure 3.4: Type 1 and 2 receptor subunits accumulate in the same endosomal compartment. *IL13R α 1-eGFP (A) co-localize with JAK3-TagRFP (B) and H6-IL2R γ (C) in endosomes (arrow heads). (D) Shows the overlay image. Square insets show zoomed in image of endosomal co-localization of type 1 and type 2 receptor subunits. Scale bar 10 μ m*

3.3 IL-2R γ positive cortical endosomes are multi-vesicular bodies

Fluorescence imaging has a limited spatial resolution. To characterize the endosomes at the ultrastructural level, Transmission Electron Microscopy (TEM) was performed with various sets of labeling on cells expressing type 1 receptor complex. These experiments were performed in collaboration with the Electron Microscopy Facility (EMF) of the CRTD. As ligand endocytosis is specific to the endosomes; IL-4-biotin gold labeling was used to visualize the IL-4 localization on the endosomes. IL-4 ligand was labeled with biotin through a Sulfo-NHS linker so that tagging does not interfere with the binding of IL-4-biotin to IL-4R α . To avoid fluid phase uptake, cells were incubated with IL-4-biotin at 4°C. Cells were washed to remove unbound IL-4-biotin and incubated at 37°C to allow the internalization of IL-4R α -bound IL-4-biotin.

Before proceeding for the EM, the endosomal localization of IL-4-biotin was verified by fluorescence confocal imaging using Cy3-streptavidin. Transfected cells incubated with Cy3-streptavidin in the absence of IL-4-biotin do not exhibit any non-specific binding of Streptavidin to the membrane or JAK3-eGFP-positive speckles (Figure 3.5A) However, in cells stimulated with IL-4-biotin, Cy3 streptavidin showed colocalization with JAK3-positive endosomes as shown by arrow heads (Figure 3.5B).

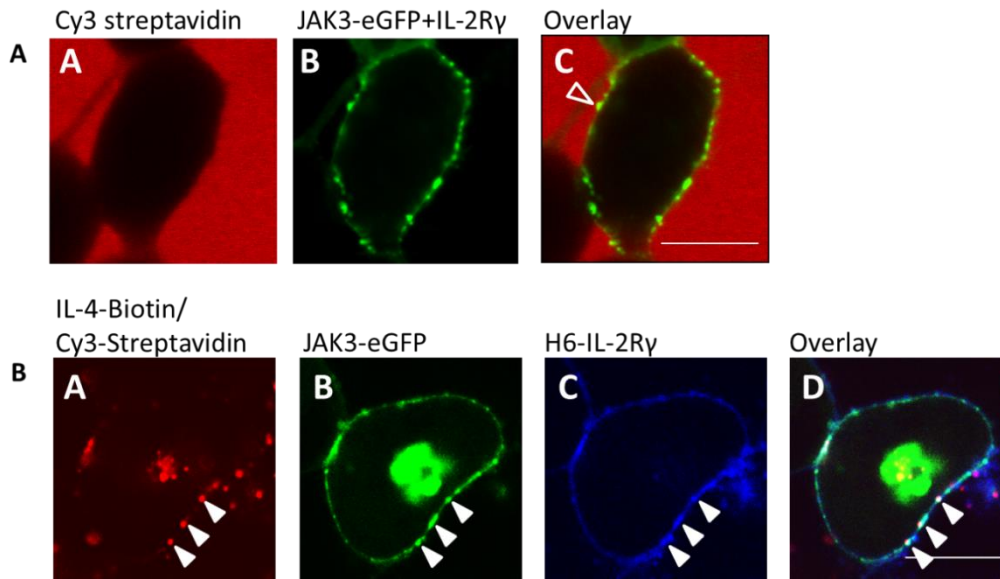


Figure 3.5: IL-4-biotin specificity. (A) Cy3 streptavidin staining on transfected cells does not show non-specific binding to the membrane or endosomes (open arrow). (B) In cells stimulated with IL-4-biotin, Cy3 streptavidin specifically binds to IL-4-biotin (A) and therefore colocalizes with JAK3-eGFP (B) and IL-2R γ (C) positive endosomes, shown by arrow heads. Scale bar 10 μ m.

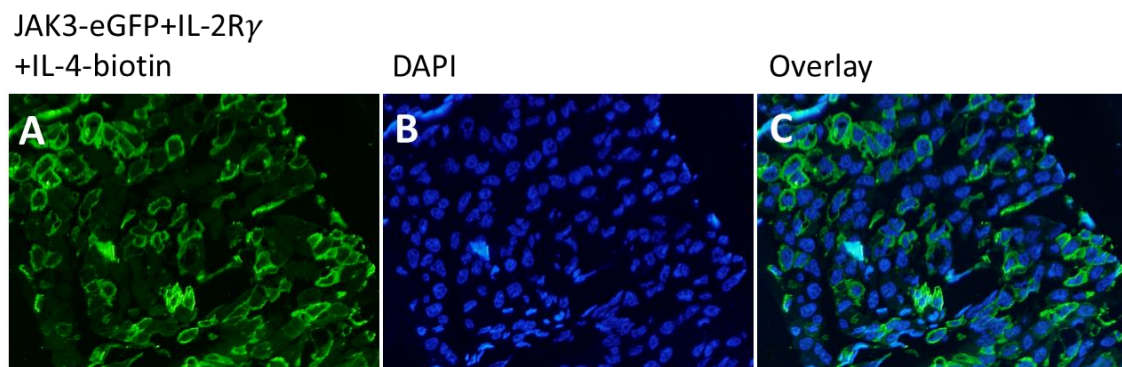


Figure 3.6: Representative images of fluorescent image of fix sections on grid. (A) Cells expressing JAK3-eGFP. (B) Nuclei are counterstained with DAPI. (C) Overlay of both GFP and DAPI channel. Appropriate samples are selected from the fluorescent image and imaged by TEM.

As we had previously established that JAK3-eGFP is always a marker for the endosome, fluorescent images were taken to identify cells expressing JAK3-eGFP. From the same samples, corresponding TEM images were taken to reveal the ultrastructure of the eGFP-positive cortical endosomes.

Cells were stimulated with IL-4-biotin for 30min. After internalization of the ligand, cells were fixed, embedded in 10% gelatin, infiltrated in 2.3 M sucrose and subsequently frozen into liquid nitrogen. 70nm thin Tokuyasu cryo-sections were thawed and placed on a grid for immunogold staining[49]. Because streptavidin-gold did not work, the sections were finally stained with anti-biotin and protein A, conjugated with 10 nm gold. TEM images shows that endosomes are multivesicular bodies (MVB) lying just beneath the plasma membrane (Figure 3.7).

JAK3-eGFP+IL-2R γ
+IL-4-biotin

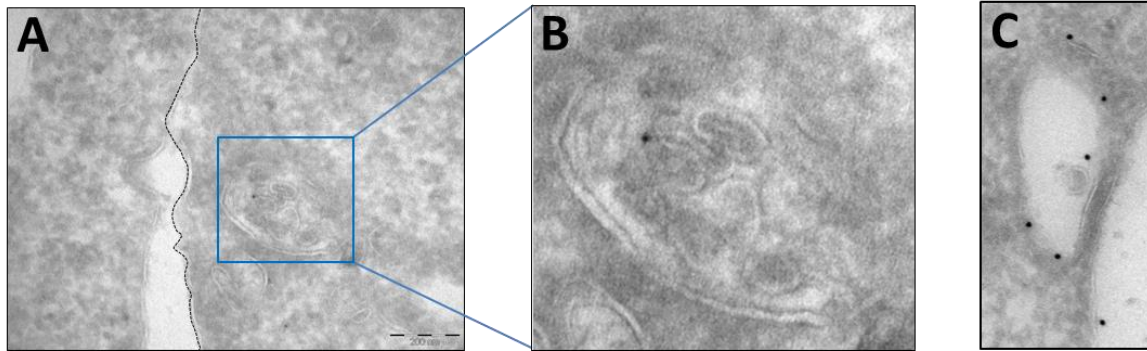


Figure 3.7: TEM image of gold labeled IL-4 marking endosome. (A) Endosome labeled with 10nm gold labeled IL-4-biotin beneath the plasma membrane (Black dotted line). Scale bar 200 nm. (B) Close up image of endosome showing multivesicular structure. (C) Endosome labeled with 10 nm gold labeled IL-4-biotin.

To directly detect JAK3 and IL-2R γ in the multivesicular endosomal structures, we proceeded to JAK3-eGFP staining. Cells expressing JAK3-eGFP and IL-2R γ were fixed, infiltrated, frozen and 70nm sections were taken. Sections were stained with primary anti-GFP and were detected with secondary antibodies coupled to ultra-small gold ~1nm, followed by silver enhancement. Antibodies conjugated to ultra-small gold particles can diffuse into the section which results in stronger labeling, because the signal is not confined to the surface but present throughout the section. These samples revealed that JAK3-eGFP is present on the limiting membrane and internal vesicles of the endosome as well as on the plasma membrane. The IL-2R γ subunits marked by JAK3-eGFP appear to be enriched in multivesicular endosomes beneath the plasma membrane. However, this method could not be used for quantification because diffusion into the section is not homogenous and therefore the antigens are not equally accessible.

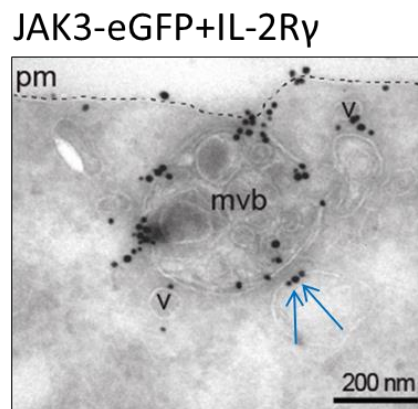


Figure 3.8: TEM image of JAK3-eGFP nano gold particle enhanced with silver labeling. Black dots represent the gold particle that is present on the limiting membrane, on internal vesicle as well as on the plasma membrane. Black dotted line represents the plasma membrane. Unlike the standard gold particle, size of this gold particle is unequal due to silver enhancement. Blue arrow shows different sizes of gold particles. Scale bar 200nm.

For the quantification of gold particles to estimate receptor density, the sections were therefore labeled with larger gold particles that do not penetrate into the section. As a result, the staining is weaker than in silver enhanced samples, but because the labeling is confined to the section surface all surface antigens are equally accessible, making these samples suitable for quantification. Thawed cryo-sections were stained with primary anti-GFP and protein A-10nm gold instead of ultra-small gold.

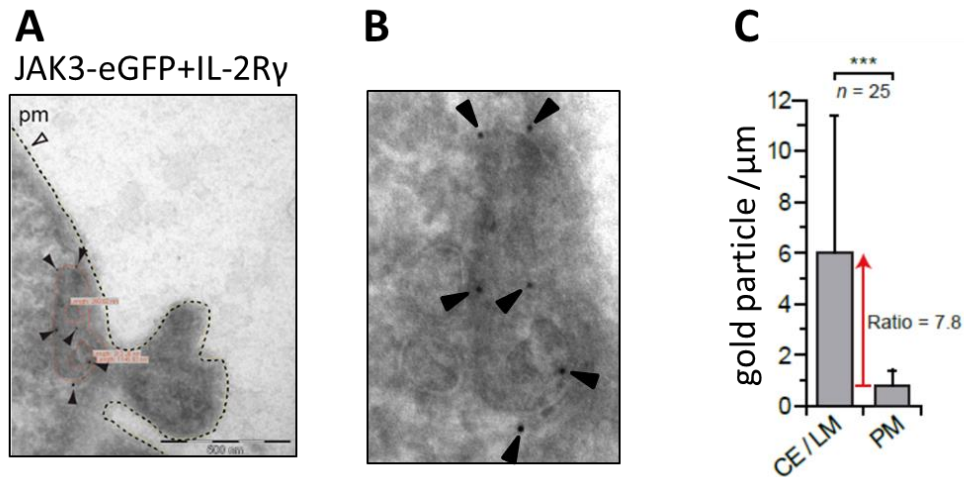


Figure 3.9: Quantification of gold particles. (A) Sections were stained with anti-eGFP antibody and detected by 10nm gold particles. Black dotted line represents length of plasma membrane. Open arrow shows gold particle on the plasma membrane. Black dotted line represents membrane surrounding the endosome and intravesicular bodies. Close arrow shows JAK3-eGFP labeled with 10nm gold particles. (B) Close up image of gold-labeled endosome (C) Quantification of IL-2R γ /JAK3-eGFP complexes at the limiting membrane of endosomes (CE/LM) and on the plasma membrane (PM). Error bars indicate SD.

To quantify the densities, total length of the plasma membrane and number of gold particle present on the membrane were calculated. For endosomes, the length of the surrounding as well as inner vesicles membranes was measured and the numbers of gold particles present on them were counted. Receptor density was correlated to the number of gold particles. This corresponds to about 8 times higher density of JAK3-eGFP per unit length of membrane in the endosome compared to the adjacent plasma membrane, clearly showing that the receptors are enriched in the cortical endosomes.

Image	Cortical endosomes			Plasma membrane	
	# gold total	# gold LM	[μ m] membrane	# gold	[μ m] membrane
1	6	4	1.1	1	3.5
2	4	3	1.2	1	1.8
3	4	3	1.8	0	2.2
4	4	1	0.8	1	3.2
5	1	1	1.5	0	3.3
6	3	3	0.8	0	1.9
7	2	1	1.5	2	2.8
8	3	1	1.6	0	2.0
9	4	3	2.4	0	2.7
10	4	4	0.9	0	1.3
11	1	3	1.2	3	3.0
12	6	2	1.4	2	3.1
13	4	4	1.4	1	1.2
14	1	6	1.4	3	3.4
15	7	7	0.8	4	3.6
16	4	3	3.3	16	12.3
17	1	1	1.1	5	2.4
18	1	1	0.7	4	4.6
19	1	1	1.4	4	3.1
20	8	8	0.9	2	2.8
21	3	3	3.8	18	17.2
22	4	3	2.0	13	7.4
23	1	1	2.2	7	3.6
24	1	1	0.8	4	3.8
25	9	6	1.5	1	1.9

Table 1: Quantification of immunogold labeled IL-2R γ /JAK3-eGFP complexes in the membrane by TEM. Gold particles were counted in cortical endosomes in total and at the limiting membrane as well as at the plasma membrane of the same image.

3.4 Multivesicular bodies are associated with actin meshwork:

As previously observed, IL-2R γ is known to be endocytosed via a specific actin-mediated and dynamin-dependent but clathrin- and caveolin-independent pathway[58, 59][58, 59][58, 59][58, 59][58, 59]. This endocytosis route requires the activation of the Rho-family GTPase Rac1, the p21-activated kinase (Pak1/2), and cortactin, leading to locally confined actin reorganization[37-41]. To determine whether the JAK3-eGFP labeled endosomes are associated with actin, CLEM (correlative electron microscopy) labeling was performed using anti-GFP immunofluorescence as a means to identify cortical speckles and anti-actin protein-A gold labeling to detect cortical actin in the vicinity of the cortical endosomes. For this, cells expressing JAK3-eGFP/IL-2R γ were fixed and sectioned. Cryo-sections were stained with primary antibodies against GFP and actin, followed by fluorescence and gold probes, respectively. In agreement with this mechanism, image shows that IL-2R γ /JAK3-eGFP positive endosomes are surrounded by gold labeled cortical actin (Figure 3.10G).

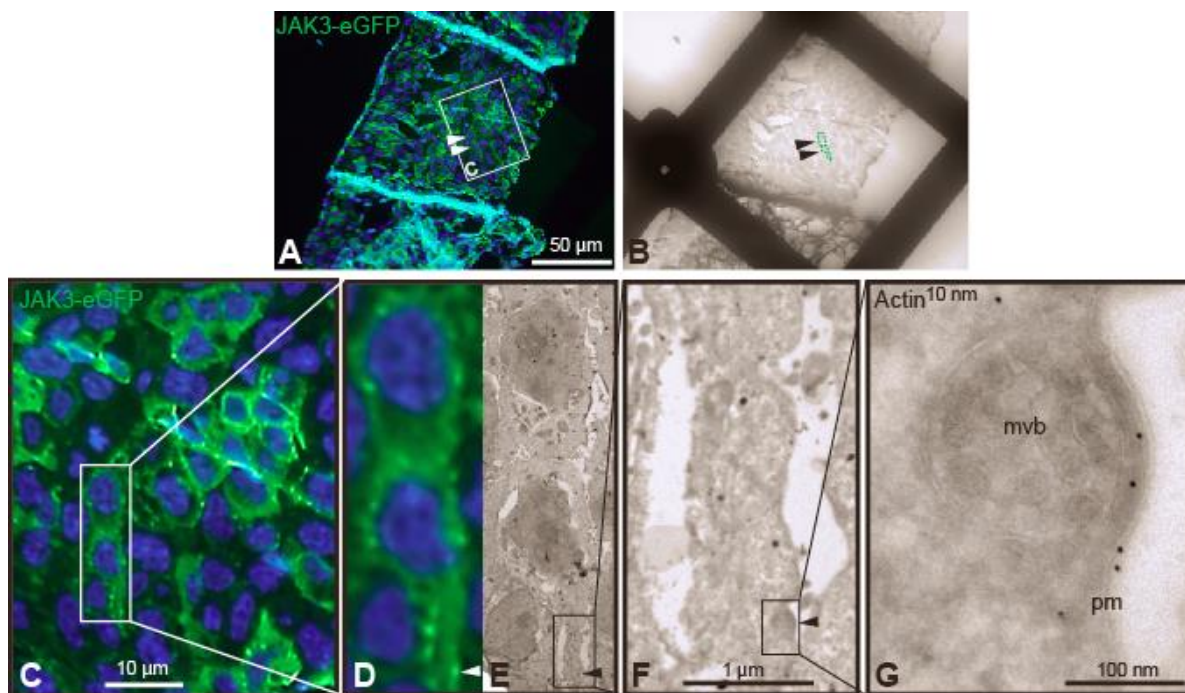


Figure 3.10: CLEM of JAK3-eGFP expressing cells. Sections were labeled with anti-GFP and anti-actin antibodies which were detected by fluorescence and gold particles, respectively. Nuclei were counterstained with DAPI. (A) Overview, fluorescence, the cells of interest (ROI) are highlighted by arrowheads, the square indicates the region displayed in C. (B) overview ROI in the TEM, ROI indicated by arrowheads. (C) GFP-labeled cells, two of which are selected for CLEM (square). (D), (E) correlative imaging of two labeled cells in the FLM (D) and the TEM (E). The arrows indicate a JAK3-eGFP labeled speckle; the square indicates the region displayed in F. (F) higher magnification, the arrow indicates an electron dense structure underneath the plasma membrane; the square indicates the region displayed in G. (G) Multivesicular body in close proximity to the actin-labeled cell cortex.

Collectively, our TEM experiments shed light on three important points. First, the cortical endosomes are multivesicular bodies. Second, endosomes are anchored in the actin cortex just below the plasma membrane, from which they are separated by only approximately 20-30 nanometers. Third, in the sections, receptor density per unit length is approximately one order of magnitude higher within the limiting membrane of the endosome than on the plasma membrane. Because the actual endosomal surface is two dimensional, this ratio corresponds to a roughly 100-fold increase in receptor density per area.

3.5 Multivesicular bodies are positive for Hrs

Although previous results in lab confirmed that these endosomes are early recycling endosomes as they stain positive for Rab5 and Rab11 (Kristina Kurgonaite, unpublished data), TEM images showed consistently that these endosomes are multivesicular bodies (MVBs). MVBs are characterized by the accumulation of small intraluminal vesicles within the endosome by invaginating towards the lumen from endosomal membrane. MVB formation is an intermediate step in endosome biogenesis where endosome matures from an early endosome to lysosome. Formations of MVBs is known to be mediated by Hrs (hepatocyte-growth-factor-regulated tyrosine kinase substrate) and ESCRT-1 (endosomal sorting complex required for transport-1) complex. Through its FYVE domain, Hrs is localized on to early endosome and during the process of invagination, it assimilates receptors destined for late endosomes or lysosomes [60]. Consistent with TEM immunostaining of these endosomes, most of these endosomes are positive for Hrs. Majority of the endosomes are also positive for both Hrs and EEA1 (early endosome antigen 1) (Figure 3.11). An interesting observation is that although they show a mixed characteristic of early, recycling and multivesicular nature they lay very close to the plasma membrane in actin cortex.

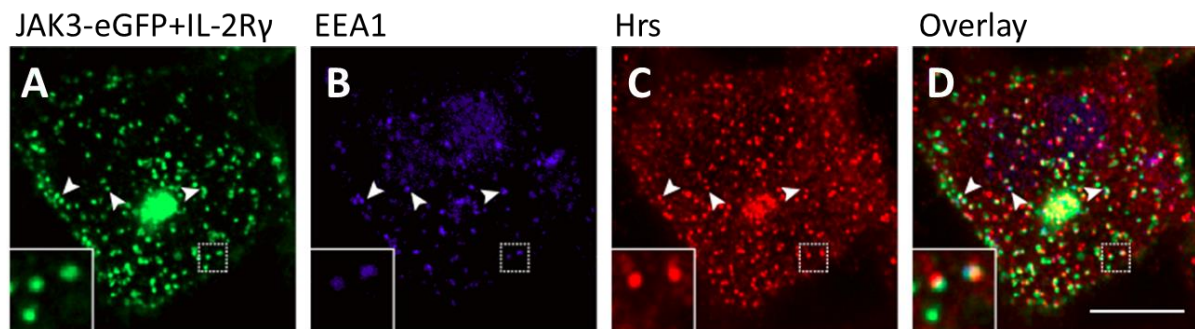


Figure 3.11: Co-immunostaining of JAK3-eGFP positive endosome with Hrs and EEA1. (A) JAK3-eGFP-positive endosome upon co-expression of JAK3 and IL-2R γ . (B) EEA1 colocalized with JAK3-eGFP positive endosome. (C) Hrs staining for JAK3-eGFP positive endosome. (D) Overlay image showing endosomes positive for both early endosomal marker – EEA1 and late endosomal marker Hrs. Square inset shows colocalized endosomes. Scale bar 10 μ m.

3.6 Endosomes are separate compartments from the plasma membrane

The endosomal structures appear adjacent to the membrane in confocal images. However, due to small size of the endosome that is approximately 300nm (from TEM) which borders on the limit of optical resolution, and because TEM delivers only single sections, it is not possible to distinguish whether these endosomes are invaginations of the plasma membrane or distinct compartments. Therefore, we performed Fluorescence Recovery After Photobleaching (FRAP) to establish whether or not they are continuous with the plasma membrane by looking at the lateral diffusion of fluorescently marked receptor complexes. In FRAP, fluorescent molecules are specifically bleached in a sample region using lasers. Upon bleaching, depending on the mobility or any other active processes, the bleached molecules are replenished dominantly by unbleached fluorescent molecules, causing fluorescence to recover. The rate and extent of this replenishment of fluorescent molecules are quantified from time-lapse imaging. From the characteristics of the recovery curve, two important information can be deduced – the rate of recovery and the saturation level of recovery. The rate of recovery signifies how fast the fluorescent molecules are being exchanged. This is fast for molecules diffusing freely in the cytoplasm, slightly slower for molecules diffusing laterally within membranes, and can even slower or entirely absent for molecules rigidly attached to the ECM or cytoskeleton. The saturation of recovery depends on the immobile fraction of molecules which do not exchange in the sample. Typical images of bleaching experiments performed on cells are shown in Figure 3.12. In our case, it was not possible to bleach the endosomes exclusively, as they lay very close to the plasma membrane. Therefore, FRAP was performed either on regions of homogenous plasma membrane or on membrane containing an underlying endosomal structure. We found diffusion time/recovery time constants of 45s in a region containing only plasma membrane and 66s for a region containing a labeled endosome close to the plasma membrane (Figure 3.13). These recovery times are consistent with the lateral diffusion in the plasma membrane [61, 62].

However, when comparing recovery saturation we found that the immobile fraction is lower in regions containing only plasma membrane fluorescence (ca 45%) than in regions containing a cortical endosome adjacent to the plasma membrane (78%). It is very difficult to measure the contribution of the plasma membrane in the recovery observed in regions with both endosome and plasma membrane owing to optical resolution limit. However, over the time of the experiment, no reconstitution of the endosomal fluorescence could be observed (Figure 3.12). We therefore interpret the increased immobile fraction as a result of the failure to traffic receptor complexes to the endosomes with comparable speed. Furthermore, this excludes the fast recovery of JAK3 between receptor bound and cytoplasmic free pool, that also resembles with JAK1 dynamics [63]. Thus, the majority of IL-2R γ /JAK3-eGFP complexes within these endosomes are not in diffusive exchange with the plasma membrane or the cytoplasmic pool within the time frame of the experiment.

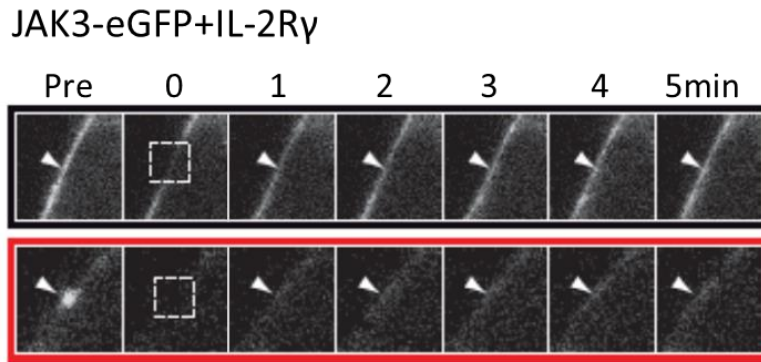


Figure 3.12: Representative image of FRAP. Square shows region of interest (ROI) with $2.5\mu\text{m}^2$ on a membrane region (black outline) and membrane with endosome (red outline). While plasma membrane recovers, endosomes do not recover during observation time showing that they are disconnected from the plasma membrane.

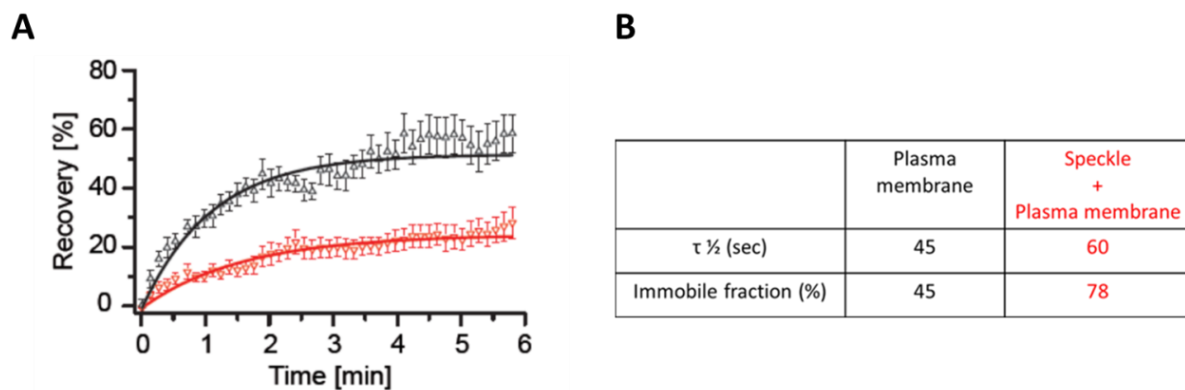


Figure 3.13: FRAP Recovery. (A) FRAP curve shows that immobile fraction is increased in endosome containing region (red) than in membrane containing region (black). (B) Table 2: Fit values of plasma membrane and speckle region showing recovery is in similar time regime but immobile fraction is increased in endosome containing plasma membrane. $n=10$ cells, error bars indicate Standard Error of the Mean (SEM).

To summarize this section, I have shown that co-expression of IL-2R γ and JAK3 results in the formation of endosomes that are present beneath the plasma membrane and are separated by 20-30nm. TEM shows that these endosomes are associated with actin cortex beneath the plasma membrane. Both type 1 and type 2 IL-4R subunits are present in the endosome. These endosomes are also accessible by ligand. However, confocal and TEM images give information only about steady state, it does not elucidate the dynamics of the transport of receptor molecules into the endosome from the plasma membrane. To understand receptor trafficking and measure the temporal dynamics of receptor endocytosis and signaling, quantitative live cell approaches need to be adopted.

Chapter 4

Results II: Quantitative analysis of trafficking of Interleukin receptors

4.1 Preface

Endocytosis was generally thought as a process of down regulating receptor-mediated signaling, by reducing the accessibility of the receptors to ligands. Increasing evidence suggests that endocytosis and signaling may be coupled and endocytosis contributes synergistically to signaling. This has led to the “signaling endosome hypothesis”. There are many endocytosis pathways known and one of the thoroughly studied pathways is clathrin-dependent pathway. For many years, it was believed to be the most common pathway for receptor-mediated endocytosis. However, more recently the involvement of clathrin-independent pathways has been established [64]. These pathways are characterized by markers like GPI-anchored proteins and are used by autocrine mobility factor, TGF- β receptor, IL-2R β , toxins and viruses [38]. It is also reported that IL-2R subunits are clustered in lipid ordered microdomains , also called “rafts”, from where they are internalized by a clathrin-and caveolae-independent pathway[39]. This pathway requires Dynamin for scission of the vesicles from the plasma membrane. Internalization of the IL-2R subunits is regulated by the Rho family GTPase Rac1, which in turn controls the canonical actin polymerization and branching cassette comprised of Pak1/2, cortactin, WASP and the actin branching modulator Arp2/3.

So far, I have shown that co-expression of JAK3 and IL-2R γ forms endosomes and both type 1 and type 2 receptor subunits are accumulated into these endosomes. These endosomes are

distinct compartments close to the plasma membrane and are surrounded by the actin cortex. Hence, we termed this population of signaling compartments “Cortical Endosomes”. However, these results give us only static images. To measure the dynamics of receptor endocytosis, the trafficking needs to be measured using live cell imaging. To achieve this, we labeled our proteins with different tags which allow us to visualize them simultaneously. As explained earlier, I used JAK3-eGFP as a marker for the cortical signaling endosomes. As explained in chapter III, receptors were again tracked with triNTA-A647 dye which reversibly binds to N-terminal His tag of the receptor [65, 66]. Depending on the experiments, Alexa647 labeled IL-4 ligand was also used [47].

4.2 Signaling components accumulates in the endosome

To assay the dynamics of trafficking of receptors into these endosomes, a pulse chase experiment was performed which quantifies the uptake of the respective ligand bound to the receptor.

Fluorescent Alexa-647 labeled ligand IL-4-A647 was used to track IL-4R α receptor trafficking. Labeling of IL-4 with fluorescent dyes does not interfere with binding to IL-4R α . In addition, labeled ligand specifically stains cells expressing the IL-4R α subunit. Cells expressing type 1 receptor complex were incubated with IL-4-A647 at 4°C to avoid a background fluid phase uptake, while allowing efficient binding to surface expressed IL-4R α . Cells were then washed to remove unbound IL-4-A647. Endocytosis was then allowed to initiate by moving the cells to room temperature. Results show that at 0 min, while membrane dynamics remains blocked, because of low temperature, IL-4-A647 bound to the IL-4R α is homogenously distributed in the cell membrane (Figure 4.1, b). However, after shifting the cells to room temperature, IL-4-A647 was accumulated in the endosomes within 7 min (Figure 4.1, e). The overlay shows clear co-localization of IL-4-A647 to the endosome marked by JAK3-eGFP+IL-2R γ (Figure 4.1, f). We thus conclude that type 1 IL-4R subunits are transported into JAK3-positive endosomes from the plasma membrane.

4.3 Dynamics of receptor trafficking in to the endosome

We have shown morphologically using EM and using FRAP that the endosomes are distinct membrane compartments. We have also shown that IL-4: IL-4R α complex is trafficked into these endosomes. However, the receptors are also found localized to the endosomes independent of the ligand. In this section, using live cell imaging, we therefore want to answer the following questions: Whether a much slower process of replenishment of receptors occurs between the plasma membrane and the endosomes and whether the presence of ligands affects the kinetics of the trafficking.

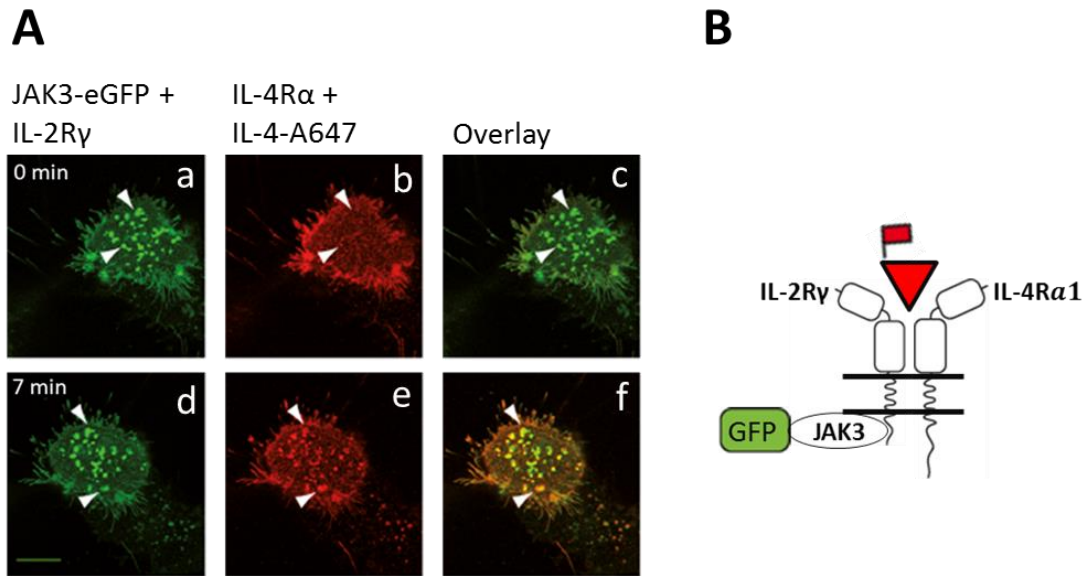


Figure 4.1: Ligand co-localization in endosome. (A) Upper panel: At 0 min IL-4-A647 distribution is homogenous (b) and do not colocalize with JAK3-eGFP positive endosome (a) as shown in the overlay image (c). Lower panel: As the temperature is increasing, IL-4R bound IL-4-A647 is redistributed in to the endosomes within 7 min (e). Overlay image (f) shows at 7 min co-localization of IL-4-A647 with JAK3-eGFP positive endosomes (d). (B) Schematic of Type 1 receptor complex. Scale bar 5 μ m.

To determine the trafficking kinetics of receptors into endosomes, we designed a receptor loading assay which quantifies accumulation of ligands and receptor into the cortical endosomes at different time points. To establish whether receptor trafficking dynamics are affected by the IL-4 ligand, the receptor was labeled independent of the ligand using a His-tag specific dye which binds to the hexa-histidine tag on the N-terminus of the receptors. Cells expressing type 1 IL-4R components were incubated with trisNTA-A647 dye at 4°C for proper binding to the His-tagged receptors. Cells were washed to remove unbound dye and transferred to 37°C to resume endocytosis. To check the background due to unspecific binding of trisNTA dye, the same procedure was followed with cells transfected with receptors lacking the hexa-histidine tag. Cells were fixed after incubation for a particular time period, and were imaged with a confocal microscope. Confocal images were quantified to assay the receptor uptake.

The intensities of the internalized receptor were quantified for each endosome. Since at initial time points, the intensity of the externally added labeled ligand is very low, the endosomes were in parallel marked by JAK3-eGFP. To measure the trafficking of receptor components in the endosomes, intensity from the pixels were calculated in the red channel that corresponds to the pixel area in the green channel. To calculate the concentration of internalized receptor and ligand, we measured the average intensity of a 3x3 pixel area shown by black inset within the endosome (Figure.4.2). Each endosome was selected manually and intensity was calculated by an automated MATLAB script.

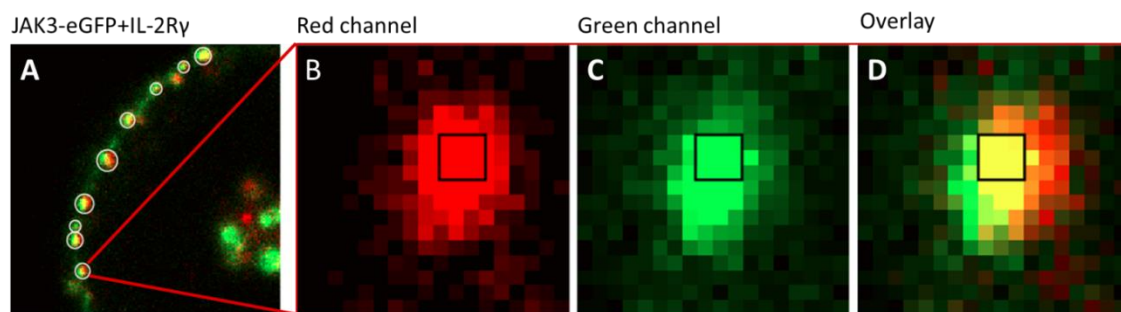


Figure 4.2: Size of quantification within the endosome. (A) Co-expression of JAK3-eGFP and H6-IL-2R γ forms endosomes near the plasma membrane. Circle around the endosome depict that they are of different size. Figure B, C, D shows close up image of endosome. Black square shows the area within the endosome measured to quantify the intensity.

It is important to set the conditions of imaging so that the range on intensities to be measured in the experiment lies in the linear range of the detectors. To ascertain this, different laser powers were used to measure the intensities. Counts per pixel measured from endosomes were plotted as histogram. The range of counts per pixel was 0-25 for 1% laser power and 0-70 for 1.5% laser power. For a pixel dwell time of 50 μ s was chosen for all the experiments as the measurements at 1% laser power at this setting were within the linear range of APD, which is about 500 KHz. This specification allowed us to measure accurately the trafficking of fluorescent ligand or receptor into the endosome.

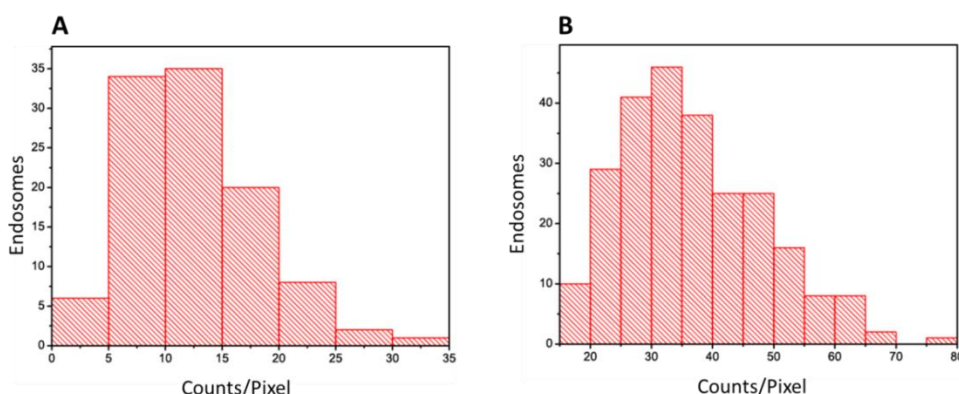


Figure 4.3: Histogram of counts/pixel at different laser power. Cells were imaged with two sets of different laser power. (A) With 1% laser power, the measured counts are between 0-35 with maximum counts around 10-15. (B) With 1.5% laser power, the counts are between 0-80 with maximum counts around 35. For the experiments, 1% laser power was selected as with this laser power, the counts are within linear range of APD around 500 KHz.

Figure 4.4A shows example image of loading of labeled receptors at 0 min and 30 min in JAK3-eGFP positive endosomes. At 0 min, there is no accumulation of receptor H6-IL-4R α /H6-IL-2R γ in red channel (Figure 4.4b). However, the endosomes become saturated with receptor H6-IL-4R α /H6-IL-2R γ within 30 minutes (Figure 4.4e). The square inset shows in the green channel the area within the endosome from which the photon intensity in red channel was calculated. These intensities, which represent the uptake of receptors, were then plotted against different time after temperature release.

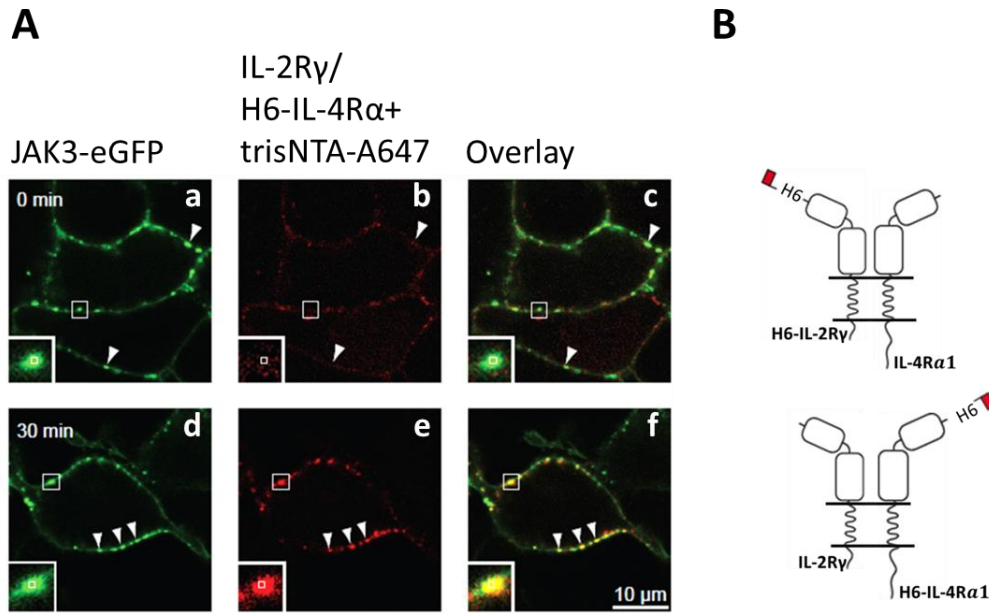


Figure 4.4: Representative image of Loading Assay. (A) 0min panel: at 0min no receptors are detectable in the Alexa647 channel (b) within the JAK3-positive endosomes (a). 30min panel: at 30min JAK3-positive endosomes (d) are saturated with alexa647-labeled receptors (e). Square inset within the endosome shows area of intensity measurement. Panels (c) and (f) show the overlay. (B) Schematic of receptor complex with N-terminally His-tagged receptors which are labeled with TrisNTA dye.

First, we checked the background intensity of the His tag dye for similar concentrations used for the experiments. The intensity of endocytosed IL-4Rα is normalized to the average intensity of H6-IL-2Rγ. The saturation level of IL-4Rα is 30% of IL-2Rγ. The nonspecific background measured with just the dye is 10% (Figure 4.5). This confirms that experimental procedure using His tag dye is functional and can be used.

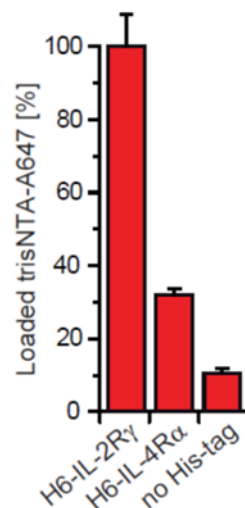


Figure 4.5: Nonspecific background of His tag dye. Intensity of tris-NTA is calculated after 30min incubation from JAK3-eGFP positive endosomes. Intensity of IL-2Rγ is taken as 100%. Compare to IL-2Rγ, IL-4Rα has 30% background and 10% unspecific background. Error bar indicates SEM.

4.4 Receptor trafficking is independent of the type of receptor

Next, we compared the trafficking rate of IL-4R α and IL-2R γ in the absence of ligand. As measured from the pulse chase experiment, IL-4R α and IL-2R γ are trafficked into the endosome with similar time constants of 8.5 ± 1.3 min and 6.6 ± 0.7 min respectively (Figure 4.6). The only difference between IL-4R α and IL-2R γ is in their saturation level. This saturation difference is presumably due to the difference in the expression level of receptors under physiological condition. The quantification of the trafficking shows that even though the endosomes appear as stable structures, they accumulate receptors continuously. The timescales of this trafficking is about 10 minutes, and therefore, too slow to be detected by FRAP assays. The loading experiments, however, strongly establish that there is a slower process of continuous trafficking of receptors occurring, which replenishes the endosomes.

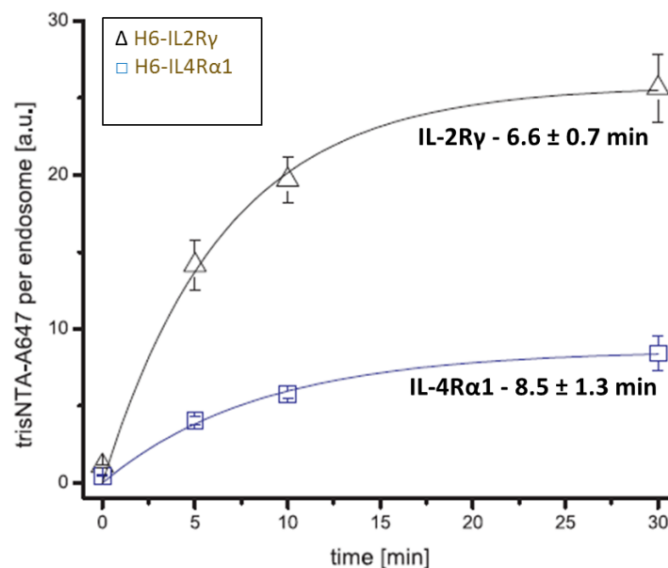


Figure 4.6: Trafficking kinetics of IL-4R α and IL-2R γ . Both receptors shows similar trafficking rate but they have difference in saturation levels. Error bar indicates SEM.

4.5 Receptor trafficking to the endosomes is independent of the presence of IL-4

The classical assumption is that binding of ligands to receptors activate them to trigger internalization. Therefore, we wanted to confirm whether the continuous trafficking between the plasma membrane and the cortical endosomes is affected by the presence of ligand. We checked the internalization of IL-4R α in the presence and absence of ligand. Intensity of accumulated TrisNTA-A647 in each endosome was calculated for different time points and plotted against time. The graph shows that the trafficking rate of IL-4R α is 8.5 ± 1.3 min in the presence of ligand (Figure 4.7). Surprisingly, the rate of internalization for IL-4R α was measured to be similar in the absence of ligand. Therefore, the IL-4R α internalization is independent of ligand occupancy and does not require pre-dimerization with IL-2R γ , which is

dependent on ligand binding. Considering these characteristics of the receptor trafficking, the model which emerges is that of the receptors acting like a “conveyor belt” shuttling the ligand constantly into the endosome.

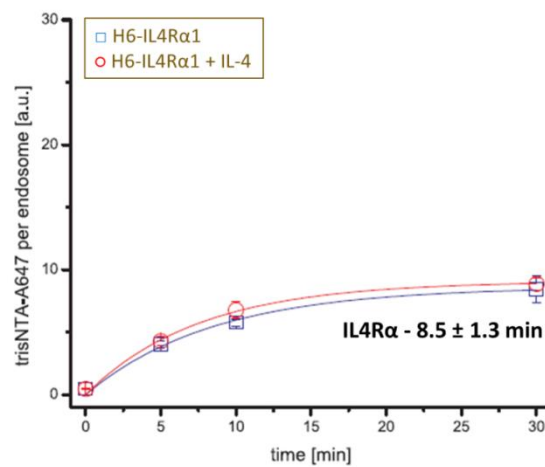


Figure 4.7: Trafficking kinetics of IL-4Ra. Trafficking rate of IL-4Ra is similar in presence and absence of ligand. Error bar indicates SEM.

4.6 Signaling and receptor internalization is sensitive to perturbation of Rac1/Pak1 driven endocytosis

As previously described, endocytosis of IL-2R γ occurs via a Rac1/Pak1 regulated pathway. As IL-4R α shares the common γ chain, we hypothesized that a similar pathway of trafficking using Rac1/Pak1 for IL-4R complex subunits as well. Indeed, previous results from the lab showed that IL-4R mediated signal transduction was sensitive to Rac1 or Pak inhibition. However, it was not clear the trafficking of which signaling components was affected. We therefore performed a pulse chase experiment in the absence or presence of Rac1 inhibitor EHT-1864[67]. Cells were pre-incubated with EHT-1864 at 4°C for 20min. IL-4-A647 was then added to the cells in the presence of drug for binding to IL-4R α . After IL-4-A647 incubation, cells were washed to remove unbound ligand but the presence of drug was continued while endocytosis was allowed to resume at room temperature. For the control, same procedure was followed in the absence of drug. As indicated by closed arrows in Figure 4.8A, IL-4-A647 is colocalized with JAK3-eGFP endosome in absence of EHT. IL-4R α mediated uptake of IL-4-A647 is reduced in the presence of drug (lower panel “+EHT”) in comparison.

To quantify the effect of drug inhibition on receptor trafficking kinetic, we performed a similar loading assay along with an additional step of pre-incubation of the cells with the drug. We set the intensity from non-treated control cells as 100%. Figure 4.8B shows that internalization of IL-4R α is reduced to 31% and IL-2R γ to 52% compared to controls. Since Rac1 and Pak1 serve pleiotropic functions, cells are strongly affected by the respective inhibitors EHT and IPA. Specifically, they round up upon drug treatment, presumably due to effects on the actin cytoskeleton. Thus, the measured intensities may have a large error. In

addition, the most strongly affected cells could not be analyzed. Therefore, these measured values represent a conservative estimate of the true reduction in trafficking. From the receptor trafficking assay, we conclude that both IL-4R α and IL-2R γ are trafficked into the endosome independent of ligand via Rac1/Pak1 pathway.

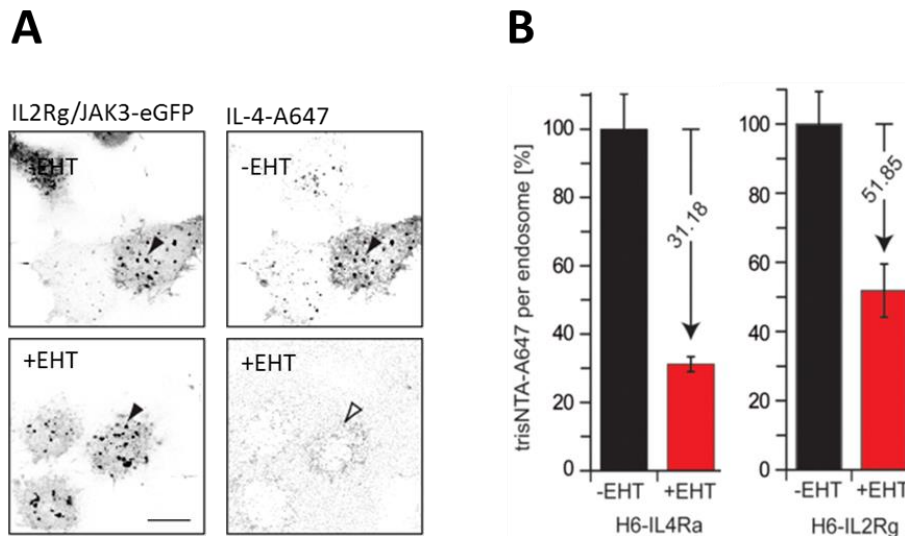


Figure 4.8: Effect of EHT-1864 on internalization of IL-4R subunits. (A) Upper panel: Close arrow shows accumulation of ligand in the endosome in the absence of drug. Lower panel: In the presence of drug, the ligand is absent in the endosomes due to inhibition of the trafficking machinery. Open arrow shows the absence of IL-4-A647 in JAK3-eGFP endosomes. (B) Receptor internalization is partially blocked; IL-4R α up to 31% and IL-2R γ up to 52% compare to non-treated cells. Error bar indicates SEM.

Next we checked the effect of inhibition of Rac1/Pak1-mediated endocytosis on signaling through either type 2 receptor complexes (IL-4R α /IL-13R α 1) either at endogenous concentrations or following overexpression of both subunits. For endogenous conditions, cells were transfected with STAT6, whereas for overexpression, cells were transfected with the IL-4R α /IL-13R α 1/STAT6. Cells were pretreated with inhibitors to exert the effect of drug. Cells were then washed out and stimulated with ligand IL-4 in presence and removal (denoted by “W”) of inhibitors EHT and IPA [67, 68]. Activity of pSTAT6 was analyzed by western blot for both sets of experiment. Results show that for endogenous type 2 receptor complex, signaling occurs only in presence of ligand (Figure 4.9A). Furthermore, blocking of Rac/Pak pathway also blocked pSTAT6 signaling. This signaling can be restored again after removal of drugs and the strength of the restored signal is comparable to pSTAT6 signal in non-treated cells. Similar results have been shown for Type 1 receptor complex (Kristina Kurgonaite, unpublished data). This concludes that endocytosis is an important step for signaling to occur and endocytosis occurs upstream of the signaling. However, for ectopic type 2 receptor complex (Figure 4.8B), when both subunits are overexpressed, we observed two things. First, in the absence of the ligand, we do see signaling which could be a result of stoichiometric interaction of overexpressed receptor. Upon addition of ligand, the signal intensity is increased due to activation by the ligand. Second, in the presence of drugs EHT/IPA, signaling is only partially blocked.

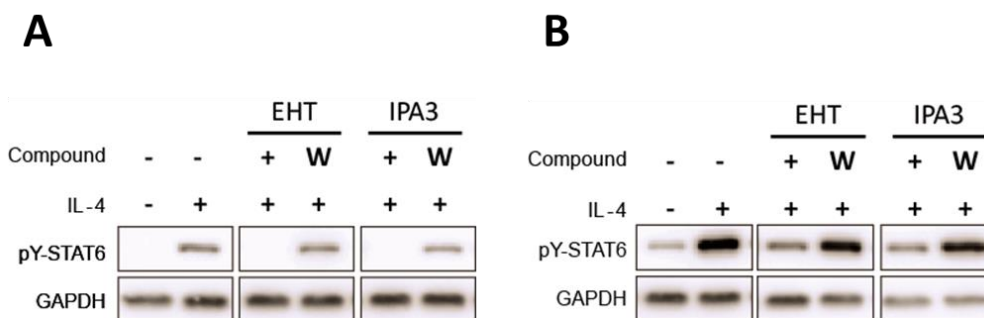


Figure 4.9: Effect of Rac/Pak inhibitors on pSTAT6 signaling. (A) Western blot showing an effect on pSTAT6 signaling under endogenous condition. Signaling is absent in absence of IL-4 and is activated in presence of IL-4. Signaling is completely inhibited in the presence of inhibitors but it can be restored after removal of drugs, which is denoted by “W” (wash out). (B) For ectopic type complex signaling is on even in absence of IL-4 but it is much stronger in presence of IL-4. In the presence of drug, signaling is reduced but not abolished and upon removal of drug (denoted by “W”), signaling is increased.

4.7 Endosomes maintain signaling

To compare the trafficking rates with the STAT6 phosphorylation kinetics we performed a pulse-chase. We used the endogenous type 2 signaling machinery for quantifying STAT6 phosphorylation. pSTAT6 signaling was determined under two different conditions: In continuous presence of ligand and after a pulse exposure of ligand. In first case, cells were stimulated with IL-4 at 4°C. Cells were then incubated at 37°C to induce endocytosis in presence of IL-4. For the second condition, after incubation at 4°C, cells were washed to remove ligand from the extracellular media and cells were incubated at 37°C to induce endocytosis in the absence of IL-4. In the second condition, signaling should be mainly coming from the endocytosed ligand population. Cells were then lysed after particular time intervals and the signal was detected by Western blot for both the conditions. Example image shows that pSTAT6 signal increases with time (Figure 4.10). Intensity of the bands were analyzed by ImageJ and plotted against time. As shown in the figure 4.11, for both the conditions, response curves shows a sigmoid shape ($EC_{50} = 12.6$ min). Onset of the response is slightly delayed with respect to receptor trafficking. The increase of the response persists for more than 30 min, without reaching a plateau. The stability of IL-4R α /IL-4 complexes at the cell surface has a half-life of about 6.5 min [64]. By this time, 95% of the ligand should be dissociated during the course of the experiment (30 min). Thus, the time dependence of the signaling response suggests that occupied, activated receptors remain present after internalization, presumably in the cortical endosomes, and maintain a long lasting output towards a transient stimulus.

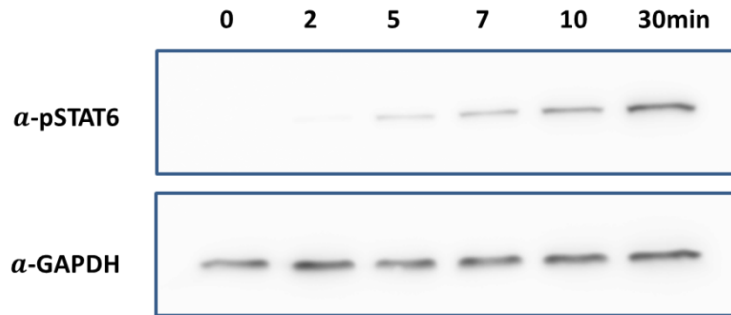


Figure 4.10: pSTAT6 kinetics. Upper panel shows pSTAT6 signaling is increasing with time. Lower panel shows control-GAPDH intensity representing number of cells for each sample.

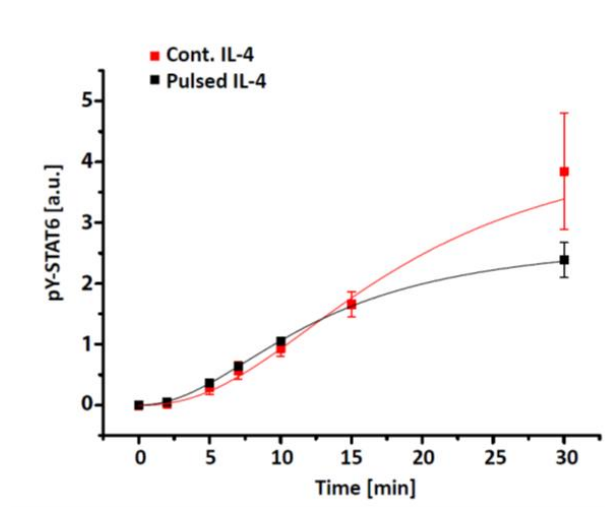


Figure 4.11: pSTAT6 kinetics. The graph shows intensity of pSTAT6 signal plotted against different time point. Red fit represents STAT6 kinetics in continuous presence of ligand whereas black fit shows in absence of ligand. Both the conditions shows sigmoid shape curve with delayed onset. Signaling is sustained for half an hour without reaching a plateau. $N=3$, Error bar indicates SEM.

In summary, I was able to prove that both type 1 and type 2 receptor subunits are accumulated in signaling endosome. These endosomes are separate compartment where ligand and receptors are constantly trafficked via Rac1/Pak1 pathway. Once the receptors are activated in the endosome, it may buffer the pathway against temporal fluctuations in ligand concentration on the extracellular sites, thus aiding in maintenance of signaling

Chapter 5

Results Part III: Regulation of receptor at the molecular level

Preface 5.1

In the previous chapters, I have established that the cytokine receptor containing endosomes lie adjacent to the plasma membrane. In addition, these distinct endosomes utilize the Rac1/Pak regulated actin polymerization machinery to replenish receptor populations in them. In this chapter, I seek to identify the regulator molecules which couple the receptor subunits to the actin machinery to achieve this contentious endocytosis

So far, the most upstream molecule in the cascade regulating actin machinery in the cytokine receptor endocytosis is the small GTPase Rac1. Small GTPases act as molecular switches to control many cellular pathways. They are toggled between “on” and “off” state by two regulatory molecules. GTPase activating protein (GAPs) promote the hydrolysis of GTP to GDP through the intrinsic GTPase activity, in turn switching it in “off” state. Guanine exchange factors (GEFs), on the other hand, allow GDP to dissociate, facilitating new GTP binding and switching the GTPase to “ON” state [69] (Figure 5.1). Among all the others, the Rho families GTPases – Rho, Rac1 and Cdc42 - are of special interest as they are known as regulators/modulators of actin cytoskeleton and are already known to be involved in several endocytic pathways. Specifically, involvement of the Rho family GTPase Rac1 in the actin mediated internalization of IL-2 receptor had previously been shown in the IL-2 context [39].

There are more than 60 GEFs identified for Rho GTPases. Among these, Vav proteins are a group of GEF proteins known to activate Rac1 [70, 71]. They are well studied in both cellular

and structural terms [72]. Vav belongs to diffuse B-cell lymphoma (Dbl) family of Rho-GEFs. Vav family consist of three isoforms in mammals; Vav1, Vav2 and Vav3. Vav1 is expressed exclusively in hematopoietic system whereas Vav2 and Vav3 show a broader expression. Vav proteins are a multi-domain protein and all mammalian Vav proteins have identical domain structures consisting of a Calponin homology (CH) domain – actin binding domain, an acidic (AC) domain, the Dbl (DH) domain that contains the Rho-GEF activity, a Plekstrin-homology (PH) domain which interacts with polyphosphoinositides, zinc finger (ZF) domain, proline rich (PR) rich region and two Src Homology 3 (SH3) and one Src Homology 2 (SH2) domain for protein protein interaction. The N-terminal of Vav is involved in its GEF activity whereas the C-terminal is important for interaction with specific phospho tyrosine (pY) residues of other proteins. Vav is the only GEF that has DH/PH motif in the same protein and SH2 – SH3 domains a characteristic of signal transducer proteins [73].

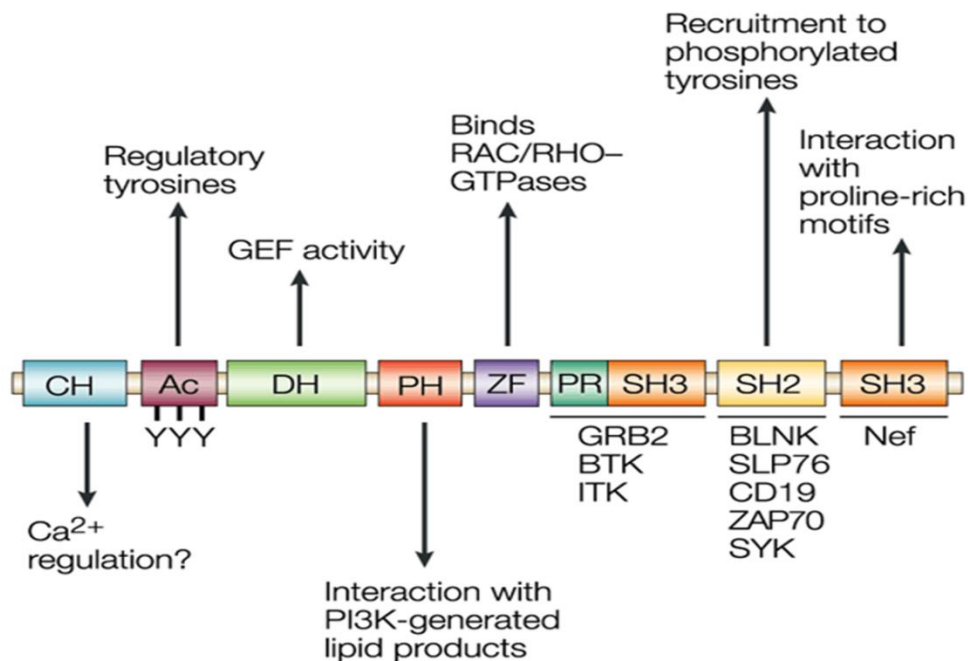


Figure 5.1: Structure of Vav. Vav is a multidomain protein. N-terminus of Vav is important for its GEF activity and C-terminus of Vav is important for the interaction with other proteins. Adapted from [74].

Rho/Rac1 GEFs can be activated in many different ways including plasma membrane translocation (Tiam1), migration from nucleus to plasma membrane (Cdc42), interaction with G-proteins (Ras GRF, PDZ-RhoGEF) or lipids (Sos,Dbl). In contrast, Vav is activated upon phosphorylation [74]. The AC domain of Vav contains three conserved tyrosines (Y) that are involved in auto inhibition of Vav GEF activity. In its inactive form, Vav is in a closed confirmation by binding of the AC domain in to active site of the DH domain, thus blocking GEF activity. Vav GEFs are activated upon phosphorylation of conserved acidic domain tyrosines (Y142, Y159, and Y172) that disrupt this autoinhibitory interaction between the acidic domain and the GEF catalytic Dbl homology domain [75, 76].

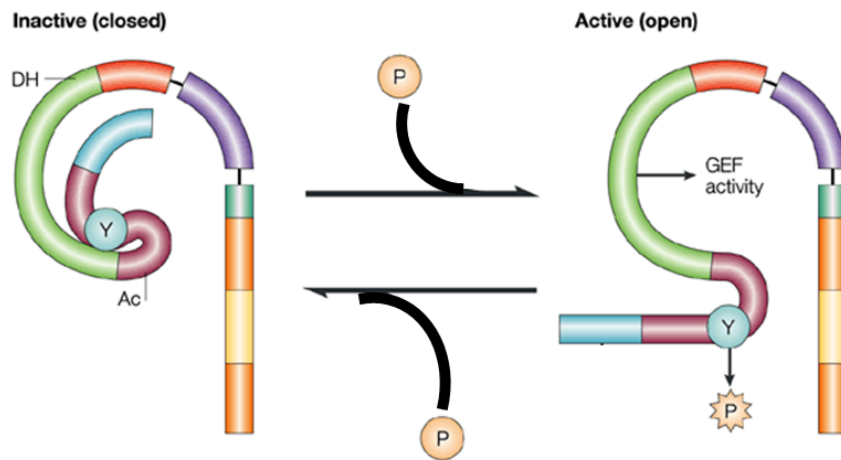


Figure 5.2: Structure if inactive and active form of Vav. In an inactive form Vav is in close confirmation by blocking the access of phospho -tyrosine residues in acidic domain. Upon phosphorylation of tyrosine residues in AC domain auto inhibitory loop opens which allows access of DH domain which promotes GEF activity. Adapted from [74].

Vav2 is known to regulate many signaling pathways downstream of receptor activation. Apart from the receptors, the upstream elements regulating Vav pathway are protein tyrosine kinases and adaptor molecules. Together with EGFR, PDGFR, BCR and TCR, Vav has been known to be involved 35 different membrane receptor pathways [77-79]. Also direct interaction of Vav with prolactin receptor [80], EPO-R [81], insulin receptor β subunit[82], gp130 and CD5 [83]have been reported [84]. For EGF receptors, Vav2 is known to slow down the receptor internalization and degradation thereby promoting enhanced signaling [85]. Importantly, involvement of Vav2 is also reported for IL-2 mediated signaling [69]. Moreover, both Rac and Vav knockout phenotype in the hematopoietic system is consistent with inhibition of IL-2R γ associated cytokine receptor signaling [86, 87]. Taken together, the link between Vav2 and cytokine receptor appears to be strong. However, the precise role of Vav2 and its mechanistic effects in cytokine receptor signaling are unknown. We suspected that Vav2 might be modulating the signaling by acting as regulator for endosome formation upstream of it.

To begin with, I wanted to check which isoform of Vav is present in our model system- the HEK cell line. Because HEK cells are epithelial cell line, I investigated the presence of only Vav2 or Vav3 but not Vav1. Non transfected cells were lysed and analyzed by western blot. Figure 5.3 shows that only Vav2 is detectable in HEK293T cell line. So, I proceeded with Vav2 for the further experiments.

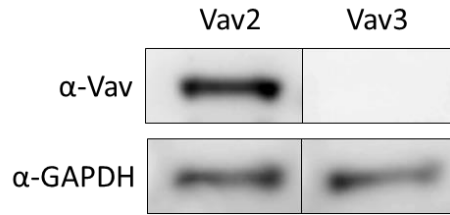


Figure 5.3: Detection of Vav2 and Vav3 in HEK293T cells by western blot. Image shows that Vav2 is present in HEK293T cells but Vav3 cannot be detected. GAPDH serves as a control.

5.2 Interaction of GEF with endosomes

Next, I wanted to check whether Vav2 localized to endosomes. Expression of non-activated Vav2 shows homogeneous distribution throughout the cell. However, we expected activated Vav2 to be localized specifically. To verify the association of activated Vav2 with the receptors, I performed immunostaining against pVav2, which signifies the active fraction of Vav2, in which autoinhibition of the GEF activity is released by phosphorylation of the linker domain. Cells were transfected with type 1 receptor complex and were stained against pVav2. Figure 5.4 shows association of JAK3-eGFP positive endosome (A) with pVav2 (B).

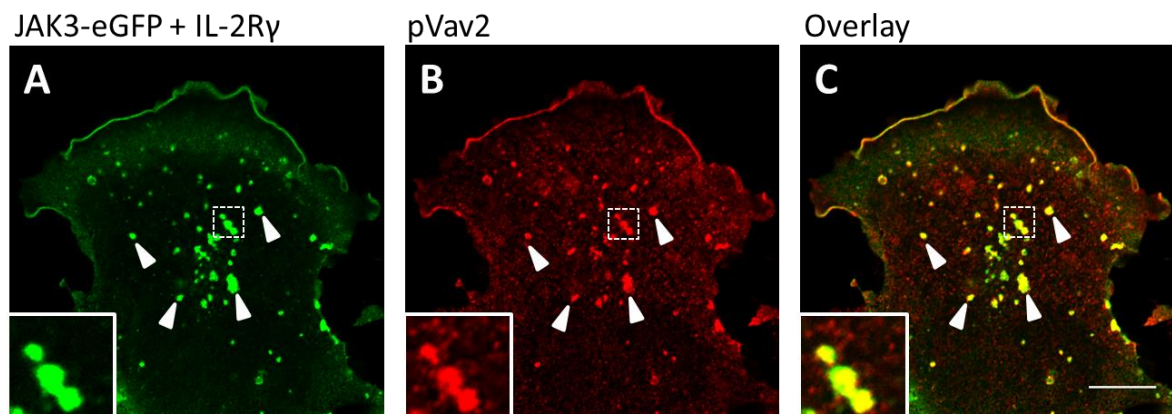


Figure 5.4: pVav2 association with endosomes. (A) Green channel shows JAK3-eGFP endosomes. (B) Red channel shows pVav2 expression in endosomes and along the periphery. (C) Overlay image shows pVAV2 is present in JAK3-eGFP positive endosome, shown by arrow heads. Square inset shows close up image of colocalized endosome. Scale bar 10 μ m.

Immunostaining shows association of pVav2 with endosome; however, this does not prove that Vav2 is directly interacting with the receptors and associated components. Thus, I used biochemical pull down assays to investigate whether there is a direct interaction between vav2 and any of the receptor components. Cells were transiently expressed with GFP tagged JAK3 and IL-2R γ alone, as well as JAK3 + IL-2R γ complex where either of them was tagged with GFP. Cells were lysed 24hr post transfection and pull down was performed with GFP and was detected with α -Vav2 and α -pVav2 antibody. Western blot shows that JAK3 + IL-2R γ complex interacts with Vav2 as well as pVav2 (Figure 5.5). Cytoplasmic JAK3 also

interacts with Vav2 and activated pVav2. While IL-2R γ can bind to Vav2, it fails to pull down pVav2. This suggests that Jak3 is required for activation of Vav2 and in the absence of JAK3, Vav2 is bound to IL-2R γ , but is not activated.

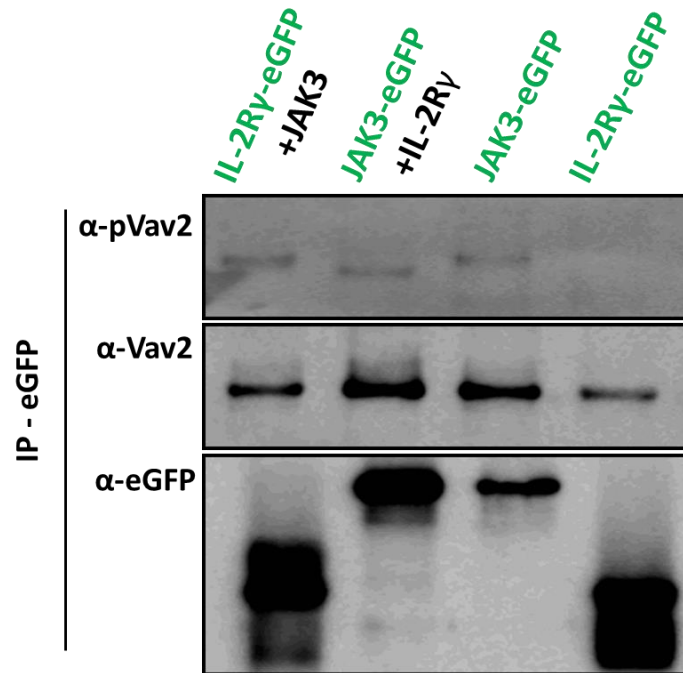


Figure 5.5: Interaction of Vav2 and pVav2 with type 1 receptor components via pull down. First two lane shows JAK3 and IL-2R γ interacts with Vav2 and pVav2. Third lane shows cytoplasmic JAK3 is able to interact with both but IL-2R γ cannot interacts with pVav2. eGFP serves as a control.

5.3 Domain specific interaction of Vav2

We wanted to further characterize the specific interaction site of Vav2 with JAK3 and IL-2R γ . To map this interaction, we created truncated forms of Vav2 with different domains deleted. I created two N-terminal domains; (1) N-term, (2) Δ SH2SH3 and three C-terminal domains consist of two SH3 domains; (1) SH3a, (2) SH2 domain and (3) SH3b (Figure 5.6). To avoid the background detection of interaction of endogenous Vav2 with JAK3 and IL-2R γ , domains were tagged with hemagglutinin (HA) tag. For the experiment, cells were transiently expressed with N-terminal and C-terminal domains together with JAK3-eGFP+IL-2R γ or JAK3+IL-2R γ -eGFP complexes as well as JAK3-eGFP and IL-2R γ -eGFP separately. GFP pull downs were detected with α -HA antibody to study domain specific interaction.

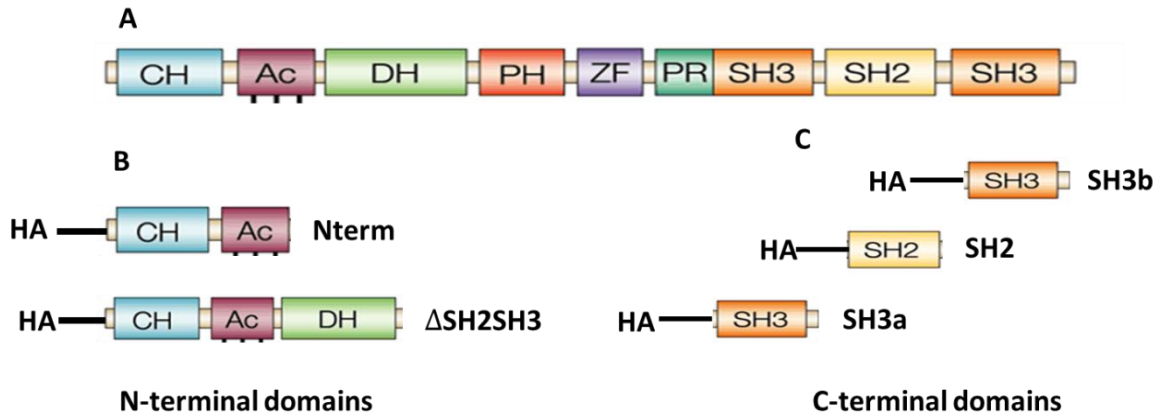


Figure 5.6: Domain specific interaction of Vav2. (A) Structure of Vav2 (B) N-terminal domains of Vav2 tagged with HA. “Nterm” consist of CH and AC domain; ΔSH2SH3 consist of CH, AC and DH domain. (C) C-terminal domain of Vav2. Three individual domains SH3a, SH2, SH3b tagged with HA. Adapted from [74].

Figure 5.7A shows that JAK3+IL-2R γ -eGFP complexes interact with both Nterm and ΔSH2SH3 constructs (red rectangle). JAK3-eGFP alone does not interact with the N-terminal domains. However, the C-terminal domains-SH3b and SH2 interact with JAK3-eGFP+IL-2R γ /JAK3+IL-2R γ -eGFP as well as JAK3 alone (Figure 5.7B). Presumably, interaction of SH2 and SH3b to JAK3+IL-2R γ is due to a binding of the Vav domains with JAK3. However, SH3a doesn't interact with either of them. Thus, I conclude that Vav2 is interacting with IL-2R γ with its N-terminal part and with JAK3 via its C-terminal part.

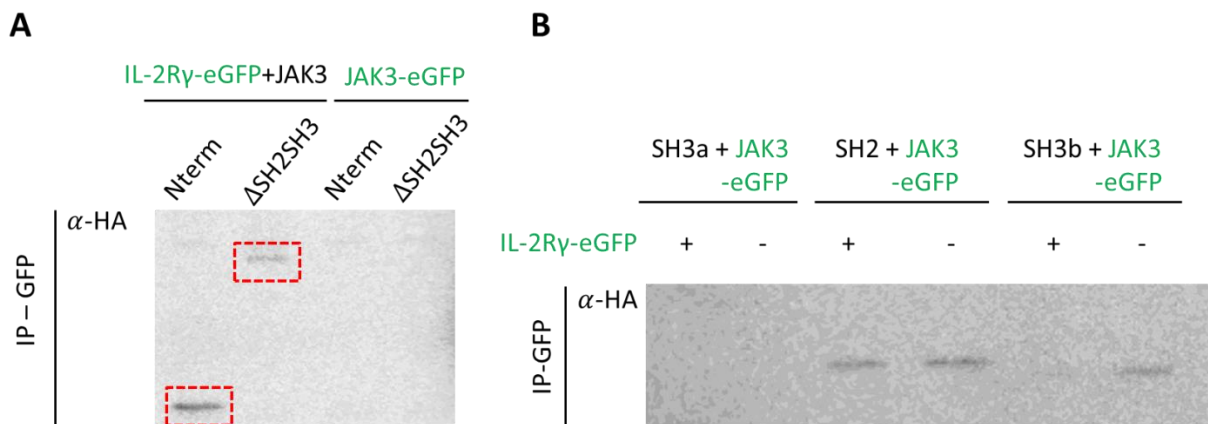


Figure 5.7: Interaction of N-terminal and C-terminal domains of Vav2. (A) First two lanes show that Nterm and ΔSH2SH3 interacts with JAK3+IL-2R γ complex. Bands are marked by red rectangular. Last two lanes show JAK3 doesn't interact with N-terminal domains. (B) Domain SH3a doesn't interact with JAK3+IL-2R γ complex or JAK3 alone. SH2 and SH3b interact with both the complex and JAK3 alone. This pull down shows that C-terminal of Vav2 is interacting with JAK3+IL-2R γ via JAK3 binding.

5.4 The IL-2R γ cytoplasmic region is important for the endosome formation

We mapped the interaction site of JAK3 and IL-2R γ on Vav2. In a similar way, I wanted to check which region of IL-2R γ is important for endosome formation. To check this, we created a truncated version of cytoplasmic tail of receptor (Figure 5.8). IL-2R γ cytoplasmic region was truncated from $\Delta 80$ to $\Delta 25$ amino acid lengths. This means in $\Delta 80$, there are only 80 amino acid after trans-membrane domain; in $\Delta 70$, there are only 70 amino acids after trans membrane domain and so on.

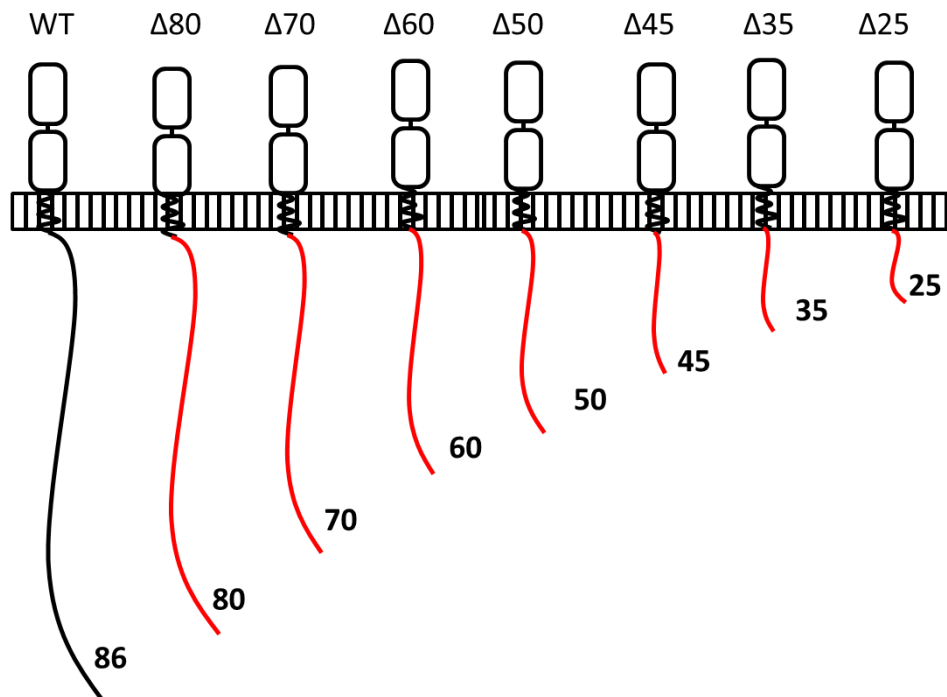
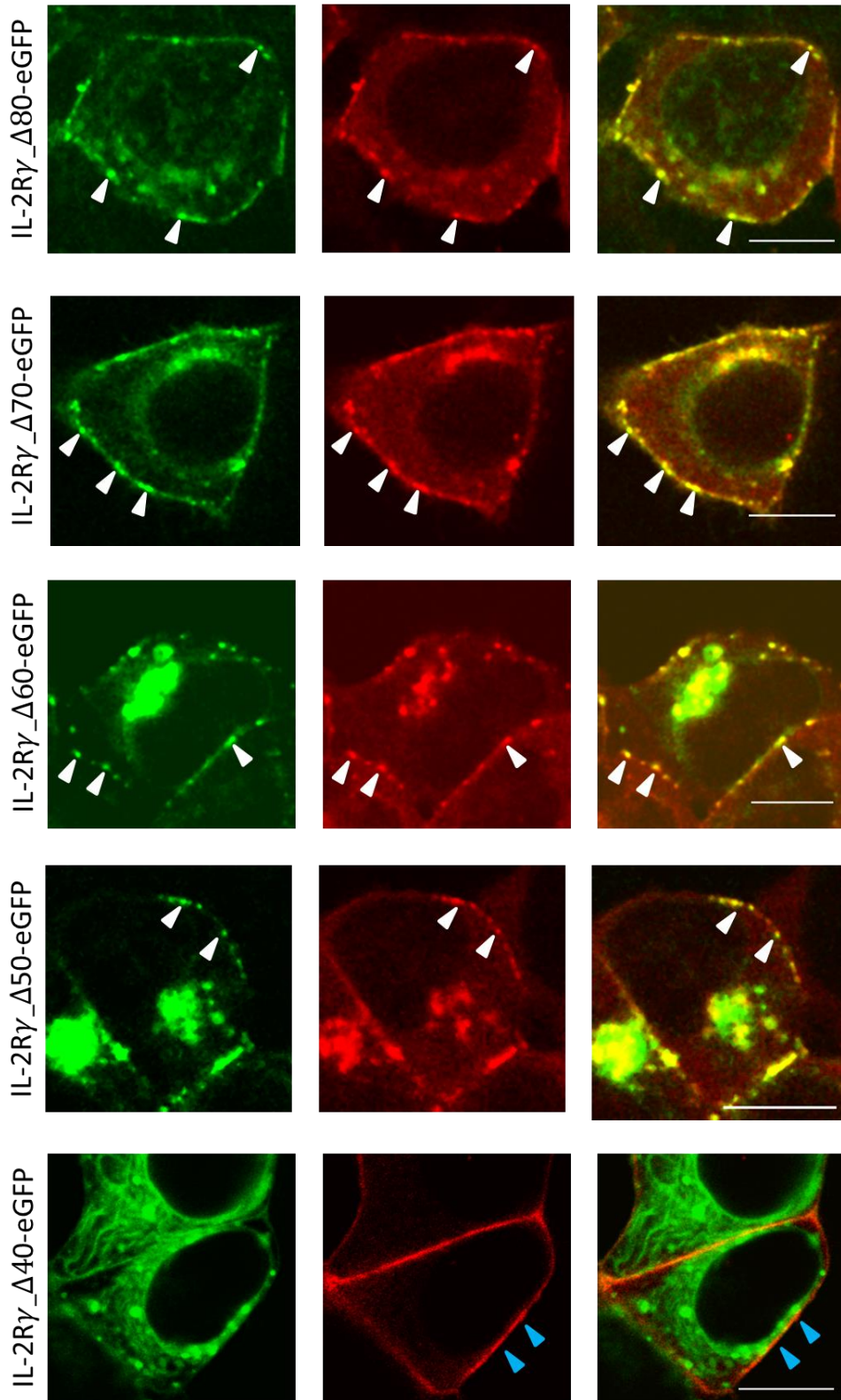


Figure 5.8: Schematic representation of truncated mutants of IL-2R γ . Figure shows N-terminal extra cellular domain, transmembrane domain and cytoplasmic tail region of IL-2R γ . The names depict that proceeding from left cytoplasmic tail of IL-2R γ is truncated after wild type (WT-86 amino acids), from 80 amino acids ($\Delta 80$) up to 25 amino acids ($\Delta 25$).

Cells were co-expressed with truncated IL-2R γ and JAK3-TagRFP. Cells were fixed and imaged with confocal microscope for endosome formation. Images (Figure 5.9) show that from wild type (86aa) till $\Delta 50$, endosome formation could be observed. Endosome formation is absent from $\Delta 40$ to $\Delta 25$. For $\Delta 40$ to $\Delta 25$ though JAK3 binding is present endosome formation is absent. In this experiment, IL-2R γ was tagged with eGFP on its C-terminal. To abate the possibility that GFP tagging could hinder endosome formation, we repeated the same experiment where IL-2R γ was tagged on its N-terminal. The presence of GFP on either N-terminus or the C-terminus did not affect the endosome formation. Regardless of the position of the GFP tag, we do not observe endosome formation after $\Delta 50$ -50 amino acids. We suspect that this region could be the putative binding site for the Vav2 and thus, results in absence of endosome formation.



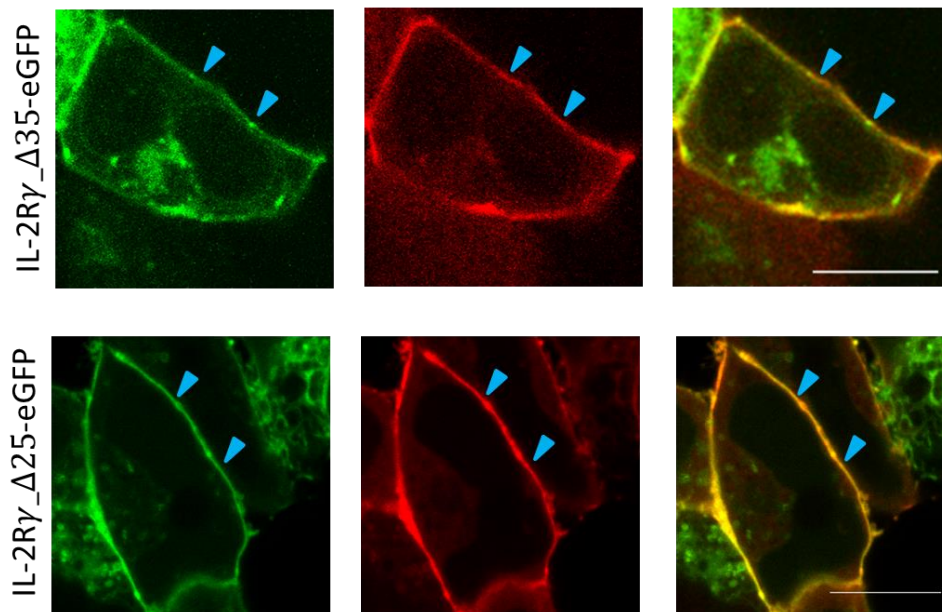


Figure 5.9: Endosome formation by IL-2R γ truncated mutants. Left panel shows expression of truncated mutants of IL-2R γ tagged with eGFP on C-terminus (green channel). Middle panel shows JAK3-TagRFP expression (red channel) and right panel shows overlay of both the channels. From IL-2R $\gamma_{\Delta 80}$ -eGFP to IL-2R $\gamma_{\Delta 50}$ -eGFP shows endosome formation (white arrow heads) with coexpression of JAK3. On expression of IL-2R $\gamma_{\Delta 50}$ -eGFP, endosome formation is abolished. From IL-2R $\gamma_{\Delta 40}$ -eGFP to IL-2R $\gamma_{\Delta 25}$ -eGFP, JAK3 and IL-2R γ co expression shows only homogenous plasma membrane distribution (blue arrow heads) but no endosome formation. Scale bar 10 μ m.

5.5 Interaction of Vav2 with IL-2R γ truncations

To verify if the 50 amino acid region of IL-2R γ from the transmembrane domain is crucial for Vav2 binding, I did a pull down assay with cells transiently expressing VAV2, JAK3 and IL-2R γ truncated mutants tagged with eGFP.

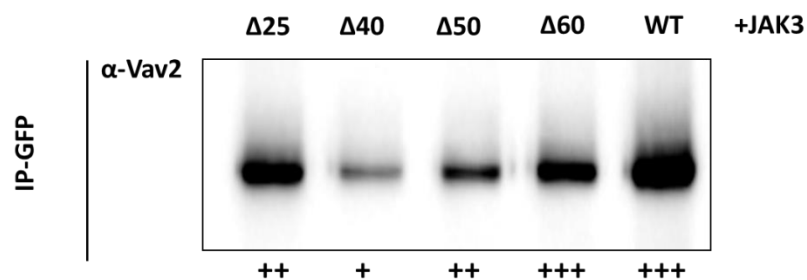


Figure 5.10: Pull down assay of Vav2 with IL-2R γ truncated mutants. Vav2 shows interaction with all the mutants. Interaction is decreasing with decreasing number of amino acids on the tail region except $\Delta 25$. Interaction of Vav2 with $\Delta 40$ and $\Delta 25$ could be due to the indirect interaction with JAK3.

Vav2 shows interaction with all truncated mutants of IL-2R γ (Figure 5.10). From WT to $\Delta 50$ Vav2 interaction was expected as they are able to form endosomes. The interaction of Vav2 with $\Delta 40$ and $\Delta 25$ could be due to the indirect interaction of Vav2 to IL-2R γ via JAK3.

Next, we wanted to check interaction of IL-2R γ and Vav2 in the absence of JAK3 to avoid indirect interaction. Since IL-2R γ is not recruited to the plasma membrane in the absence of JAK3, we directly targeted IL-2R γ to the membrane (Figure 5.11A) by creating a myristoylated version of IL-2R γ . The extracellular and the trans-membrane domain of IL-2R γ were removed and the molecule was myristoylated before the cytoplasmic region. This enables IL-2R γ to escape the secretory pathway and is targeted directly to the plasma membrane. As shown in the image, myristoylated IL-2R γ (Myr-IL-2R γ -eGFP) is able to translocate to the membrane even in the absence of JAK3 (Figure 5.11B).

To check if Myr-IL-2R γ -eGFP is able to recruit JAK3, cells were transiently expressed with Myr-IL-2R γ -eGFP-eGFP and JAK3-TagRFP and imaged by confocal microscope. Figure 5.9 shows Myr-IL-2R γ -eGFP is able to recruit to JAK3, but their co expression does not form endosomes.

To force endosome formation with cytokine receptor components, we co-transfected cells with Myr-IL-2R γ -eGFP and wild type IL-2R γ and JAK3-TagRFP. As shown in the figure 5.13 expression of JAK3 together with wild type IL-2R γ is able to form endosomes (a,d). Also, Myr-IL-2R γ -eGFP is recruited to the endosome (b,e). This suggests a putative role of transmembrane domain or a cooperative effect with Jak3 in receptor recruitment to the plasma membrane.

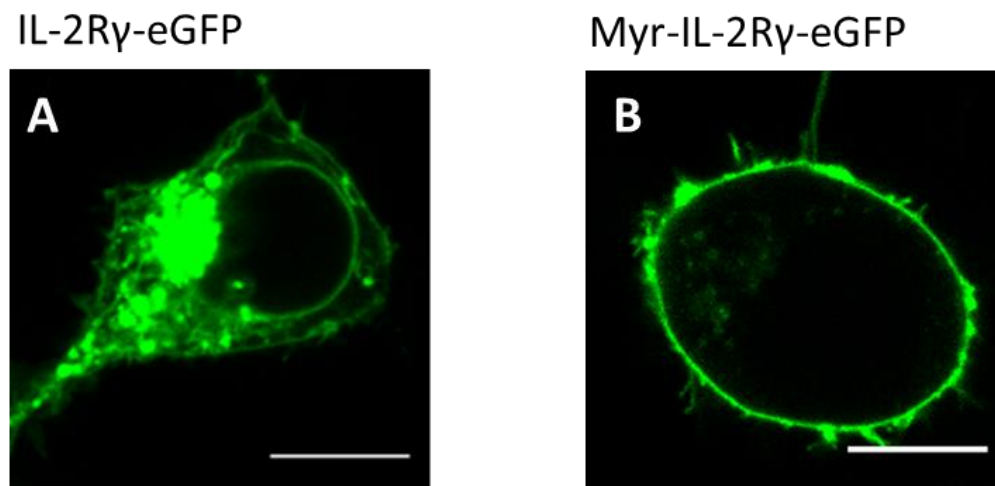


Figure 5.11: Myr-IL-2R γ -eGFP expression. (A) IL-2R γ is alone is localized in perinuclear region. (B) Myristoylated IL-2R γ is recruited to the membrane even in the absence of JAK3. Scale bar 10 μ m.

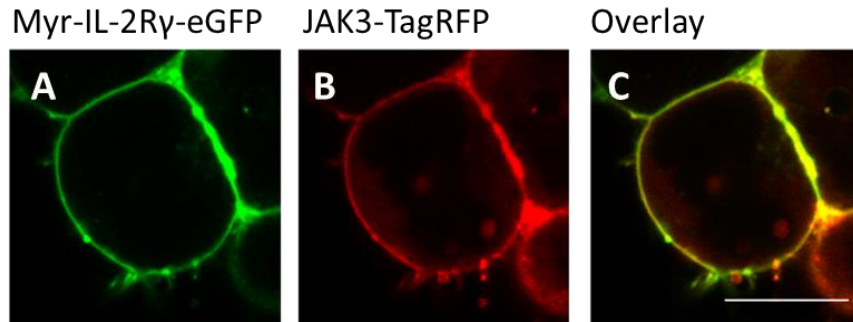


Figure 5.12: Myr-IL-2R γ -eGFP fails to form endosome. (A) Myr-IL-2R γ -eGFP is recruited to the membrane. (B) JAK3 is also recruited to the membrane by IL-2R γ c. (C) Overlay shows that JAK3 and IL-2R γ is recruited to the membrane but they fail to form endosomes. Scale bar 10 μ m.

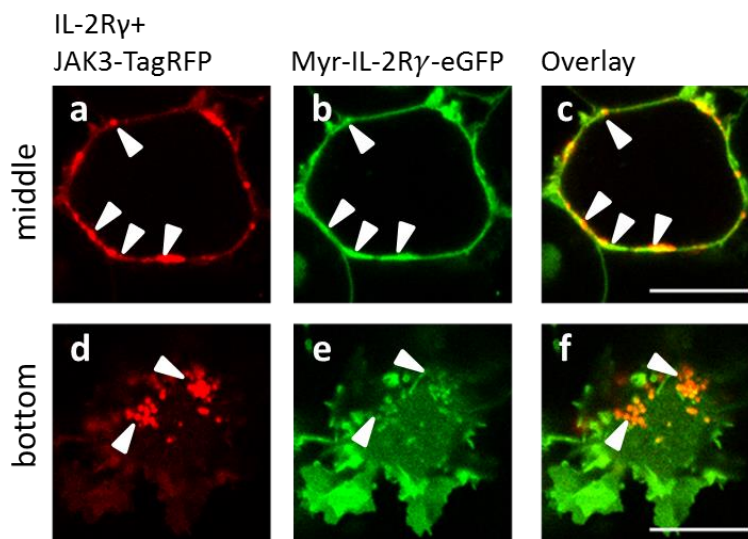


Figure 5.13: Myr-IL-2R γ -eGFP is failed to recruit in to pre-formed endosomes. (a,d) Red channel shows endosome formation by IL-2R γ and JAK3-TagRFP. (b,e) Myr-IL-2R γ -eGFP is recruited to the preexisting endosomes. (c,f) Overlay image shows that Myr-IL-2R γ -eGFP is recruited to the plasma membrane and colocalize JAK3/IL-2R γ positive endosome. Scale bar 10 μ m.

5.6 Vav2 can modulate signaling

So far I mapped the interaction sites of Vav2 and showed that may be it indirectly related to endosome formation. Next I wanted to check if Vav2 is required for signaling. STAT6 phosphorylation and STAT6 dependent reporter gene assays provide a highly specific readout for IL-4R signaling. To check whether Vav2 has a role in signaling, cells expressing gain of function (GOF) and loss of function mutants (LOF) of Vav2 were checked for pSTAT6 signaling compare to wild type. As reported previously, the first five N-terminal domains of Vav1-CADPZ function together to regulate its GEF activity [76]. Based on this study, we considered the N-terminal domains with c-terminal parts lacking, as loss of function mutants. Also, it has been reported for Vav1 that phosphorylation of Tyr174 is important for its GEF activity [71, 76]. However, additional phosphorylation of Tyr142 and Tyr160 facilitate activation of Vav1 by making Tyr174 assessable in auto inhibitory loop [88, 89].

Phosphorylation of Tyr142 and Tyr160 makes Tyr174 accessible for the further phosphorylation and in turn GEF activation [76]. On the basis of these studies, we performed a Tyrosine (Y) to aspartic acid (D) mutation at the amino acid position corresponding to similar mutation in Vav1, which holds Vav2 in open active configuration. I made three gain of function mutants; GOF1 - Y172D, GOF2 - Y142D + Y159D, GOF3 - Y142D + Y159D + Y172D (Figure 5.14).

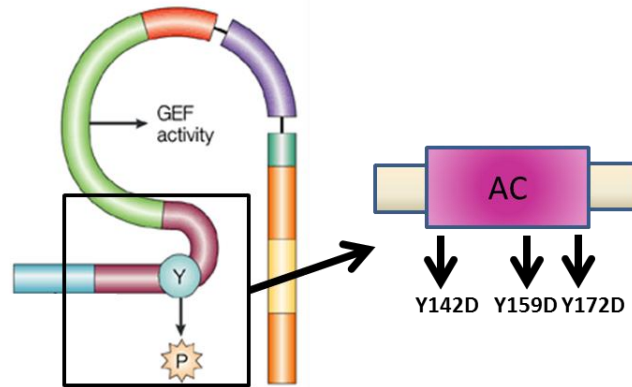


Figure 5.14: Schematic of mutation in Vav2 acidic domain (AC). Three Mutations were created at three different tyrosine residues in AC domain to make activated form of Vav2. Adpated from [74].

Cells were co transfected with STAT6 and GOF or LOF mutants of Vav2. Cells were stimulated with IL-4 ligand for 30 min and checked for pSTAT6 level. Figure 5.15 shows that compared to wild type Vav2, N-term domain constructs show decreased signaling whereas Δ SH2SH3 constructs show increased signaling. While both GOF2 and GOF3 show increased signaling compared to the wild type. Thus, I conclude that Vav2 can modulate the pSTAT6 signaling.

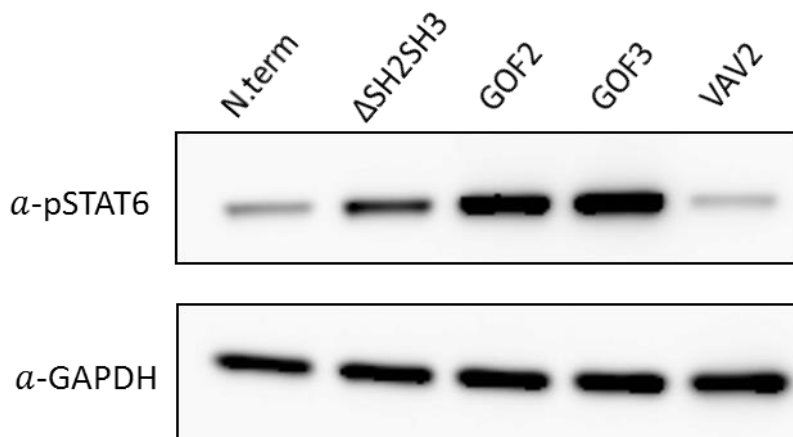


Figure 5.15: Effect of gain of function and loss of function of Vav2 on pSTAT6 signaling. The blot shows that compared to endogenous pSTAT6 intensity loss of function N-term gives equal signal intensity but Δ SH2SH3 gives more signaling. Compared to gain of function (GOF2 and GOF3) the signal intensity is less. GOF gives much stronger signal intensity compare to endogenous or LOF Vav2.

Furthermore I also tried knockdown of Vav2. Cells were first treated with esiRNA Vav2 and control RULC esiRNA (Renilla luciferase) and later transfected with STAT6. Cells were lysed after IL-4 ligand incubation and pSTAT6 level was analyzed by western blot. However, shows that in presence of esiRNA Vav2, level of endogenous Vav2 is reduced but it does not have any effect on pSTAT6 signaling (Figure 5.16). This could be due to the redundancy of Vav isoforms.

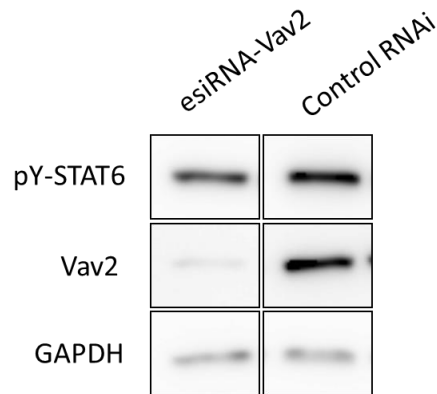


Figure 5.16: Effect of Vav2 esiRNA on pSTAT6 signaling. In the presence of esiRNA Vav2 is diminished but it does not show any effect on pSTAT6 signal compared to control RULC esiRNA. GAPDH was used as a control representing number of cells.

To summarize, I have shown that activated Vav2 is localized endosomes and directly interacts with the receptor complex. I have mapped the interaction sites of Vav2 with IL-2R γ and JAK3. I have also shown that the 50 amino acid region of IL-2R γ is crucial for endosome formation. Although we could not establish a direct link between the putative roles of Vav2 in endosome formation, Vav2 gain of function mutant enhances signaling. We could not see any effect upon esiRNA knockdown. This may be a result of redundancy in Vav isoforms. To overcome the effects of redundant isoform of Vav, multiple isoform knockouts of Vav are required. It is also possible that Vav2 is dispensable and other regulatory proteins function to activate the actin machinery resulting in endosome formation and signaling.

5.7 Outlook

JAK3 mutant fails to form endosome

An important link between Vav2, signaling and endocytosis is provided by JAK3 mutants involved in severe combined immunodeficiency (SCID). A few SCID related mutants of JAK3 had been already investigated [57, 90]. Our lab in addition discovered that these SCID related JAK3 mutants fail to form endosomes (Figure 5.14 A, unpublished data). Figure 5.17B shows both JAK3 mutants JAK3-K556A-eGFP (K5) and JAK3-R402H-eGFP (R4) fail to form endosomes compare to the wild type. We wanted to check whether Vav2 and pVav2 interacts with these Jak3 mutants or not. Cells were co-transfected with IL-2R γ and K5 or R4 JAK3 constructs. Immunoprecipitation was performed using antibody against eGFP and blots probed for Vav2 and pVav2. eGFP was probed as a positive marker. As shown in Figure

5.17C, the pseudokinase mutant JAK3-K5 is able to bind Vav and pVav2 (Figure 5.17C). However, the R4 mutant, which affects the SH2 domain is able to interact with Vav2 but does not selectively pull down pVav2.

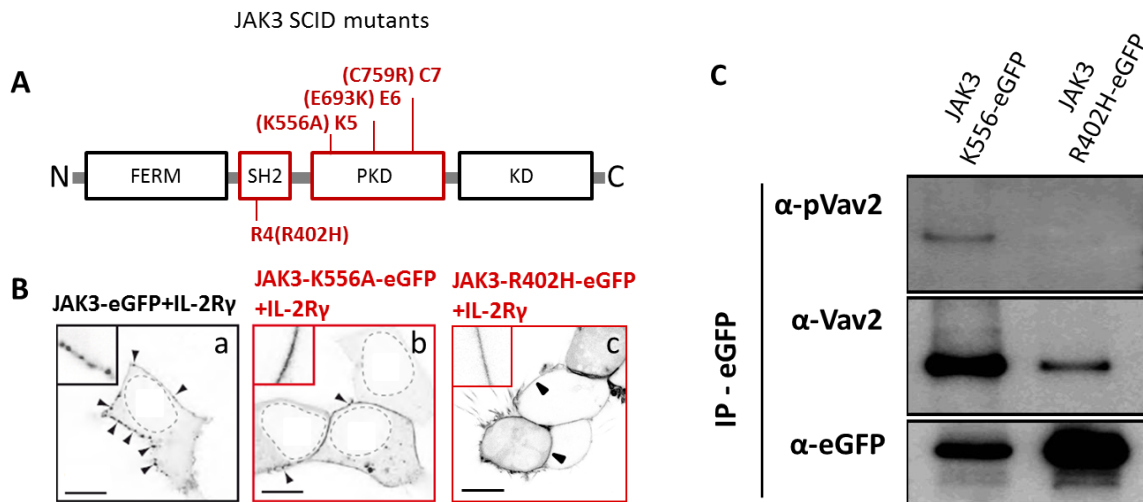


Figure 5.17: Co expression and immuno precipitation of JAK3 SCID mutants. (A) Schematic of JAK3 kinase, showing mutations in pseudo kinase domain, K5, E6, C7 and in SH2 domain, R4. (B) Confocal images of coexpression of IL-2R γ with wild type as well as JAK3 mutants shows that IL-2R γ forms endosomes upon co expression with wild type JAK3 (a). Co-expression of IL-2R γ with K5 and R4 (b,c) failed to form endosomes. (C) Pull down assay shows K5 mutant is able to interact with Vav2 and pVav2 while R4 interacts with Vav2 but not with pVav2.

We presume that R4 is unable to bind pVAV2 because of the mutation in its phospho tyrosine binding pocket [91]. This results in impaired stabilization of Vav2 being in open active configuration by JAK3. To compensate this, we created a phosphomimic Vav2 gain of function mutants, which should not require JAK3 to stabilize it in its active state. Cells were transfected with either wild type IL-2R γ and JAK3 or JAK3-R4, IL-2R γ and the Vav2 GOF constructs. However, while the Vav2-GOF construct affected overall cell morphology, formation of the JAK3 positive cortical endosomes was not rescued (Figure 5.18B).

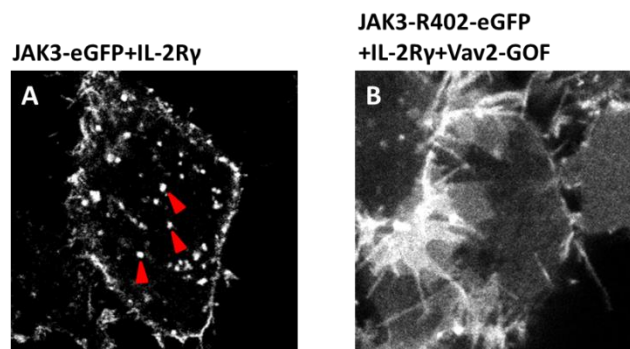


Figure 5.18: JAK3-R402H-eGFP fails to form endosome in the presence of Vav2 gain of function. (A) Endosome formation, pointed by red arrow heads upon co expression of JAK3 and IL-2R γ . (B) co expression of R4, IL-2R γ and Vav2 gain of function do not form any endosomes.

Future directions

Although I could show that Vav2 is a suitable candidate as a GEF by showing that Vav2 is involved in endosome formation and directly interacts with the receptor, the function of Vav as a GEF in cytokine receptor internalization needs further detailed investigations. Our experiments, suggests further investigations along the following lines:

1) Why does Vav loss of function not affect signalling?

As described before, Vav has three isoforms; Vav1, Vav2 and Vav3. In our experiments we could not detect Vav3 by standard western blotting. However, reappraisal of published transcriptome data shows that Vav3 is present in HEK293T cells at the level of about 20% of Vav2 [92]. Although it is widely assumed that Vav1 is present only in hematopoietic cells, we also found that Vav1 is present at 10% of the level of Vav2 in HEK293T cells. Therefore, future experiments should involve knocking out all the three isoforms to clearly elucidate the function of Vav. There is also a possibility of a different GEF functionally substituting for Vav. In addition the knock down efficiency achievable by esiRNA may in principle be insufficient, and other approaches such as genetic knockouts may be required.

2) Why is Vav2 pulled down with truncated mutants of IL-2R γ ?

A possibility is that Vav2 is connected to JAK3 and IL-2R γ of different complexes and not within the same complex. This might explain the pull down of Vav2 in truncated versions of IL-2R γ . The 40aa of IL-2R γ may also be important for other protein-protein interactions. During preparation of this thesis another paper has been published that implicated Vav2 in IL-2R internalization. The signalling factor PI3K is a specific regulator of the clathrin-independent dynamin-dependent endocytosis of IL-2 receptors [93]. PI3 kinase facilitates conversion of PIP2 to PIP3 and induction of Vav2 which activates Rac1. Activated Rac1 is recruited to the sites containing IL-2R and enhances the actin polymerization rate. This suggests a potential role of PI3 Kinase in endosome formation, that will have to be experimentally separated from the contribution of Vav.

Discussion

During recent years many studies have revealed that synergistic interactions of cell signalling processes and endocytosis are important for various cellular processes including e.g. animal development, metabolism, motility, differentiation, and immune responses. It is therefore well established that signalling and endocytosis processes are functionally and mechanistically linked in many receptor systems. This also means that the degree to which signalling and endocytic machinery can be independently manipulated in experiments is limited and a variety of tools are required to elucidate the relationships between these machineries.

In this thesis, I explored the significance of endosomes for cytokine signalling. Previous studies had established that, upon binding of ligands, cytokine receptors oligomerize, which brings the associated JAK kinases into close proximity, resulting in activation by cross-phosphorylation [55]. For certain cytokine receptor pathways it had also been observed that the activated receptors localized in endosomes upon activation. However, the details of how and why the receptors localize to endosomes were not known. It also remains to be elucidated whether endocytosis serves as a termination mechanism or has a positive role in signalling.

The Weidemann and Bökel labs focused on one cytokine receptor, IL-4R, which forms two types of complexes; termed type1 and type2. Type1 IL-4R complexes comprise of the receptor subunits IL-4R α and IL-2R γ bound by IL-4, whereas type2 complexes comprise of the subunits IL-4R α and IL-13R α 1 bound by either IL-4 or IL-13 [53]. Extensive studies have been carried out on the receptor affinity, receptor localization and receptor internalization of IL-4R components [94, 95]. However, these studies have not elucidated the mechanistic details of pathway activation under physiological conditions.

Worch *et al.* showed that neither IL-4R α nor IL-2R γ exist as pre-formed dimers at the plasma membrane [96]. This suggests that ligand binding must take place to drive the receptors to undergo complex formation. Weidemann *et al.* reported for the first time a systematic investigation of the receptor-complex formation at single molecule resolution in live cells [47]. Under over-expressed conditions and using FCCS, they reported that ligand could induce detectable dimerization in type 2 IL-4 receptor system, but for type 1 IL-4R complexes, IL-2R γ recruitment was not detected. This suggested that the type 1 receptor complex formation may be facilitated by a more complex mechanism. This required precise measurement of affinities between the receptors. Before I joined the project, complex formation between the receptor subunits of the different IL-4R complexes was characterised using an improved FCCS approach in living cells (TW, unpublished data). Using this approach we observed that respective ligands can indeed induce the formation of all three receptor complexes on the plasma membrane albeit with low efficiency. FCCS also allows the quantification of the average numbers for individual receptor and complex species within the focal volume. From this, dissociation constants for these complexes (K_{d2D}) can be estimated. Since the complex formation and dissociation take place at the plasma membrane

the two-dimensional $K_{d,2D}$ is given in units of receptors/ μm^2 . The $K_{d,2D}$ values we obtained were 200 ± 40 receptors/ μm^2 for the IL-4R α :IL-4/IL-13R $\alpha 1$ interaction, 530 ± 100 receptors/ μm^2 for IL-4R α /IL-13:IL-13R $\alpha 1$, and 1100 ± 170 receptors/ μm^2 for IL-4R α :IL-4/IL-2R γ .

Although these values for affinities are surprisingly low, they do make sense with respect to signalling strength of the respective complexes. The dimerization probabilities deduced from the K_d values measured by FCCS, follows the order - IL-4/type 2 > IL-13/type 2 > IL-4/type 1. According to the classical view that receptor dimerization is the limiting factor for pathway activation, higher affinities should translate into stronger signalling output. In agreement with this old hypothesis [97], our affinity data correlates with the signalling strength which was determined by the level of pSTAT6 signalling intensity for all three receptor complexes (Kristina Kurgonaite, unpublished data). In contrast, in the structural study by Laporte *et al*, the affinities between isolated ectodomains (IL-4:IL-4R α /IL-13R $\alpha 1$ and IL-4:IL-4R α /IL-2R γ) as measured in free solution failed to correlate with the signalling strength, thus requiring complex explanations for the relative signalling strength [98].

Curiously, physiological cytokine receptor concentrations are about 1 receptor/ μm^2 [99], which is at least two orders of magnitude below the measured k_d values. Thus, even at full ligand occupancy dimerization will be very low at the plasma membrane. In our overexpressed condition we worked at plasma membrane receptor density of around 300 to 500 receptors/ μm^2 , which was just about sufficient to detect complex formation. However, this observation suggests that a concentration step is required to facilitate receptor dimerization. Simultaneously, we observed that the receptor components were localized into speckle like structures in the live cells. We suspected these to be endosomes, which potentially could actively enrich the population of receptors, allowing overcoming the weak affinities and thereby, facilitating complex formation.

To test this hypothesis, we proceeded with the molecular characterization of the speckle like structures. We found that these endosomes are positive for both early recycling Rab markers Rab5, Rab11. In addition, I could show that they are also labelled by immunostaining against the ESCRT factor Hrs, a marker for multi-vesicular bodies [100]. Consistently, I could show by electron microscopy that these endosomes are multi-vesicular bodies of approx. 300nm in diameter that are tightly associated with the actin cortex. Quantification of IL-2R γ /JAK3-eGFP-gold particles on the plasma membrane and on the limiting membrane of the multivesicular endosomes from TEM images have shown that the number of gold particles per unit length is enriched approximately 10 fold on the limiting membrane compared to the adjacent plasma membrane. Considering that the endosomal limiting membrane is a two dimensional surface, we can approximate the ratio of receptor density per area between endosomal and plasma membrane surface density from the linear density by squaring. The receptor subunit IL-2R γ is therefore enriched about 100 fold within the endosomal limiting membrane. This enrichment takes the local receptor concentration into the range of measured K_d values, which is also the range at which receptor dimerization can efficiently take place.

To further understand the mechanism of enrichment, we probed the route of trafficking of the IL-4 receptors into the endosomes. Previous studies had already established that IL-2R γ chain can be internalized in both constitutive and ligand induced manner [40, 101]. IL-2R chain can be internalized, in the IL-2R context by Rac1/Pak1 mediated mechanism [37]. It has been also shown for the IL-4 system that the presence of ligand IL-4 induces internalization of IL-4R α but they did not specify which pathway [43]. In these experiments, the receptor internalization was tracked using radio labelled ligand IL-4 and the surface bound receptors were quantified by acid stripping methods over time scales of hours. Instead, we used receptors carrying a hexahistidine tag on their N-terminus, which could be specifically labelled with fluorescent dyes and can be monitored independent of ligand. Since this approach allows live cell imaging, our experiments represent a more accurate measurement of the rapid dynamics of receptor trafficking which occurs on a time scale of minutes. We observed that IL-4R α is internalized with similar rate irrespective of the presence of ligand. This, to our knowledge, is the first report quantitatively describing constitutive trafficking of the IL-4R α to a defined internal structure. This is in stark contrast to other pathways like TGF β and RTKs, where receptor uptake is generally shown to be a consequence of pathway activation [9]. We also observed that the trafficking kinetics of IL-4R α and IL-2R γ are similar with a half time around 8 min. These trafficking kinetics explains the slow endosomal recovery rate observed by FRAP, and also suggest that all three receptor subunits are trafficked to the same target compartment using the same pathway. We prove this presumption by using pharmacological inhibition to interfere with a specific endocytosis route. It is well established that IL-2R subunits are internalized via Rac/Pak mediated actin regulatory pathway [41]. Consistent with this, we observed that type 1 IL-4R subunits IL-4 and IL-4R α are also trafficking via Rac1/Pak1 pathway, as receptor and ligand internalization was inhibited when this pathway was specifically blocked using drugs. This further leads to inhibition of signalling (Kristina Kurgonaitė, unpublished data)

The absolute enrichment we observe from EM is about 100 times and the rate of internalization is with a half time of about 8 min. The enriched concentrations in the endosomes are a steady state value. To maintain this enriched concentration in the endosomes ($C_{endosome}$) compared to the concentration at the plasma membrane (C_{pm}), the rate of internalization (k_{in}) must be much faster compared to the rate of trafficking out (k_{out}).

$$k_{in} \times C_{pm} = k_{out} \times C_{endosome}$$

$$C_{endosome} = 100 \times C_{pm}$$

$$\therefore k_{in} = 100 \times k_{out}$$

This kind of maintenance of steady state concentration is in contrast to other regulated endocytic pathways such as clathrin-mediated endocytosis, where phosphorylation of receptors lead to recruitment of ubiquitin ligases, which serves as an internalization signal and drives an active internalization, resulting in an increased internalization rate upon activation. As a consequence, e.g. EGF receptors are only transiently localized to the endosomes from which they signal.

Based on the following observations: 1. The receptors have very low affinity at the plasma membrane 2. The receptors are enriched in endosomes. 3. The receptors are trafficked constitutively in an actin machinery dependent manner irrespective of the presence of the ligand; we propose a new model for the function of endosomes, where the endosomes fulfill a thermodynamic role in cytokine signalling. The endosomes act as a site of subcellular receptor enrichment, where the dynamics of trafficking are tuned so that it results in an increased concentration of the receptors, thereby enabling them to overcome their weak affinities and dimerize in the presence of ligand. The observation that this concentration is maintained even in the absence of the ligands suggests that the endosomes are poised to signal as soon as the ligands are internalized with the receptors.

To confirm that in accordance with our model, the receptor dimerization indeed takes place in endosomes, FLIM/FRET technique was used to detect receptor dimerization within the endosome (Christian Bökel, unpublished data). For detecting active receptor complex formation, life time shift in donor IL-4R α CyPet was measured with acceptor IL-2R γ YPet or IL-13R α 1 YPet in the presence of ligand IL-4 at the plasma membrane and within the endosome. For low affinity type 1 receptor, we detected pronounced reduction in donor lifetime only within the endosome (2.06 ± 0.05 ns vs. 1.57 ± 0.06 ns, $p < 0.01$) while the effect was much less pronounced at the plasma membrane (2.29 ± 0.05 ns vs. 2.18 ± 0.07 ns). In contrast, for the higher affinity type 2 receptor complex we observed strong reduced donor life time shifts both within the endosome (2.16 ± 0.06 ns vs. 1.78 ± 0.04 ns; $p < 0.01$) as well as at the plasma membrane (2.34 ± 0.04 ns vs. 1.85 ± 0.04 ns, $p < 0.01$). In agreement with the FCCS results, presence of ligand induces some degree of dimerization at the plasma membrane. However, it should be noted that this is again an overexpression system. Under physiological conditions, when the receptor concentrations are low at the plasma membrane, we still expect oligomerization to be happening exclusively within the endosomes.

We further reasoned that if the endosomes only serve a thermodynamic purpose of allowing complex formation by enriching the receptor densities, their necessity could be by-passed by expressing high enough concentration of receptors on the plasma membrane. Active signalling from the plasma membrane can be inferred by probing pSTAT6 in the presence of Rac/Pak inhibitors EHT and IPA. When only one of the receptors is over expressed, no signalling takes place, indicating insufficient dimerization even in the presence of ligand occupied receptors. However, when both the receptors are overexpressed, signalling is restored even when endosome formation is blocked, confirming our hypothesis that the primary reason behind absence of signalling from the plasma membrane is the insufficient concentration of receptors. Under physiological conditions, the endosomes provide a means to overcome this low concentration by enriching the receptor subunits in a confined compartment.

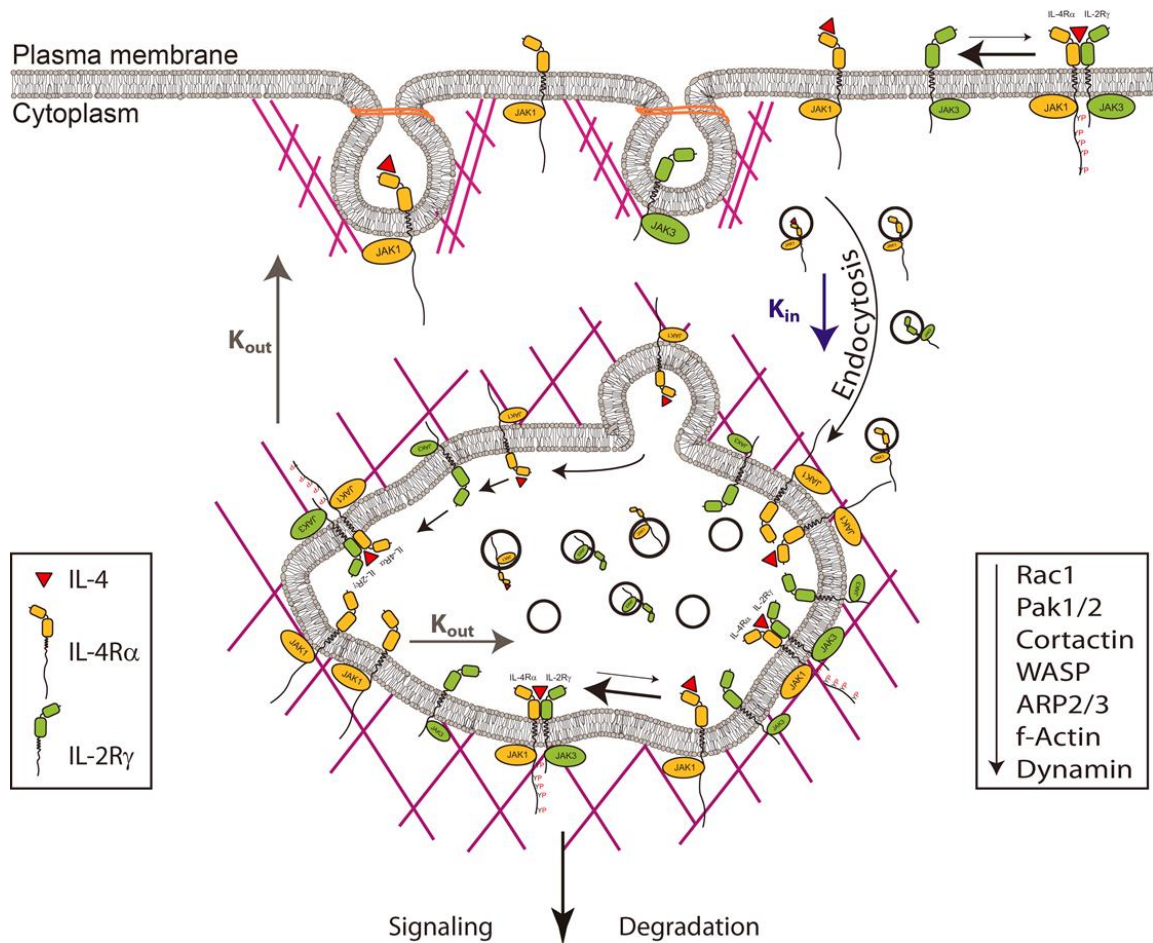


Figure 6.1: Schematic model of type 1 IL-4R trafficking and signaling. IL-4R subunits IL-4R α (orange) and IL-2R γ (green) do not form active receptor complex on the plasma membrane due to low affinity between receptor subunits. Receptor subunits are constitutively internalized independent of ligand IL-4 (red) from the plasma membrane into the endosome that are stably anchored within actin cortex (magenta lines) via Rac/Pak pathway. This leads to the high concentration of receptors within the endosome. Endosome facilitates to overcome weak affinity and receptor forms active complex within endosome.

Signalling from endosomes where high steady state concentration is maintained by low exit rates may also provide other advantages. For example, dependent on the dynamics of trafficking, the signalling can be buffered against extracellular fluctuations in ligand concentration through sustained signalling. We showed this by assaying the pSTAT6 kinetics after pulse chase exposure of ligand. We observed that the signalling still increased 30 minutes after ligand removal, although, according to the published half-life of the ligand receptor complex ≈ 7 min [64]. If the active receptors remained at the membrane, by this time 95% of ligand should have dissociated into the external milieu. Presumably colocalization in to the small internal volume of the endosomes allows efficient re-binding of ligand to the receptor.

According to our model, endosomes therefore fulfil a thermodynamic function for IL-4R signalling. However, it could be that endocytosis is not the only mechanism for receptor concentration and activation in the cells. In different cell types or for different cytokine

receptor systems, different mechanisms of enrichment might take place. It has been reported that for IL-7R, which also shares IL-2R γ , the receptors are enriched in 'raft' like membrane domains, which may itself provide a required concentration step [44]. On the other hand, localization and concentration of receptors in raft may be a prerequisite step for internalization, as shown for the IL-2R where clustering of the different IL-2R subunits α - γ in rafts is followed by receptor internalization [39].

It is evident that the IL-4R internalization and actin dynamics are intimately connected. However, a tight regulation of the actin meshwork is critical for various modes of uptake. While I have shown that the Rac/Pak pathway functionally links the actin machinery to IL-4 receptor endosomal trafficking, the molecular details of the regulation and evidence of a direct coupling molecule were still missing. Rac1 is a member of the small GTPase family of regulatory molecules, whose activity state is typically controlled by guanine nucleotide exchange factors (GEFs). In our system we suspected this GEF to be Vav2, as Vav GEFs are known to modulate actin machineries in many other pathways [70, 73, 75, 85, 87, 102]. In addition, the Rac and Vav knockout phenotypes are consistent with a loss of IL-2R γ mediated cytokine receptor signalling [87]. I tested this hypothesis by showing that Vav2 is localized in IL-2R γ and JAK3 positive endosomes. Furthermore, using pull down assays, I showed that Vav2 interacts with both the receptor subunit IL-2R γ and the associated kinase JAK3. Importantly, 50 aa of receptor tail are crucial because deleting this region results in inhibition of endosome formation. Interestingly, unlike wild type JAK3, mutation of tyrosine binding pocket of the JAK3-SH2 domain prevents the internalization of mutant JAK3/IL-2R γ complexes. Mutant Jak3 protein does not pull down pVav2 and exhibits inhibited endosome formation, showing a direct correlation between endosome formation and signalling. Conversely, constitutively active mutants in Vav2 lead to increased pSTAT6 levels, proving that Vav2 can act upstream of signalling. However, loss of function mutants and esiRNA mediated knockdown did not show any effect on pSTAT6 signalling. This could be due to several different reasons. Firstly, it could be due to the redundancy of Vav isoforms. Secondly, activation of the pathway may require only small quantities of GEF, which may remain even after knockdown. Thirdly, there might be other GEFs controlling this machinery that are structurally different but functionally redundant.

In summary, my work has contributed mechanistic detail to a larger effort by the Weidemann and Bökel labs analyzing how cytokine signalling, specifically through IL-4R, works at the single molecule to tissue level. I contributed to the ultra-structural characterization of the endosomes and quantitative analysis of receptor endocytosis. I have shown how endosomes can facilitate sustained signalling that may help with the long range cytokine signalling in the human body. Finally, I investigated how endocytosis machinery might be regulated at molecular level through one of the commonly employed GEFs. Putting together all the pieces of the puzzle, we could show that endocytosis fulfils a positive role in cytokine signalling by providing a local enrichment compartment for receptors that allow them to overcome the thermodynamic barrier for efficient complex formation. Therefore, endosomes fulfil an entirely different role compared to previously known functions from other pathways. Our experiments provide renewed support to the old model that receptor dimerization is the

limiting step for signal transduction [103]. However, instead of dimerization occurring at the plasma membrane as it was previously assumed, for IL-4R it occurs in the endosome. Low affinities between subunits resolve how cytokine receptors are kept in an inactive state at the plasma membrane. Furthermore, endosomal signalling buffers the pathway against local fluctuations in ligand concentration. In addition, concentration of ligands and receptors in a signalling endosome allows the cell to integrate weak signals over time. This may be particularly relevant to immune cells, as they migrate through the body, where they are exposed to highly variable signalling micro-environments. This might explain why cytokine signalling is tightly associated with haematopoietic system.

It will be interesting to know for what range of receptors our newly discovered mechanism of endocytosis dependent oligomerization may hold true. The process may for different pathways also be tuned by regulating the rate of trafficking into the endosomes and rate of degradation, which results in different steady state functional concentrations at the endosome. However, this requires further detailed investigations into the mechanisms of endocytosis and intracellular trafficking. The extent to which such processes can be tuned effectively may even eventually be exploited to have desired effects in terms of treatments for diseases caused by misregulation of cytokine receptor signalling.

Abbreviations

AC	AaaAcidic domain
CLEM	Correlative Electron Microscopy
CLIC	Clathrin independent carriers
DbI	Diffuse B-cell lymphoma
DH	DbI domain
EEA1	Early Endosome Antigen 1
EGF	Epidermal growth factor
EGFR	Epidermal growth factor receptor
ESCRT	Endosomal Sorting Complex Required for Transport
ESCRT-1	Endosomal Sorting Complex Required for Transport-1
esiRNA	Endoribonuclease-prepared siRNAs
FCCS	Fluorescence Cross Correlation Spectroscopy
FRAP	Fluorescence Recovery After Photobleaching
GEEC	GPI-AP-enriched early endosomal compartments
GEF	Guanine nucleotide exchange factor
GFP	Green Fluorescence Protein
GOF	Gain of function
GPCRs	G protein coupled receptors
HA	Hemagglutinin
HEK	Human embryonic kidney
Hrs	Hepatocyte-growth-factor-regulated tyrosine kinase substrate
IL-13R α 1	Interleukin 13 receptor alpha chain
IL-2R γ	Interleukin 2 receptor gamma chain
IL-4	Interleukin 4
IL-4R α	Interleukin 4 receptor alpha chain
IRS	Insulin receptor substrate

JAK3	Janus kinase 3
MVB	Multivesicular bodies
NGF	Nerve Growth Factors
N-WASP	Neural Wiskott–Aldrich Syndrome Protein
Pak1	p-21 activated kinase 1
PDGER	Platelet derived growth factor receptor
PH	Plekstrin-homology domain
PI3-kinase	Phosphatidylinositol 3-kinase
PRR	Proline rich region
Rac1	Ras-related C3 botulinum toxin substrate
ROI	Region of interest
RTKs	Receptor tyrosine kinases
SARA	Smad anchor for receptor activation
SH2	Src Homology 2
SH3	Src Homology 3
STAT	Signal transducer and activator
TCR	T-cell receptor
TEM	Transmission Electron Microscopy
TGF- β	Transforming growth factor beta
XSCID	X-linked severe combined immunodeficiency
ZF	Zinc finger domain

References

1. Gilman, A.G., *G proteins: transducers of receptor-generated signals*. Annu Rev Biochem, 1987. **56**: p. 615-49.
2. Venkatakrisnan, A.J., et al., *Molecular signatures of G-protein-coupled receptors*. Nature, 2013. **494**(7436): p. 185-94.
3. Bethani, I., et al., *Spatial organization of transmembrane receptor signalling*. EMBO J, 2010. **29**(16): p. 2677-88.
4. Boulay, J.L., J.J. O'Shea, and W.E. Paul, *Molecular phylogeny within type I cytokines and their cognate receptors*. Immunity, 2003. **19**(2): p. 159-63.
5. Ihle, J.N., *Cytokine receptor signalling*. Nature, 1995. **377**(6550): p. 591-4.
6. Goldstein, J.L., R.G. Anderson, and M.S. Brown, *Coated pits, coated vesicles, and receptor-mediated endocytosis*. Nature, 1979. **279**(5715): p. 679-85.
7. Zerial, M. and H. McBride, *Rab proteins as membrane organizers*. Nat Rev Mol Cell Biol, 2001. **2**(2): p. 107-17.
8. Lasiecka, Z.M. and B. Winckler, *Mechanisms of polarized membrane trafficking in neurons -- focusing in on endosomes*. Mol Cell Neurosci, 2011. **48**(4): p. 278-87.
9. Platta, H.W. and H. Stenmark, *Endocytosis and signaling*. Curr Opin Cell Biol, 2011. **23**(4): p. 393-403.
10. Sorkin, A. and M. von Zastrow, *Endocytosis and signalling: intertwining molecular networks*. Nat Rev Mol Cell Biol, 2009. **10**(9): p. 609-22.
11. Glenney, J.R., Jr., et al., *Ligand-induced endocytosis of the EGF receptor is blocked by mutational inactivation and by microinjection of anti-phosphotyrosine antibodies*. Cell, 1988. **52**(5): p. 675-84.
12. Felder, S., et al., *Kinase activity controls the sorting of the epidermal growth factor receptor within the multivesicular body*. Cell, 1990. **61**(4): p. 623-34.
13. Lamaze, C. and S.L. Schmid, *Recruitment of epidermal growth factor receptors into coated pits requires their activated tyrosine kinase*. J Cell Biol, 1995. **129**(1): p. 47-54.
14. Waterman, H. and Y. Yarden, *Molecular mechanisms underlying endocytosis and sorting of ErbB receptor tyrosine kinases*. FEBS Lett, 2001. **490**(3): p. 142-52.
15. Vieira, O.V., et al., *Acquisition of Hrs, an essential component of phagosomal maturation, is impaired by mycobacteria*. Mol Cell Biol, 2004. **24**(10): p. 4593-604.
16. Hurley, J.H. and P.I. Hanson, *Membrane budding and scission by the ESCRT machinery: it's all in the neck*. Nat Rev Mol Cell Biol, 2010. **11**(8): p. 556-66.
17. Howe, C.L. and W.C. Mobley, *Signaling endosome hypothesis: A cellular mechanism for long distance communication*. J Neurobiol, 2004. **58**(2): p. 207-16.
18. Baass, P.C., et al., *Compartmentalized signal transduction by receptor tyrosine kinases*. Trends Cell Biol, 1995. **5**(12): p. 465-70.
19. Di Guglielmo, G.M., et al., *Distinct endocytic pathways regulate TGF-beta receptor signalling and turnover*. Nat Cell Biol, 2003. **5**(5): p. 410-21.
20. Grimes, M.L., et al., *Endocytosis of activated TrkA: evidence that nerve growth factor induces formation of signaling endosomes*. J Neurosci, 1996. **16**(24): p. 7950-64.
21. Watson, F.L., et al., *Neurotrophins use the Erk5 pathway to mediate a retrograde survival response*. Nat Neurosci, 2001. **4**(10): p. 981-8.
22. Ascano, M., D. Bodmer, and R. Kuruvilla, *Endocytic trafficking of neurotrophins in neural development*. Trends Cell Biol, 2012. **22**(5): p. 266-73.

23. Grimes, M.L. and H.M. Miettinen, *Receptor tyrosine kinase and G-protein coupled receptor signaling and sorting within endosomes*. J Neurochem, 2003. **84**(5): p. 905-18.
24. Luttrell, L.M. and R.J. Lefkowitz, *The role of beta-arrestins in the termination and transduction of G-protein-coupled receptor signals*. J Cell Sci, 2002. **115**(Pt 3): p. 455-65.
25. Tsao, P.I. and M. von Zastrow, *Type-specific sorting of G protein-coupled receptors after endocytosis*. J Biol Chem, 2000. **275**(15): p. 11130-40.
26. Confalonieri, S., et al., *Tyrosine phosphorylation of Eps15 is required for ligand-regulated, but not constitutive, endocytosis*. J Cell Biol, 2000. **150**(4): p. 905-12.
27. Haugh, J.M. and T. Meyer, *Active EGF receptors have limited access to PtdIns(4,5)P(2) in endosomes: implications for phospholipase C and PI 3-kinase signaling*. J Cell Sci, 2002. **115**(Pt 2): p. 303-10.
28. Di Guglielmo, G.M., et al., *Compartmentalization of SHC, GRB2 and mSOS, and hyperphosphorylation of Raf-1 by EGF but not insulin in liver parenchyma*. EMBO J, 1994. **13**(18): p. 4269-77.
29. Dobrowolski, R. and E.M. De Robertis, *Endocytic control of growth factor signalling: multivesicular bodies as signalling organelles*. Nat Rev Mol Cell Biol, 2012. **13**(1): p. 53-60.
30. Tsukazaki, T., et al., *SARA, a FYVE domain protein that recruits Smad2 to the TGFbeta receptor*. Cell, 1998. **95**(6): p. 779-91.
31. Itoh, F., et al., *The FYVE domain in Smad anchor for receptor activation (SARA) is sufficient for localization of SARA in early endosomes and regulates TGF-beta/Smad signalling*. Genes Cells, 2002. **7**(3): p. 321-31.
32. Gurdon, J.B. and P.Y. Bourillot, *Morphogen gradient interpretation*. Nature, 2001. **413**(6858): p. 797-803.
33. Bokel, C., et al., *Sara endosomes and the maintenance of Dpp signaling levels across mitosis*. Science, 2006. **314**(5802): p. 1135-9.
34. Yeh, E., et al., *Neuralized functions cell autonomously to regulate Drosophila sense organ development*. EMBO J, 2000. **19**(17): p. 4827-37.
35. Johannes, L. and S. Mayor, *Induced domain formation in endocytic invagination, lipid sorting, and scission*. Cell, 2010. **142**(4): p. 507-10.
36. Bustelo, X.R., V. Sauzeau, and I.M. Berenjeno, *GTP-binding proteins of the Rho/Rac family: regulation, effectors and functions in vivo*. Bioessays, 2007. **29**(4): p. 356-70.
37. Grassart, A., et al., *Clathrin-independent endocytosis used by the IL-2 receptor is regulated by Rac1, Pak1 and Pak2*. EMBO Rep, 2008. **9**(4): p. 356-62.
38. Grassart, A., et al., *Pak1 phosphorylation enhances cortactin-N-WASP interaction in clathrin-caveolin-independent endocytosis*. Traffic, 2010. **11**(8): p. 1079-91.
39. Lamaze, C., et al., *Interleukin 2 receptors and detergent-resistant membrane domains define a clathrin-independent endocytic pathway*. Mol Cell, 2001. **7**(3): p. 661-71.
40. Subtil, A., A. Hemar, and A. Dautry-Varsat, *Rapid endocytosis of interleukin 2 receptors when clathrin-coated pit endocytosis is inhibited*. J Cell Sci, 1994. **107** (Pt 12): p. 3461-8.
41. Sauvonnnet, N., A. Dujancourt, and A. Dautry-Varsat, *Cortactin and dynamin are required for the clathrin-independent endocytosis of gammac cytokine receptor*. J Cell Biol, 2005. **168**(1): p. 155-63.
42. Bulut, G.B., et al., *Ubiquitination regulates the internalization, endolysosomal sorting, and signaling of the erythropoietin receptor*. J Biol Chem, 2011. **286**(8): p. 6449-57.

43. Friedrich, K., et al., *The two subunits of the interleukin-4 receptor mediate independent and distinct patterns of ligand endocytosis*. Eur J Biochem, 1999. **265**(1): p. 457-65.
44. Henriques, C.M., et al., *IL-7 induces rapid clathrin-mediated internalization and JAK3-dependent degradation of IL-7R α in T cells*. Blood, 2010. **115**(16): p. 3269-77.
45. Radtke, S., et al., *Cross-regulation of cytokine signalling: pro-inflammatory cytokines restrict IL-6 signalling through receptor internalisation and degradation*. J Cell Sci, 2010. **123**(Pt 6): p. 947-59.
46. Devergne, O., C. Ghiglione, and S. Noselli, *The endocytic control of JAK/STAT signalling in Drosophila*. J Cell Sci, 2007. **120**(Pt 19): p. 3457-64.
47. Weidemann, T., et al., *Single cell analysis of ligand binding and complex formation of interleukin-4 receptor subunits*. Biophys J, 2011. **101**(10): p. 2360-9.
48. Harper, C.B., et al., *Targeting membrane trafficking in infection prophylaxis: dynamin inhibitors*. Trends Cell Biol, 2013. **23**(2): p. 90-101.
49. Slot, J.W. and H.J. Geuze, *Cryosectioning and immunolabeling*. Nat Protoc, 2007. **2**(10): p. 2480-91.
50. Tokuyasu, K., et al., *Aortic lesions in nonlaying hens with endogenous hyperlipidemia*. Arch Pathol Lab Med, 1980. **104**(1): p. 41-5.
51. Sprague, B.L., et al., *Analysis of binding reactions by fluorescence recovery after photobleaching*. Biophys J, 2004. **86**(6): p. 3473-95.
52. Kelly-Welch, A.E., et al., *Interleukin-4 and interleukin-13 signaling connections maps*. Science, 2003. **300**(5625): p. 1527-8.
53. Nelms, K., et al., *The IL-4 receptor: signaling mechanisms and biologic functions*. Annu Rev Immunol, 1999. **17**: p. 701-38.
54. Wang, X., et al., *Structural biology of shared cytokine receptors*. Annu Rev Immunol, 2009. **27**: p. 29-60.
55. Leonard, W.J. and J.X. Lin, *Cytokine receptor signaling pathways*. J Allergy Clin Immunol, 2000. **105**(5): p. 877-88.
56. Romagnani, S., *The role of lymphocytes in allergic disease*. J Allergy Clin Immunol, 2000. **105**(3): p. 399-408.
57. Hofmann, S.R., et al., *Jak3-independent trafficking of the common gamma chain receptor subunit: chaperone function of Jaks revisited*. Mol Cell Biol, 2004. **24**(11): p. 5039-49.
58. Lamaze, C., et al., *Regulation of receptor-mediated endocytosis by Rho and Rac*. Nature, 1996. **382**(6587): p. 177-9.
59. Mayor, S. and R.E. Pagano, *Pathways of clathrin-independent endocytosis*. Nat Rev Mol Cell Biol, 2007. **8**(8): p. 603-12.
60. Gruenberg, J. and H. Stenmark, *The biogenesis of multivesicular endosomes*. Nat Rev Mol Cell Biol, 2004. **5**(4): p. 317-23.
61. Lippincott-Schwartz, J., E. Snapp, and A. Kenworthy, *Studying protein dynamics in living cells*. Nat Rev Mol Cell Biol, 2001. **2**(6): p. 444-56.
62. Teruel, M.N. and T. Meyer, *Translocation and reversible localization of signaling proteins: a dynamic future for signal transduction*. Cell, 2000. **103**(2): p. 181-4.
63. Giese, B., et al., *Long term association of the cytokine receptor gp130 and the Janus kinase Jak1 revealed by FRAP analysis*. J Biol Chem, 2003. **278**(40): p. 39205-13.
64. Wang, Y., B.J. Shen, and W. Sebald, *A mixed-charge pair in human interleukin 4 dominates high-affinity interaction with the receptor alpha chain*. Proc Natl Acad Sci U S A, 1997. **94**(5): p. 1657-62.

65. Hintersteiner, M., et al., *Covalent fluorescence labeling of His-tagged proteins on the surface of living cells*. *Chembiochem*, 2008. **9**(9): p. 1391-5.
66. Lata, S., et al., *Specific and stable fluorescence labeling of histidine-tagged proteins for dissecting multi-protein complex formation*. *J Am Chem Soc*, 2006. **128**(7): p. 2365-72.
67. Shutes, A., et al., *Specificity and mechanism of action of EHT 1864, a novel small molecule inhibitor of Rac family small GTPases*. *J Biol Chem*, 2007. **282**(49): p. 35666-78.
68. Deacon, S.W., et al., *An isoform-selective, small-molecule inhibitor targets the autoregulatory mechanism of p21-activated kinase*. *Chem Biol*, 2008. **15**(4): p. 322-31.
69. Evans, G.A., et al., *Interleukin-2 induces tyrosine phosphorylation of the vav proto-oncogene product in human T cells: lack of requirement for the tyrosine kinase lck*. *Biochem J*, 1993. **294** (Pt 2): p. 339-42.
70. Abe, K., et al., *Vav2 is an activator of Cdc42, Rac1, and RhoA*. *J Biol Chem*, 2000. **275**(14): p. 10141-9.
71. Han, J., et al., *Role of substrates and products of PI 3-kinase in regulating activation of Rac-related guanosine triphosphatases by Vav*. *Science*, 1998. **279**(5350): p. 558-60.
72. Bustelo, X.R., *Understanding Rho/Rac biology in T-cells using animal models*. *Bioessays*, 2002. **24**(7): p. 602-12.
73. Hornstein, I., A. Alcover, and S. Katzav, *Vav proteins, masters of the world of cytoskeleton organization*. *Cell Signal*, 2004. **16**(1): p. 1-11.
74. Turner, M. and D.D. Billadeau, *VAV proteins as signal integrators for multi-subunit immune-recognition receptors*. *Nat Rev Immunol*, 2002. **2**(7): p. 476-86.
75. Aghazadeh, B., et al., *Structural basis for relief of autoinhibition of the Dbl homology domain of proto-oncogene Vav by tyrosine phosphorylation*. *Cell*, 2000. **102**(5): p. 625-33.
76. Yu, B., et al., *Structural and energetic mechanisms of cooperative autoinhibition and activation of Vav1*. *Cell*, 2010. **140**(2): p. 246-56.
77. Bustelo, X.R. and M. Barbacid, *Tyrosine phosphorylation of the vav proto-oncogene product in activated B cells*. *Science*, 1992. **256**(5060): p. 1196-9.
78. Bustelo, X.R., J.A. Ledbetter, and M. Barbacid, *Product of vav proto-oncogene defines a new class of tyrosine protein kinase substrates*. *Nature*, 1992. **356**(6364): p. 68-71.
79. Margolis, B., et al., *Tyrosine phosphorylation of vav proto-oncogene product containing SH2 domain and transcription factor motifs*. *Nature*, 1992. **356**(6364): p. 71-4.
80. Clevenger, C.V., et al., *Vav is necessary for prolactin-stimulated proliferation and is translocated into the nucleus of a T-cell line*. *J Biol Chem*, 1995. **270**(22): p. 13246-53.
81. Krumenacker, J.S., et al., *Prolactin receptor signaling: shared components with the T-cell antigen receptor in Nb2 lymphoma cells*. *Endocrine*, 1998. **9**(3): p. 313-20.
82. Uddin, S., et al., *Insulin-dependent tyrosine phosphorylation of the vav protooncogene product in cells of hematopoietic origin*. *J Biol Chem*, 1995. **270**(13): p. 7712-6.
83. Gringhuis, S.I., et al., *Signaling through CD5 activates a pathway involving phosphatidylinositol 3-kinase, Vav, and Rac1 in human mature T lymphocytes*. *Mol Cell Biol*, 1998. **18**(3): p. 1725-35.

84. Bustelo, X.R., *Regulatory and signaling properties of the Vav family*. Mol Cell Biol, 2000. **20**(5): p. 1461-77.
85. Thalappilly, S., et al., *VAV2 regulates epidermal growth factor receptor endocytosis and degradation*. Oncogene, 2010. **29**(17): p. 2528-39.
86. Saveliev, A., et al., *Function of the nucleotide exchange activity of vav1 in T cell development and activation*. Sci Signal, 2009. **2**(101): p. ra83.
87. Dumont, C., et al., *Rac GTPases play critical roles in early T-cell development*. Blood, 2009. **113**(17): p. 3990-8.
88. Lopez-Lago, M., et al., *Tyrosine phosphorylation mediates both activation and downmodulation of the biological activity of Vav*. Mol Cell Biol, 2000. **20**(5): p. 1678-91.
89. Miletic, A.V., et al., *Vav1 acidic region tyrosine 174 is required for the formation of T cell receptor-induced microclusters and is essential in T cell development and activation*. J Biol Chem, 2006. **281**(50): p. 38257-65.
90. Chen, M., et al., *Complex effects of naturally occurring mutations in the JAK3 pseudokinase domain: evidence for interactions between the kinase and pseudokinase domains*. Mol Cell Biol, 2000. **20**(3): p. 947-56.
91. Radtke, S., et al., *The Jak1 SH2 domain does not fulfill a classical SH2 function in Jak/STAT signaling but plays a structural role for receptor interaction and up-regulation of receptor surface expression*. J Biol Chem, 2005. **280**(27): p. 25760-8.
92. Sultan, M., et al., *A global view of gene activity and alternative splicing by deep sequencing of the human transcriptome*. Science, 2008. **321**(5891): p. 956-60.
93. Basquin, C., et al., *The signalling factor PI3K is a specific regulator of the clathrin-independent dynamin-dependent endocytosis of IL-2 receptors*. J Cell Sci, 2013. **126**(Pt 5): p. 1099-108.
94. Mueller, T.D., et al., *Structure, binding, and antagonists in the IL-4/IL-13 receptor system*. Biochim Biophys Acta, 2002. **1592**(3): p. 237-50.
95. Zhang, J.L., et al., *The high-affinity interaction of human IL-4 and the receptor alpha chain is constituted by two independent binding clusters*. J Mol Biol, 2002. **315**(3): p. 399-407.
96. Worch, R., et al., *Focus on composition and interaction potential of single-pass transmembrane domains*. Proteomics, 2010. **10**(23): p. 4196-208.
97. Whitty, A., et al., *Interaction affinity between cytokine receptor components on the cell surface*. Proc Natl Acad Sci U S A, 1998. **95**(22): p. 13165-70.
98. LaPorte, S.L., et al., *Molecular and structural basis of cytokine receptor pleiotropy in the interleukin-4/13 system*. Cell, 2008. **132**(2): p. 259-72.
99. Park, L.S., et al., *Characterization of the human B cell stimulatory factor 1 receptor*. J Exp Med, 1987. **166**(2): p. 476-88.
100. Bache, K.G., et al., *Hrs regulates multivesicular body formation via ESCRT recruitment to endosomes*. J Cell Biol, 2003. **162**(3): p. 435-42.
101. Hemar, A., et al., *Endocytosis of interleukin 2 receptors in human T lymphocytes: distinct intracellular localization and fate of the receptor alpha, beta, and gamma chains*. J Cell Biol, 1995. **129**(1): p. 55-64.
102. Sauzeau, V., et al., *Loss of Vav2 proto-oncogene causes tachycardia and cardiovascular disease in mice*. Mol Biol Cell, 2007. **18**(3): p. 943-52.
103. Heldin, C.H., *Dimerization of cell surface receptors in signal transduction*. Cell, 1995. **80**(2): p. 213-23.

Acknowledgements

I would like to thank my PhD advisors, Prof. Petra Schwille, Dr. Thomas Weidemann and Dr. Christian Bökel for guiding me through the project during the last three years. I would like to thank Petra for always supporting me and urging me to give better presentations. I express my gratitude to Thomas for teaching me various aspects of imaging, helping with the project and have always been very supportive. Christian has been a great mentor during the last three years, especially with the biological aspects of the project. I have learnt a lot from the Schwille and Bökel labs and I am glad I spent my three years with these two labs.

I would also like to thank Thomas Kurth for the help with electron microscopy studies that are an important part of this thesis. I would also express my gratitude to Christoph Herold, who was very kind to help with MATLAB codes for analysis. I am also very grateful to Karin, Sarah and Raquel who were very cooperative and helped me in many ways in the daily life in the lab.

I am also very grateful to all the past and current members of the Schwille lab –Remi, Viktoria, Christoph, Grzegorz, Erdinc, Jens, Carina, Eugene, Zdenek, Paul, Sonal, Christoph F, Janine, Franziska, Jakob, Alena, Ariadna, Ilaria, Tobias, Henri and many others, who made my three years in the lab very pleasant. I also enjoyed the conferences and the Klosters trip with almost all of you in different instances. You all will be dearly missed. I am very grateful to you for your support during my regular nervous breakdowns before the talks. I would also like thank friends outside the lab – Annett, Prayag, Priyanka and Rido, Sundar, Rupam, Rahul and Neha, Mansi who were very helpful to us and made me feel at home so far from home.

I would also take this opportunity to thank Sonal, who proofread this thesis, and for many other things during my visits to Munich. I would like to thank the tango group – Sonal, Grzegorz, Kristina, Alena, Jakob and Andrea for introducing me to the new world of dancing I never knew. It was great to dance with you guys, and I hope we find many future opportunities to gather again.

I would like to thank people from Boekel lab- Kristina, Olga and Eugene. I enjoyed their company while having lunch at menza. I thank to Marcus for helping with all kind of translations that made my life much easier. I thank Olga for proof reading my thesis.

I would also like thank Remi and Anna, Jens, Sundar, Rahul, Carina, Grzegorz, Erdinc, Viktoria, Alex and Maya who became very close friends and made our first life abroad easy and very memorable. I am grateful to them for all the help, including the moving of the apartment. We were appalled by your enthusiasm and willingness to help. We could not have ever done it so easily without you. We enjoyed all the events - the trips to the mountains or the get-togethers we had. We are also grateful to Grzegorz for his warm hospitality in Poland. I am grateful to him for turning what could have been a cold lonely winter into a very warm, joyable affair by inviting us to his family in Dziewiethlin, Poland. Remi, I know, we will visit you soon!

No words are enough for my family. My brother and his family, my parents have always encouraged and stood by me during difficult times. Love and support from my parents and Senthil's parents have always given me courage to keep at this. I would like thank my husband without whom this would have never been possible. I am grateful for his love, support and encouragement at each step of my carrier. We both have learnt a lot about life, found great friends in here. Dresden will always be a cherished part of our lives.

Erklärung entsprechend §5.5 der Promotionsordnung

Hiermit versichere ich, dass ich die vorliegende Arbeit ohne unzulässige Hilfe Dritter und ohne Benutzung anderer als der angegebenen Hilfsmittel angefertigt habe; die aus fremden Quellen direkt oder indirekt übernommenen Gedanken sind als solche kenntlich gemacht. Die Arbeit wurde bisher weder im Inland noch im Ausland in gleicher oder ähnlicher Form einer anderen Prüfungsbehörde vorgelegt.

*Die Dissertation wurde im Zeitraum vom **September 1, 2011 bis January 30, 2014** verfasst und von **Prof. Dr. Petra Schwille, TU Dresden Biotechnologischen Zentrum der Tu Dresden** betreut.*

Meine Person betreffend erkläre ich hiermit, dass keine früheren erfolglosen Promotionsverfahren stattgefunden haben.

Ich erkenne die Promotionsordnung der Fakultät für Mathematik und Naturwissenschaften, Technische Universität Dresden an.

Declaration according to §5.5 of doctorate regulation

I herewith declare that I have produced this paper without the prohibited assistance of third parties and without making use of aids other than those specified; notions taken over directly or indirectly from other sources have been identified as such. This paper has not previously been presented in identical or similar form to any other German or foreign examination board.

*The thesis work was conducted from starting **September 1, 2011** to **January 30, 2014** of finish under the supervision of **Prof. Dr. Petra Schwille, TU Dresden Biotechnologischen Zentrum der Tu Dresden**.*

I declare that I have not undertaken any previous unsuccessful doctorate proceedings.

I declare that I recognize the doctorate regulations of the Fakultät für Mathematik und Naturwissenschaften of the Technische Universität Dresden.

Date

Signature